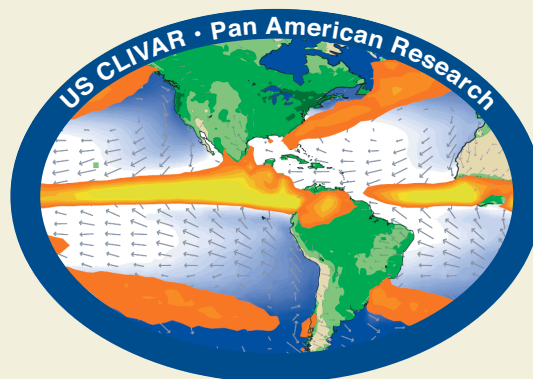
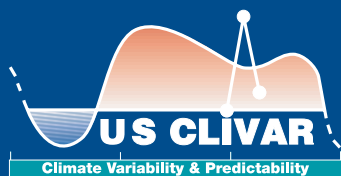


U.S. CLIVAR **Pan American Research**

A Scientific Prospectus and Implementation Plan

U.S. Pan American Sector
Implementation Panel

May 2002



Support for this publication provided by the

National Science Foundation (NSF)

National Oceanic and Atmospheric Administration (NOAA)

National Aeronautics and Space Administration (NASA)

Writers

PACS Working Groups

Editors

Steve Esbensen, Oregon State University

Todd Mitchell and Candace Gudmundson, University of Washington

Design and Graphics Support

Jill Campbell and Kay Dewar, University of Washington

U.S. CLIVAR Pan American Implementation Panel, 2002: *U.S. CLIVAR Pan American Research: A Scientific Prospectus and Implementation Plan*, U.S. CLIVAR Office, Washington, DC, 58 pp.

printed on recycled paper



U.S. CLIVAR Pan American Research: A Scientific Prospectus and Implementation Plan

Executive summary

The U.S. CLIVAR program is a contribution to an internationally coordinated World Climate Research Programme (WCRP) initiative to improve the understanding and prediction skill of physical climate variability on time scales of seasons to decades. The Pan American component of the U.S. CLIVAR program evolved from the Pan American Climate Studies (PACS) program, an early contribution to U.S. CLIVAR research, and is built on the heritage of the Tropical Ocean-Global Atmosphere (TOGA) program (1985-1995). TOGA demonstrated the feasibility of operational seasonal-to-interannual climate prediction of equatorial Pacific sea surface temperature anomalies based on numerical models of the physics of the tropical ocean-atmosphere system, and it clarified the planetary-scale atmospheric response associated with the sea surface temperature anomalies.

U.S. CLIVAR Pan American research seeks to extend the scope and improve the skill of operational climate prediction over the Americas on seasonal and longer time scales.

The three specific objectives of U.S. CLIVAR Pan American research are:

1. Promote a better understanding of and more realistic simulation of coupled ocean-atmosphere-land processes, with emphasis on
 - ◆ the response of planetary-scale atmospheric circulation and precipitation patterns to potentially predictable surface boundary conditions such as sea surface temperature, soil moisture, and vegetation;
 - ◆ the mechanisms that couple climate variability over ocean and land;
 - ◆ the seasonally varying climatological mean state of the ocean, atmosphere, and land surface; and
 - ◆ the effects of land surface processes and orography on the variability of seasonal rainfall patterns.

2. Determine the predictability of warm-season precipitation anomalies over the Americas on seasonal and longer time scales.
3. Advance the development of the climate observing and prediction system for seasonal and longer time scales.

The season-to-season “memory” of the coupled ocean-atmosphere-land system resides in the processes that determine the slowly evolving and potentially predictable changes at Earth’s surface, i.e., the sea surface temperature fields, soil moisture, snow cover, and vegetation. Sea surface temperature in both the Atlantic and Pacific oceans is known to determine much of the climate variability over the tropical Americas and to affect the wintertime climate at middle and high latitudes. Predictability of seasonal rainfall has been demonstrated and seasonal predictions having modest skill up to a year in advance are issued routinely by the U.S. National Centers for Environmental Prediction (NCEP) and other organizations. Warm-season precipitation, however, is not yet predictable. In particular, the relative contributions of sea surface temperature and land surface processes in shaping the annual march of the Pan American monsoons and the evolution of warm-season rainfall anomalies are not well understood.

U.S. CLIVAR Pan American research will focus on the phenomena that are crucial for organizing seasonal rainfall patterns, i.e., the monsoons, the oceanic ITCZs, and the tropical and extratropical storm tracks, and will emphasize the contribution of land surface processes to warm-season climate variability.

Regional rainfall anomalies over the Americas involve the intensification, weakening, or subtle displacements of these seasonally varying, climatological-mean features.

U.S. CLIVAR Pan American research necessarily encompasses a broad range of activities. Empirical and



modeling studies, as well as the development and analysis of historical datasets, will contribute to a better understanding and simulation of the phenomena that control the annual march of seasonal rainfall patterns and their variability on seasonal-to-decadal time scales. Informal groups of observers and theoreticians will work together to understand and simulate key phenomena and processes and hence to accelerate progress. U.S. CLIVAR will make a major contribution to improving the climate observing system in the oceans and seas adjacent to the Americas and will collaborate with CLIVAR Variability of the American Monsoon Systems (VAMOS) and with national and international agencies and organizations to improve the quality and coverage of atmospheric climate observations. Three field programs—North American Monsoon Experiment (NAME), Monsoon Experiment South America (MESA), and Eastern Pacific Investigation of Climate (EPIC)—will improve the understanding of key climate processes that are currently hindering advances in climate simulation and prediction over the Americas.

U.S. CLIVAR and the Global Energy and Water Experiment (GEWEX) are complementary programs in the Pan American region. The distribution of rainfall over the Americas is shaped not only by sea surface temperature patterns but also by land surface processes, particularly during the warm season, when vegetation and soil moisture are highly influential. Orography and coastal geometry mediate these effects and leave a distinctive mesoscale imprint on the rainfall patterns. These issues will be addressed in collaboration with GEWEX and its regional programs. CLIVAR will supply the coupled climate modeling expertise, with emphasis on the processes that couple climate variability over the oceans to that over the land. GEWEX will supply the hydrological expertise and emphasize the processes that couple the land surface to the overlying atmosphere.

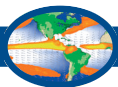
Significant economic benefits are expected from the improved understanding of the processes that control the distribution of rainfall over the Americas and the application of that knowledge to improve the models used for climate prediction on seasonal and longer time scales. Climate-sensitive areas of the economy such as agricultural water resource management will benefit from more accurate and detailed information concerning the statistical probabilities of various rainfall scenarios.

In addition, U.S. CLIVAR research will increase the accuracy and credibility of regional projections of future anthropogenic climate change over the American continents.

The climate processes addressed by U.S. CLIVAR Pan American research are the same as those involved in assessing the effects of anthropogenic climate change.

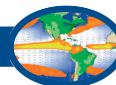
Anthropogenic changes in atmospheric gases and particulate composition modify the global energy balance. The practical consequences for people depend on how the climate system responds on regional scales to such global energy balance changes. Any regional response is likely to be tied to natural regional climate variations, and its modeling cannot be credible unless the significant natural climate variations are understood and included in the models addressing anthropogenic changes.

This scientific prospectus and implementation plan provides the motivation and scientific basis for U.S. CLIVAR Pan American research and describes how that research will be carried out in pursuit of its specific objectives. Section 1 gives a scientific description of phenomena in the ocean-atmosphere-land system that are likely to be of importance for understanding and predicting climate variations over the Americas on time scales of a season and longer. The climate and weather variations over the Americas that provide the practical and scientific motivation for U.S. CLIVAR Pan American research are discussed in Section 2. Section 3 describes the overall implementation strategy for the empirical studies, modeling, dataset development, and field studies that will be conducted under its auspices. Section 4 describes in more detail the field studies that are envisioned as part of U.S. CLIVAR, including pilot projects and activities already underway and those likely to be proposed for the 2002-2015 time frame. Sections 5-7 discuss modeling, dataset development and management, and climate observing system issues that are central to the success of U.S. CLIVAR Pan American research. U.S. CLIVAR organization and the anticipated links with other national and international programs are described in Section 8.



Contents

Executive Summary	1
1. Scientific Background for Pan American Regional Climate	4
1.1 What determines the annual mean climate?	4
1.2 What determines the seasonal march?	7
1.3 What determines anomalies over North America?	12
1.4 What determines anomalies over South America?	13
1.5 The land surface role	14
1.6 El Niño/Southern Oscillation	15
1.7 Cold tongue/ITCZ complexes	18
1.8 Stratus cloud decks	20
1.9 Subseasonal climate variability	20
2. Practical and Scientific Motivation for Pan American Climate Research	24
3. Implementation Strategy	27
3.1 Understanding and simulating Pan American climate variability	28
3.2 Atmospheric response to boundary conditions	28
3.3 Coupling between land and ocean	29
3.4 Seasonally varying mean climate	30
3.5 Evolution of tropical sea surface temperature anomalies	30
4. Field Studies	31
4.1 North American Monsoon Experiment (NAME)	31
4.2 Monsoon Experiment South America (MESA)	35
4.3 Eastern Pacific Investigation of Climate Processes in the Coupled Ocean-Atmosphere System (EPIC)	36
4.3.1 Pilot field studies	36
4.3.2 Enhanced monitoring for EPIC	38
4.3.3 EPIC 2001: An intensive observing period	41
5. Modeling Issues	42
5.1 Atmospheric General Circulation Models (AGCMs)	42
5.2 Mesoscale atmospheric models	42
5.3 Modeling the effects of the land surface	43
5.4 Ocean General Circulation Models (OGCMs)	43
5.5 Coupled ocean-atmosphere GCMs	44
6. Dataset Development and Management	46
7. Building the Pan American Climate Observing System	47
8. U.S. CLIVAR Organization and Links to Other Efforts	48
Selected References	50
Notes on Illustrations	54
Acronym Glossary	56
Color Maps for Selected Figures	57



1. Scientific Background for Pan American Regional Climate

1.1 What determines the annual mean climate?

The rainfall climatology of the Pan American region is dominated by intertropical convergence zones (ITCZs) and the continental monsoons. The tropical Atlantic and eastern Pacific tradewind regions are noted for fair weather and a large excess of evaporation over precipitation, while narrow ITCZs, which separate the regions, are marked by heavy and persistent rainfall. The positions and intensities of the ITCZs are sensitive to the underlying land surface and the sea surface temperature (SST) distribution. Rainfall over the tropical and subtropical Americas and the adjacent oceans is dominated by seasonally dependent monsoonal circulations, which produce widespread rain and upper-level anticyclones in the summer hemisphere. The northeasterly and southeasterly tradewind belts, which occupy most of the tropics and subtropics, border the major monsoonal rain areas. However, seasonal reversals of surface winds are less pronounced within the Pan American domain than they are in the Australasian sector of the tropics. The prevalent upper-tropospheric westerlies over the equatorial eastern Pacific allow for a higher degree of interaction between the Northern and Southern hemisphere circulations than occurs elsewhere in the tropics. Figure 1 shows the distribution of annual mean rainfall over the tropics based on two different sets of measurements. The continental monsoons and the oceanic ITCZs are clearly evident in both, but the oceanic ITCZs are more prominent in the microwave imag-

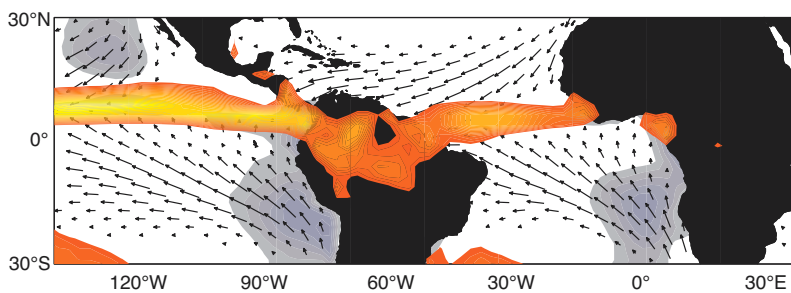


Figure 2. Climatological annual mean conditions over the Pan American region. Vectors denote surface winds, orange-yellow shading shows precipitation, and gray-blue shading denotes stratus cloud decks. Over both the Atlantic and Pacific, the ITCZ is located well to the north of the equator, and southeasterly trades extend across it. The stratus cloud decks are more extensive in the Southern Hemisphere.

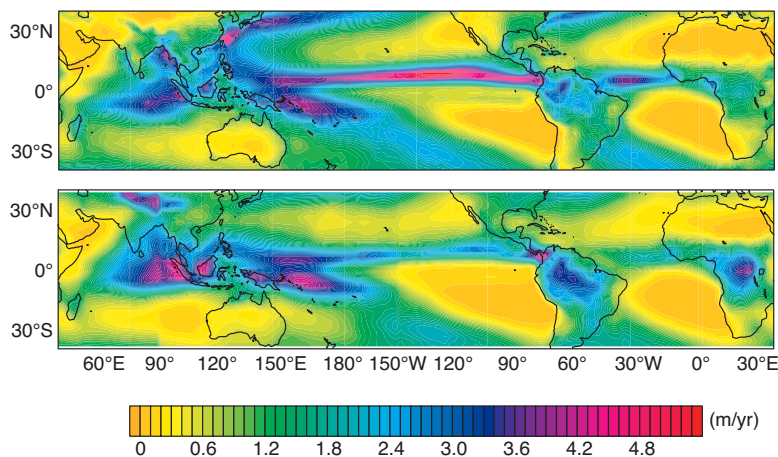


Figure 1. Annual mean precipitation over the tropics, as inferred from different data sources. The upper panel is based on the microwave sounding unit over the ocean and a land climatology compiled from station data. The lower panel shows the Geostationary Operational Environmental Satellite precipitation index (GPI) inferred from high-resolution imagery of outgoing longwave radiation. The bands of heavy precipitation over the tropical Pacific and Atlantic are the oceanic ITCZs. Quantitative estimates of precipitation can be inferred from the color bar.

ery (top panel), which is more sensitive to low-level rain systems. Both plots show the contrasting structure of the ITCZ-dominated Pan American domain and the monsoon-dominated Australasian region. The annual mean climate over the Pan American domain is marked by strong equatorial asymmetries that cannot be explained on the basis of simple considerations of sun-earth geometry. The heavy, persistent rainfall associated with the ITCZ is centered not on the equator but at 5–10°N, as indicated in Fig. 2. Stratiform cloud decks, indicated by the gray-blue shading, are of greater extent in the Southern Hemisphere and act to cool the underlying ocean by shielding it from incoming solar radiation.

The highest SSTs are observed not along the equator but to the north, where a broad latitudinal belt of high sea surface temperature extends from the Pacific coast of southern Mexico, eastward across the Caribbean Sea, into the Atlantic. The highest temperatures off southern Mexico (Figs. 3 and 4) occur with relatively light surface currents and mean wind speeds. In contrast to the western Pacific, however, both the surface currents and winds are strong over the warm ocean areas in the Caribbean and Atlantic. The narrower latitudinal bands of high sea surface temperatures close to the equator in the eastern Pacific and Atlantic oceans, between

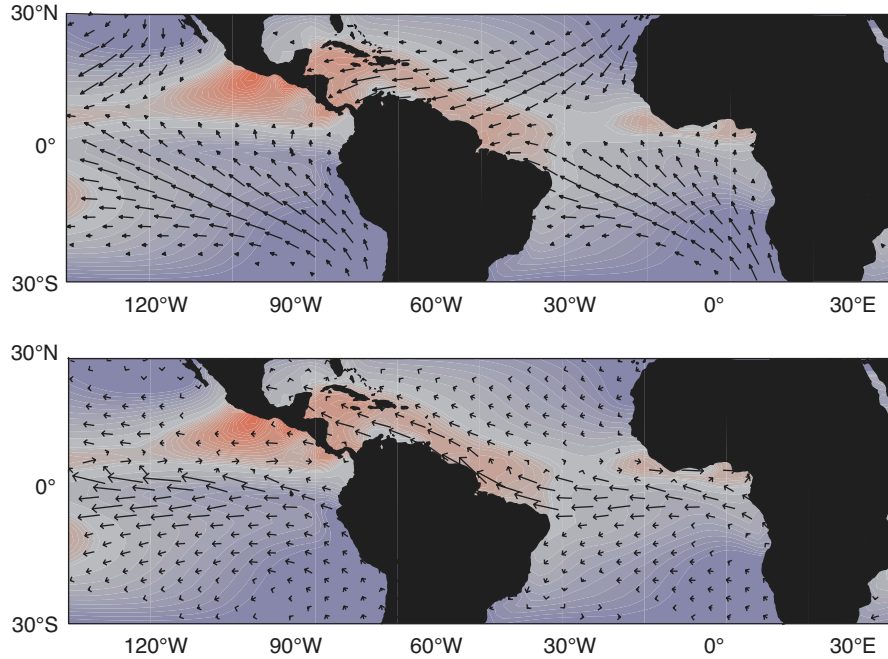


Figure 3. As in Fig. 2, but shading denotes annual mean sea surface temperature. The warmest (reddest) waters are observed not on the equator but in the Northern Hemisphere near the latitude of the ITCZ.

Figure 4. As in Fig. 3, but arrows denote surface currents. The eastward arrows at the latitude of the ITCZ correspond to the North Equatorial Countercurrent and the longer westward arrows along and just to the south of the equator correspond to the South Equatorial Current.

5°-10°N, more or less coincide with the annual mean position of the ITCZ, as shown in Fig. 3. They also coincide with the eastward-flowing North Equatorial Countercurrent (Fig. 4), which is linked to the strong meridional gradient of wind stress across the ITCZ. The easterly surface winds along the equator drive the westward-flowing South Equatorial Current, which is deflected toward the right in the Northern Hemisphere and toward the left in the Southern Hemisphere by the Coriolis force. The induced equatorial upwelling of large volumes of cold, nutrient-rich water is responsible for the pronounced “equatorial cold tongues,” indicated by the bluish shading in Figs. 3 and 4, and for the equatorial maximum in chlorophyll concentrations revealed by the Coastal Zone Color Scanner imagery in Fig. 5.

The size, shape, and location of the North and South American land masses contribute to the asymmetry of the Pan American climate. Figure 6 shows the North and South American topography. The major western continental mountain ranges over the Americas extend from northwest to southeast for the entire length of both continents. As can be seen in Figs. 2 and 3, the winds along the Pacific coast are

largely parallel to the shore of South America and are very weak along the North American shore. The southeasterly tradewinds are approximately parallel to the South American coastline, while the northeasterly tradewinds in the tropical Pacific are roughly perpendicular to the west coasts of Mexico and Central America. The tradewinds in the Gulf of Mexico and the Caribbean Sea are considerably weakened by the Mexican and Central American Sierra Madre mountain ranges as boundary-layer air crosses over the land to the Pacific. On the eastern slopes of the Rocky Mountains and the Andes, the annual mean near-surface flow

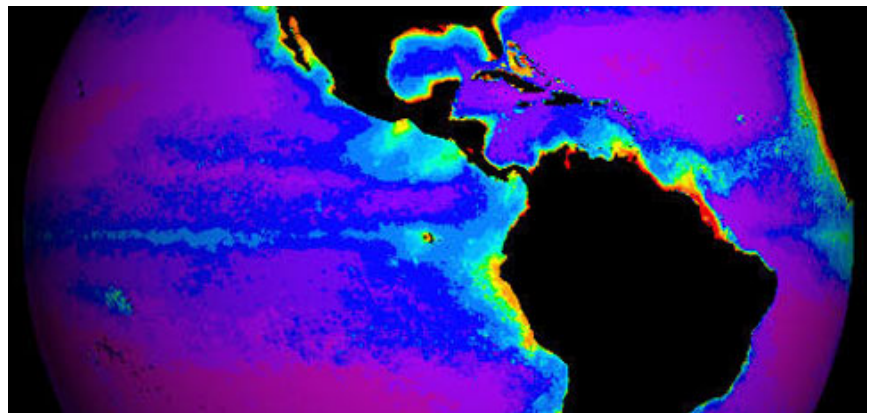
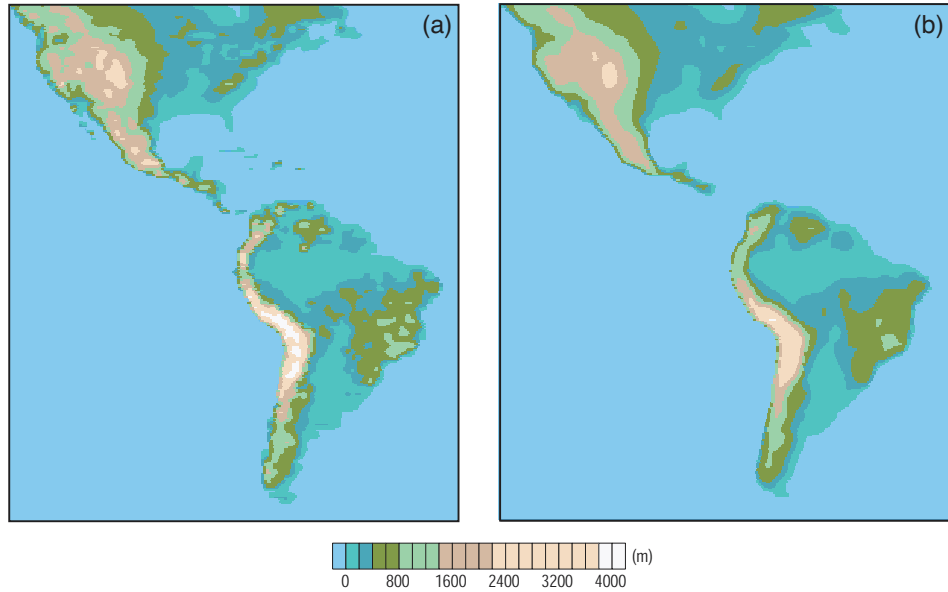


Figure 5. Annual mean chlorophyll concentrations based on Coastal Zone Color Scanner imagery. The color scale has been adjusted to enhance the weak gradients in the vicinity of the equator. The enhanced concentrations along the equator in both oceans are signatures of upwelling. Concentrations are also enhanced beneath the ITCZ, in the region of coastal upwelling along the Peruvian coast and downstream (on the Pacific side) of the gaps in the mountain ranges of Central America.



Figure 6. Topography of North and South America (a) at approximately 5' resolution and (b) at the typical 2° latitude-longitude resolution of an atmospheric general circulation model that is used in climate simulations. The smallest shading interval is 200 m.



is poleward and tends to either parallel the mountain range or move down the slope. The location of most of South America to the east of North America and at low latitudes extending into the Northern Hemisphere contributes to the north-south asymmetry. The character of the South American continent, with the Andes cordillera to the west and a land mass that extends from the Northern Hemisphere equatorial region to the high

latitudes of the Southern Hemisphere, creates distinctive climate patterns in the overlying atmosphere. Unlike North America, which lies mostly in midlatitudes, South America is a tropical continent that ends to the south in a narrow conical shape. The lowlands of the continent assume an approximate "T" shape with the west-to-east Amazon basin in the tropics and the north-to-south La Plata basin perpendicular to it and extending poleward to about 40°S. This is different from North America, where the main river basins extend equatorward from middle latitudes. The central Andes are closed to tropical moisture and dry conditions prevail there. This situation is similar to conditions over North America, and an analogy can be drawn between the North American Great Plains and the subtropical plains of South America.

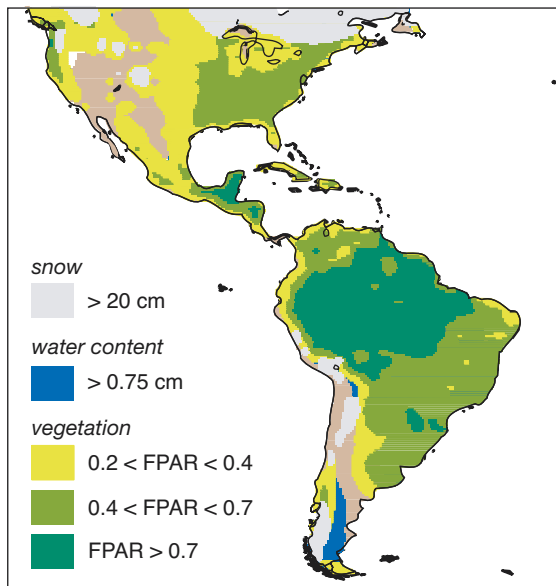


Figure 7. Annual mean distribution of snow cover, soil moisture, and vegetation over North and South America. The soil moisture is characterized by model water content in the topmost 7 cm of soil. Vegetation is documented by the satellite-derived fraction of photosynthetically active radiation (FPAR) absorbed by the green vegetation canopy. Snow depth is derived from surface observations.

The land surface also influences the climatic mean state and variability by interacting not only with winds through terrain but also with the atmospheric boundary layer and hence moist convection through its controls of sensible and latent heat flux. Figure 7 shows the annual mean distribution of soil moisture, snow cover, and vegetation. Large values of soil moisture and the vegetation index are found over tropical South and Central America and over the subtropical regions of the southeastern United States and South America. These features of the land surface that alter the surface and water balances are slowly varying and potentially predictable. Although the sea surface temperature is high and moisture readily available in the Pan American warm-pool region, the precipitation appears to be greater over tropical South America than over the warm water.

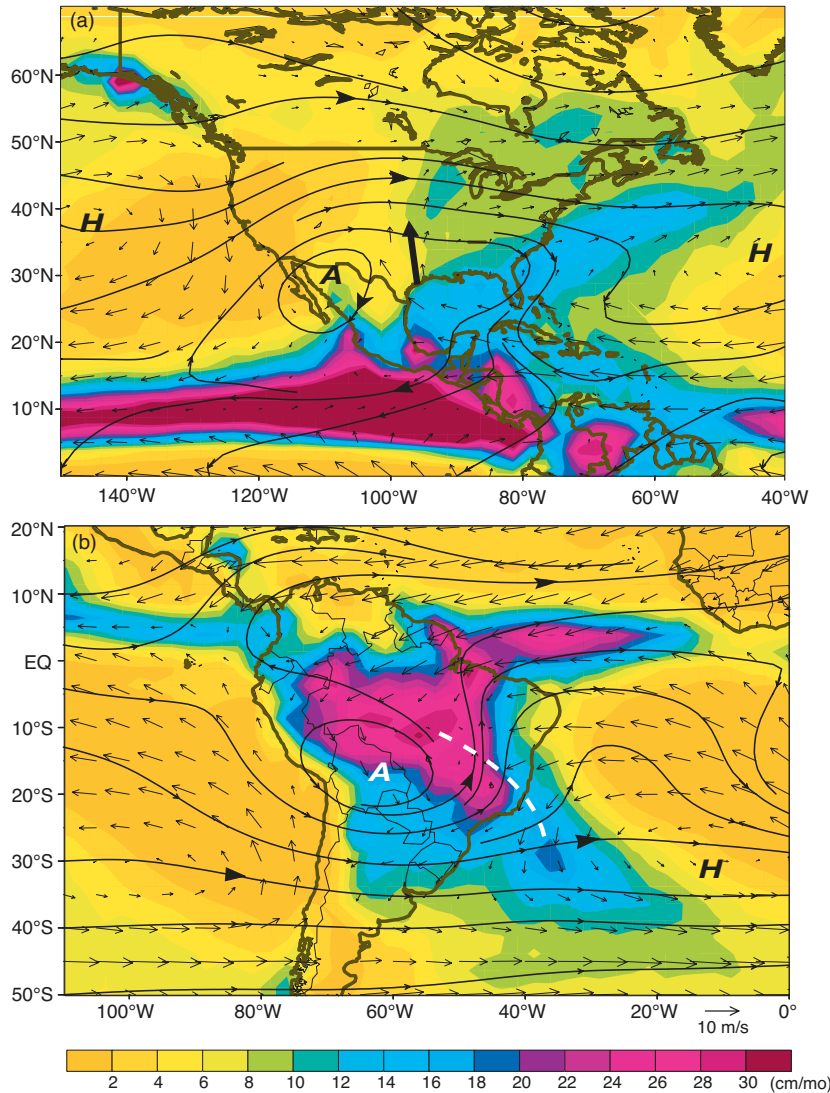


Figure 8. Mean (1979-1995) warm-season precipitation (shading) and circulation at 925 hPa (vector winds) and 200 hPa (streamlines): (a) July-September. The position of an upper-level monsoon anticyclone over the southwestern United States and northwestern Mexico is indicated by an "A". The subtropical surface high pressure centers over Bermuda and the North Pacific are indicated by an "H". The approximate location of the Great Plains low-level jet is indicated by a heavy solid arrow. (b) December-February. The position of the upper-level monsoon high over Bolivia is indicated by an "A". The South Atlantic subtropical surface high pressure center is indicated by an "H". The approximate axis of the South Atlantic Convergence Zone (SACZ) is indicated by the heavy white dashed line.

land-sea distribution in the Northern and Southern hemispheres or from the superimposed seasonal march? And to what extent do land surface processes contribute to the annual mean patterns?

1.2 What determines the seasonal march?

The march of the seasons over the Americas contains some of the classic textbook elements that are easily quantified in global atmospheric models. Warm-season maxima in rainfall occur in both hemispheres,

The strong equatorial asymmetry in the mean climate evidently is a manifestation of coupled ocean-atmosphere-land interactions, perhaps even more intricate than those involved in El Niño/Southern Oscillation (ENSO). Many questions remain. Does the ITCZ in the Atlantic and Pacific oceans result from the underlying belt of warm sea surface temperature, or is warm water a response to the ITCZ? Neither view is adequate as the ITCZ and the underlying warm water along with the surface winds, ocean currents, oceanic upwelling, stratus cloud decks, and deep atmospheric convection are all elements of a response to the land-sea geometry. Both circulations in the meridional and zonal plane are important. To what extent does the large equatorial asymmetry in the annual mean climate derive from oceanic processes related to the northwest-southeast orientation of the west coasts of South America and Africa or from atmospheric planetary waves induced by the differences in orography and the

over Columbia/Central America, and over Southern Brazil/Paraguay, with accompanying surface lows and upper-level anticyclones over the elevated terrain of northwestern Mexico and the central Andes (Fig. 8). During the Northern Hemisphere warm season, the ITCZ bands in the Pacific and the Atlantic merge with the continental monsoons of Central America and northern South America. During the Southern Hemisphere warm season, the ITCZ bands weaken to the north of the equator and the monsoon over Amazonia dominates and merges with the South Atlantic Convergence Zone (SACZ). Rainfall in the upper reaches of the Amazon is year round. Also relatively well understood and simulated are the rainy winters of the U.S. Pacific Northwest and southern Chile.

The North American monsoon system develops in May and June as synoptic-scale transient activity decreases over northern Mexico and the U.S., and

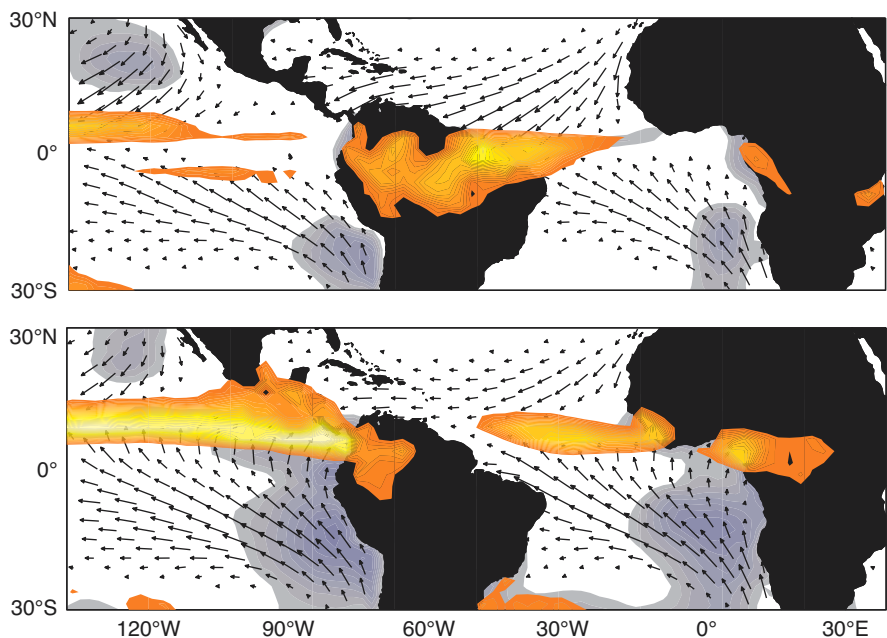
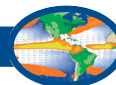


Figure 9. As in Fig. 2, but for the March-April mean (upper panel) and September-October mean conditions (lower panel). Note the double ITCZ configuration in the Pacific, symmetric about the equator in March-April, in contrast to the prominent single ITCZ near 10°N in September. A strongly contrasting structure is also observed in the Atlantic sector, with the ITCZ displaced farther north in September-October. Rainfall rates in excess of 20 cm per month are colored orange-yellow.

midlatitude storms weaken and their tracks migrate poleward. Heavy rainfall starts over southern Mexico and quickly spreads northward along the western slopes of the Sierra Madre Occidental into Arizona and New Mexico by early July. In July and August, a “monsoon high” becomes established in the upper troposphere near the U.S.-Mexican border (Fig. 8). This feature is analogous to the Tibetan anticyclone over Asia. The region of enhanced upper-tropospheric divergence in the vicinity and to the south of the upper-tropospheric high coincides with enhanced upper-tropospheric easterlies or weaker westerlies and enhanced Mexican monsoon rainfall. In contrast, the flow is more convergent and rainfall diminishes in the increasingly anticyclonic westerly flow to the north and east of the monsoon high. Upper-level divergence and precipitation apparently increase in the vicinity of the “induced” trough over the eastern U.S. The system decays in September and October, but generally at a slower pace than during development. The ridge over the western U.S. weakens, as the monsoon high and Mexican monsoon precipitation retreat southward into the deep tropics.

The monsoon system develops in the Southern Hemisphere during the austral spring with a rapid southward shift of the region of intense convection from northwestern South America to the highland region of the central Andes (Altiplano) and to the southern Amazon basin. Transient synoptic systems at higher latitudes, in contrast to the Northern Hemisphere monsoon, modulate the southward shift in convection. In particular, cold fronts enter northern Argentina and

southern Brazil, frequently accompanied by enhanced deep convection over western and southern Amazonia and by increased southward moisture flux from lower latitudes. A strong low-level jet that occurs to the east of the Andes, which is not as well documented as its counterpart over the Great Plains of North America, can enhance this moisture flux. As the austral spring progresses, and the SACZ develops, precipitation increases over the Brazilian altiplano and southeast Brazil, and the anticyclone over the central Andes becomes established. The monsoon decays in late summer as convection shifts gradually northward toward the equator. By April and May, the low-level southward flow of moisture from western Amazonia weakens, as more frequent incursions of drier and cooler air from the

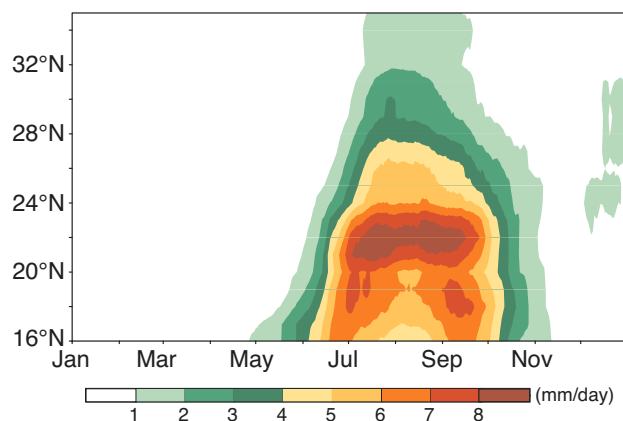
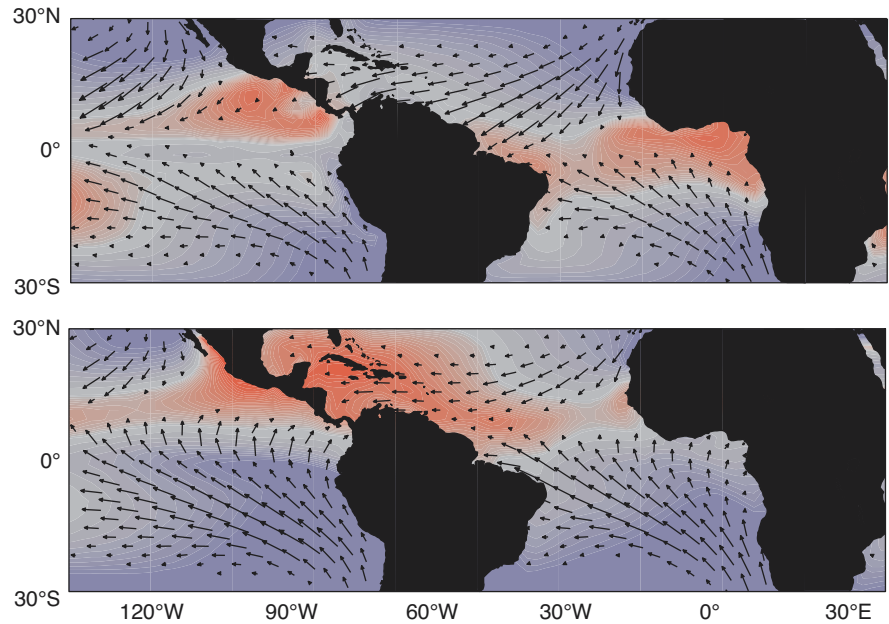


Figure 10. Time-latitude sections of the mean annual cycle of precipitation (1961-1990). Data are averaged zonally over west coast land points at each latitude.



Figure 11. As in Fig. 3, but for the March-April (upper panel) and September-October (lower panel) mean conditions. The warm pool to the north of the equator is present year round. The largest seasonal contrasts are observed along the northern flank of the equatorial cold tongue. September-October is the time of strongest meridional temperature contrast across the equator.



midlatitudes begin to occur over the interior of subtropical South America. The narrow midlatitude section of the continent is exposed to strong westerly flow and seasonal variations that are not as pronounced as those over North America at the same latitudes.

The temperature and humidity patterns of the lower troposphere are closely related to climatological precipitation patterns. These patterns are determined over land by both the advection of air from the ocean, depending on near surface winds and sea surface temperature, and on the seasonally and diurnally varying fluxes of water vapor and energy between the land and atmosphere. The water vapor and energy fluxes over the Andes have an observable effect on midtropospheric temperature during the pre-monsoon period and may affect subsequent evolution of the monsoon. Surface sensible heating warms the midtroposphere over the central Andes during the pre-monsoon period and after the monsoon onset. Strong latent heat release accompanies the deep convection over the subtropical highlands and the southern portion of the Amazon basin, changing the thermal structure of the troposphere, with this warm air eventually covering a large area, from the eastern south Pacific to the western south Atlantic.

The seasonal march also contains some surprises such as the large differences between the March-April versus the September-October climates over the tropical oceans adjacent to the Americas (Fig. 9), a single March-May rainy season in Northeast Brazil and coastal Ecuador, and, in general, the much less pronounced

rainy season during the March-May period in the eastern Amazon than in the western Amazon. A double peak structure (wet-dry-wet) in the seasonal march of precipitation is found over the west coasts of Mexico and Central America (Fig. 10). This dry period along the west coast of Mexico and Central America is called the midsummer drought. The variation in climatological precipitation is accompanied by a double peak structure in the diurnal temperature range (i.e., small-large-small) equatorward of the Tropic of Cancer. The physical and dynamical mechanisms responsible for the climatological midsummer drought are not well understood.

At the time of heaviest rainfall in the equatorial belt, March-April, a double ITCZ, symmetric about the equator, is often observed in the eastern Pacific, and the Atlantic ITCZ is on the equator. In contrast, September-October is the time of strongest equatorial asymmetry, the strongest northward cross equatorial flow, the northernmost position of the ITCZ, and the maximum extent of the Southern Hemisphere stratus cloud decks. Related to this annual march in the atmosphere is a strong modulation in the intensity of the equatorial cold tongues (Fig. 11). For example, the water temperatures near the Galapagos Islands range from 22°C in September to near 27°C in March. These sea surface temperature changes are remarkably regular from year to year in both the eastern Pacific and the Atlantic, even in the presence of El Niño, as demonstrated in Fig. 12. Why should such an oscillation exist at all? Why is the annual cycle so much stronger than

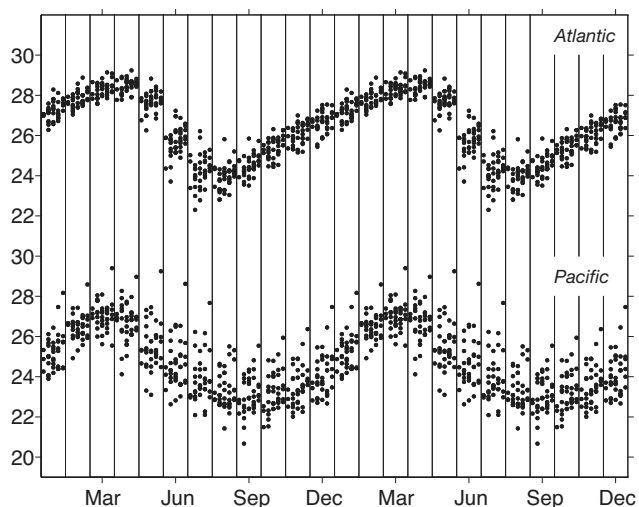


Figure 12. Scatter plot of monthly mean sea surface temperature ($^{\circ}\text{C}$) in the equatorial cold tongue regions of the Atlantic and Pacific for individual years/months, grouped by calendar month. The dots for each calendar month are staggered along the x axis to make them more visible, and the calendar year is repeated. Note the high degree of reproducibility of the seasonal march, particularly in the Atlantic, where El Niño exerts only a modest influence.

the semiannual cycle in the equatorial belt? To what extent is the seasonal march of rainfall, temperature, wind, and ocean currents in the cold tongue/ITCZ complex linked to the American and west African monsoons? The oceanic seasonal march near the equator does not follow any simple model for the oceanic response to atmospheric forcing: cold sea surface temperatures are present typically nine months of the year, with the warming confined to a period of less than three months ending in March; the usual westward surface current reverses from April through June even though the wind continues to blow from the east; and the eastward flow in the subsurface equatorial undercurrent is a maximum in May-June, following the period of weakest surface easterly wind stress. It is notable that the maximum sea surface temperature in March precedes the onset of the period of eastward flow, which advects warm water eastward. The notion that a reduction in easterly wind stress leads to reduced upwelling and so to a deeper thermocline and warmer sea surface temperature does not appear to be applicable to the seasonal march: the seasonal variations in thermocline depth and sea surface temperature (Fig. 13) do not exhibit the well-defined inverse relation characteristic of the ENSO cycle. The processes responsible for the sea surface temperature variations in the seasonal march and the ENSO cycle may be quite different.

Over the tropical eastern Pacific and Atlantic the seasonal march is more pronounced and more regular from year to year in the meridional wind stress than in the zonal wind stress because the former is more directly tied to the seasonal march of the monsoon convection over Central America and West Africa. Seasonal variations in the meridional wind stress influence the seasonal march in surface temperatures on or near the equator in several ways: wind speed affects the net sensible and latent heat flux at the air-sea interface and the amount of wind-induced mixing and entrainment in the mixed layer; wind stress curl can induce upwelling or downwelling; meridional stress can force meridional flow and change the rate of upwelling and the meridional temperature advection, etc. What is the relative importance of these processes in the seasonal march of sea surface temperature? How does the modulation of the strength of the cold tongues contribute to the absence of a rainy season at the time of the September equinox over much of equatorial South America? Does the seasonal march in the latitude of the ITCZs contribute to the greater southward displacement of the jet stream over the United States in springtime than in autumn and to the consequent heavier rainfall and a higher frequency of occurrence of severe thunderstorms to the east of the Rockies in springtime? North-south thermal contrasts and the related circulation cells in the atmosphere and ocean may be instrumental in producing the distinctive features of the seasonal march in

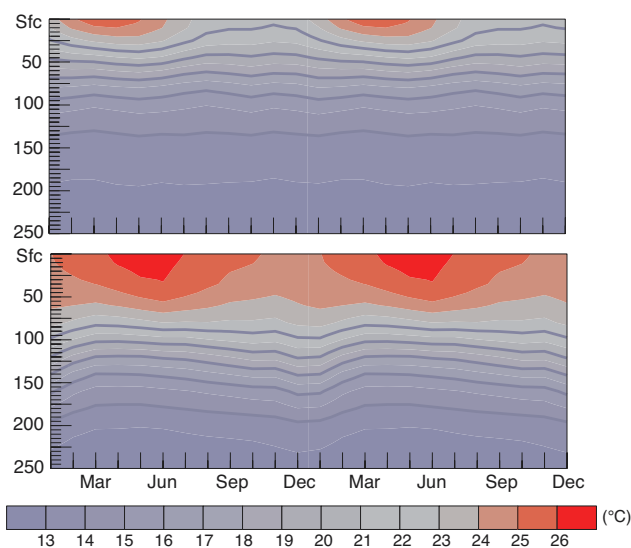


Figure 13. Depth-time sections of climatological mean temperature on the equator at 110°W (upper panel) and 140°W (lower panel) showing how the seasonal march tends to be much stronger near the surface than near the thermocline.

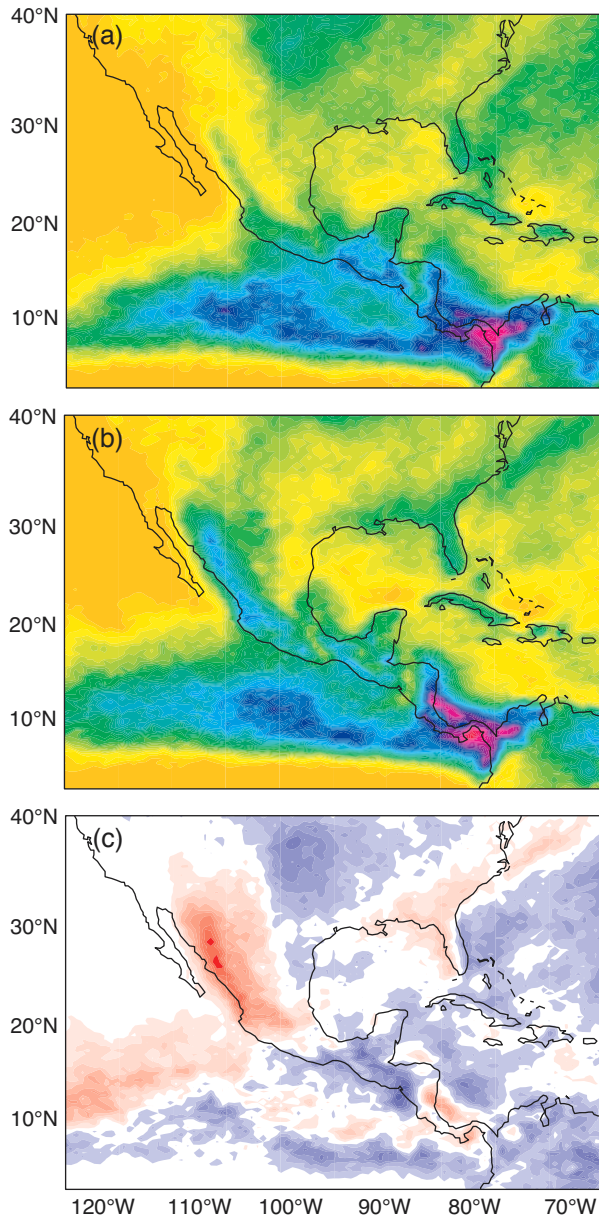


Figure 14. Frequency of cloud occurrence with tops colder than -38°C as revealed by high-resolution satellite imagery for the years 1990-1993. (a) June, (b) July, (c) the difference of July minus June. In most years, the northward shift of the rainfall in northwestern Mexico and Arizona occurs rather abruptly around July 1. Despite this shift, the same distinctive signature of the orography and coastal geometry is evident during both months over much of Central America.

the Pan American region, and they may account for some of the interannual variability as well.

Another intriguing feature of the seasonal march over the Americas is the abrupt onset of the summer monsoon from June to early July over much of northwestern Mexico and the southwestern United States, as

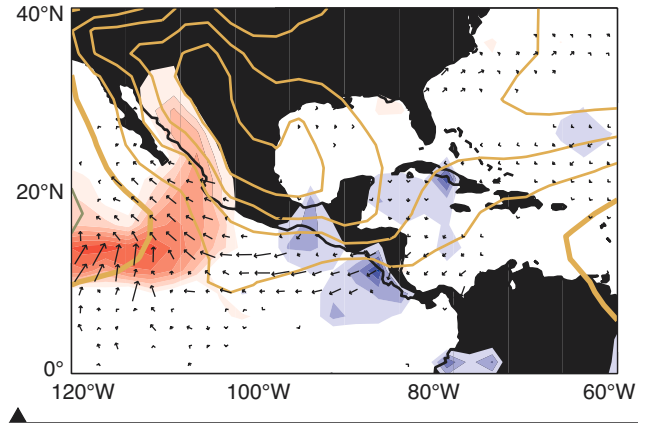


Figure 15. July minus June differences in surface winds (arrows), sea-level pressure (gold contours denote pressure increases; zero contour thickened), and rainfall (red denotes increases and blue decreases). The freshening of the trades over much of Central America is related to the rise in sea-level pressure over Mexico. The prevailing northwesterly winds along the west coast of Mexico weaken, allowing surges of moist southerly flow to penetrate into the Gulf of California. The link between month-to-month changes in the continental monsoon and the ITCZ appears to be stronger in the microwave sounding unit imagery and rain gauge data shown here than in the infrared imagery shown in Fig. 14.

reflected in the frequency of occurrence of deep convective clouds (Fig. 14). Rainfall simultaneously decreases over the northern Rockies, the U.S. Great Plains, and parts of the Caribbean and Central America, and sea-level pressure over Mexico abruptly rises (Fig. 15). The increased pressure gradient across Central America is accompanied by a freshening of the northeast trades at some locations. The reversal of the surface winds over the Gulf of California from northwesterly to southeasterly is accompanied by an abrupt increase in low-level moisture. The magnitude, abruptness, and year-to-year regularity of this shift in rainfall and associated circulation patterns are quite remarkable, considering the small changes in solar heating from June to July.

How do land surface processes contribute to the seasonal march of Pan American climate? Soil moisture, snow cover, and vegetation control the exchange of energy between land and atmosphere and the partitioning between latent and sensible heat. Figure 16 shows the soil moisture and vegetation at the equinoxes. At lower elevations, soil moisture is typically larger in spring than in fall and decreases as the summer progresses. On the other hand, biological activity associated with vegetation typically peaks in summer and then declines in most regions as winter approaches. Snow cover advances and retreats rapidly from polar

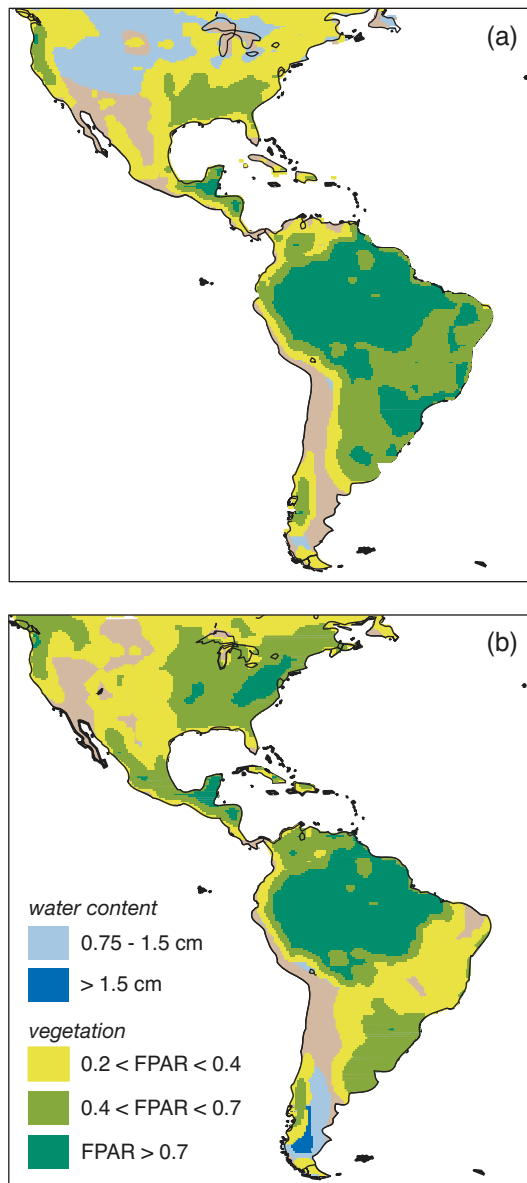


Figure 16. (a) March-April and (b) September-October mean soil moisture and vegetation (FPAR).

regions to middle latitudes over Canada and most of the United States during Northern Hemisphere fall and spring (Fig. 17). Representing the effects of these land “memory” processes in coupled ocean-atmosphere-land climate models is a major challenge.

1.3 What determines anomalies over North America?

Wintertime climate anomalies over North America are better understood than summer. The North American climate is affected on seasonal and longer time scales

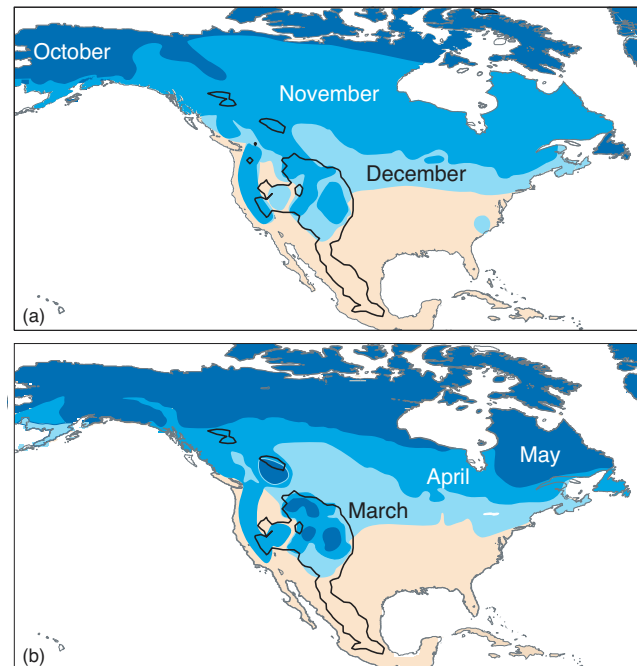


Figure 17. Seasonal march of the snow line at (a) the beginning and (b) end of Northern Hemisphere winter. Darker blues indicate cooler temperatures. Elevation contour is 1500 m.

by complex interactions between the Pacific and Atlantic oceans, the North American landmass, and the atmosphere. The El Niño/Southern Oscillation phenomenon (Section 1.6) exerts a strong influence on U.S. precipitation and surface temperature. The record El Niño event of 1997-1998 brought extreme rainfall and flooding to California in February 1998, features that were successfully predicted by atmospheric general circulation models with prescribed sea surface temperature taken from the coupled ocean-atmosphere model output one to two seasons in advance.

The links between tropical sea surface temperature anomalies and extratropical climate anomalies are not as pronounced during summer as winter. The extraordinarily wet and humid 1983 summer in southern California and Arizona may have been an aftermath of the 1982-1983 ENSO warm episode. During summer 1983, an unusual number of Pacific hurricanes tracked northward into the Gulf of California. The abrupt resurgence of the eastern equatorial Pacific cold tongue in early 1988, while sea surface temperatures to the north of the ITCZ remained above normal, might have served to draw the ITCZ northward, inducing an extratropical response and possibly contributing to the drought over the central United States during April and May of that year. The latter event is one of several episodes in



which patterns of precipitation anomalies have been simulated, with some degree of success, in forecast integrations out to a season in advance with prescribed tropical sea surface temperature anomalies.

The North American monsoon system, which affects much of Mexico and the southwestern United States, draws moisture from both the Pacific and the Gulf of Mexico. The time of onset and strength of the upper-level monsoon ridge over the southwestern U.S. during summer may influence major drought and flood episodes in the midwestern U.S. The climatological onset of summer rains over northern Mexico and Arizona around July 1 coincides with a decrease of rainfall over the Great Plains and an increase on the east coast (Fig. 18). The midwestern floods in July 1993 coincided with a delayed onset of the monsoon rains in Arizona. Interannual fluctuations in the onset date of the monsoon in the southwestern United States appear to be correlated with fluctuations in the intensity of summer rainfall in this region such that early monsoons tend to be very wet and late monsoons tend to be somewhat dry. Wet (dry) monsoons in the Southwest often follow winters characterized by dry (wet) conditions in the Southwest and wet (dry) conditions in the Pacific Northwest. Interannual variability of the summer monsoon in the American Southwest also appears to be modulated by decadal climate fluctuations in the North Pacific.

The low-level jet over the Great Plains, which transports moisture from the Gulf of Mexico, is linked to

the strength of the “Bermuda high,” which is possibly influenced by the Atlantic sea surface temperature. Little has been established empirically regarding associations between Atlantic sea surface temperature and North American climate. Anomalous soil moisture or snow cover early in the warm season, related to conditions during the previous winter, may influence subsequent hydrological and biological conditions through much of the growing season.

1.4 What determines anomalies over South America?

Climate anomalies over South America are regional manifestations of hemispheric scale climate variations. Summer rains are largest over the tropical continent and extend into the Atlantic Ocean in a northwest to southeast band (SACZ). Climate anomalies often appear as modulations of this convection band over tropical and subtropical latitudes. Persistent wet and dry conditions over tropical and subtropical eastern South America during summer appear as a dipole pattern of rainfall anomalies, with one center over southeastern Brazil in the vicinity of the SACZ and another center over southern Brazil, Uruguay, and northeastern Argentina. This seesaw pattern reflects changes in the position and intensity of the SACZ on intraseasonal and interannual time scales. Enhancement of the SACZ coincides with suppression of convection over the Inter-American Seas (Gulf of Mexico and the Caribbean Sea) and the ITCZ over the north Atlantic.

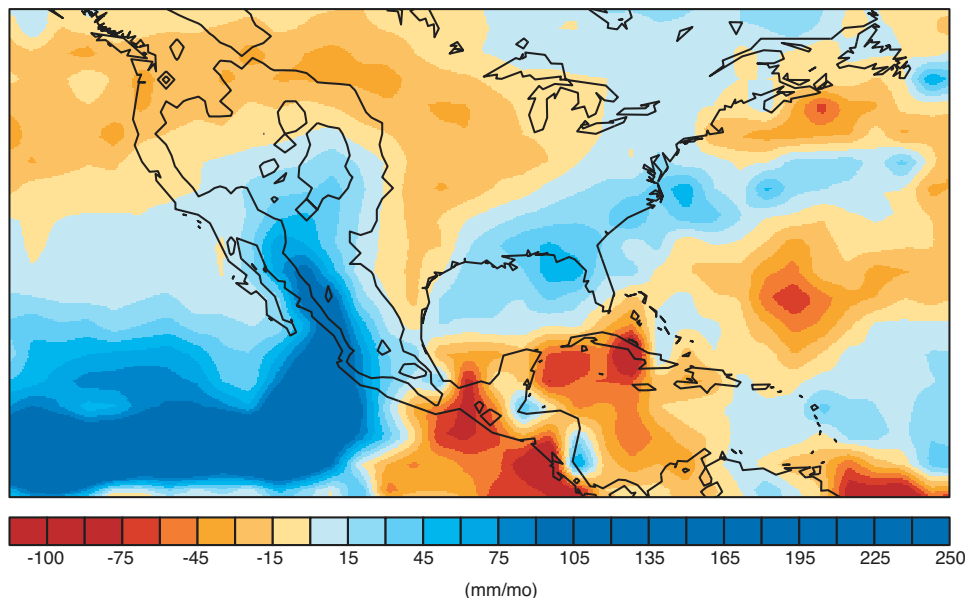


Figure 18. Climatological mean July minus June precipitation.

An example of how hemispheric scale climate anomalies influence the South American continent may be seen in the long-term trends over the middle and high latitudes of the Southern Hemisphere. A reduction of sea-level pressure over Antarctica and increased pressure over the three midlatitude ocean basins has been documented in decadal time scales. This trend influences the Atlantic moisture flux into South America, consistent with precipitation increases observed



over southern South America during the last three decades. There is also evidence of interhemispheric teleconnections between the North Atlantic and South America. For example, the positive phase of the North Atlantic Oscillation, which is associated with warm surface temperature over North America, is correlated with increased precipitation over northern and central South America in summer.

The distinctive shape of the South American land mass may determine some aspects of the climate anomalies. Unlike North America, which lies mostly in midlatitudes, South America is a tropical continent with a narrow conical extension to the south and the steep Andes cordillera to the west. Links have been established between rainy afternoon episodes in the central Andes with a weakened low-level jet on the eastern slopes resulting in tropical moisture flux reaching the central Andes highlands. There is also evidence from modeling and data assimilation studies that the enhancement of South American tropical convection may be coupled to descending motion over the stratus deck off the west coast of South America. Low-level flow east of the Andes is weakened with enhanced tropical convection as a geostrophic response to the low-level low pressure center that develops under the SACZ. The opposite phase of this seesaw pattern exhibits a weakened SACZ, strong low-level northerly flow east of the Andes, and a resulting influx of moisture from the tropics into the subtropical plains of southern Brazil and central Argentina. The central Andes are then closed to tropical moisture and dry conditions prevail. This situation is similar to conditions over North America, and an analogy can be drawn between the North-American Great Plains and the subtropical plains of South America. Both regions have mountains to the west that are dry when the plains are wet and vice-versa.

1.5 The land surface role

The land surface consists of the soil, vegetation, surface water, and ice in many forms. Soil and vegetation are altered by their interactions with the atmosphere and by the activity of people and other organisms. Vegetation regulates fluxes of water from the soil and the distribution and application of solar radiation, thus altering surface temperature. It responds not only to moisture availability but also to the availability of light, nutrients, and atmospheric stresses (e.g., heat, cold, aridity). People alter the landscape through agriculture and land use practices. Hence, the land component of the

climate system involves not only geophysics but also biology, chemistry, and sociology, with these latter factors increasing in importance on longer time scales.

Because of the rapid exchange of water between the soil and the atmosphere, the sum of the water in soil and in the atmosphere changes more slowly than either of these water reservoirs individually, hence imposing a long-term memory on the coupled land-atmosphere system. Land surface memory depends on how soil stores water, how vegetation moves it into the atmosphere, and how precipitation transports it back to the land surface. Increased evapotranspiration from wetter soil moistens the lower atmosphere and increases latent heat content and moist static energy, all of which can contribute to increased rainfall locally and downwind. Dry soil conditions have the opposite effect. The U.S. drought of 1988 provides an example of remotely forced circulation anomalies amplified by local land-atmosphere feedbacks. The extent and severity of the drought depended on both ocean temperature anomalies and soil moisture anomalies. Soil moisture conditions that were upstream of the 1993 floods over the central U.S. similarly influenced the outcome.

Water losses to the ocean and overlying atmosphere weaken land-atmosphere feedbacks most during the cold season. However, winter snowpack stores surface water seasonally and may modify North American summer precipitation and the response of the monsoon system to ENSO, resulting in a seasonal variation in the association between El Niño fluctuations and precipitation over the southwestern U.S. Abundant spring snow may lead to deficient summer rain, and sparse snow to heavier rain.

Seasonal green-up or leaf-out, with increases in leaf and vegetation cover and decreases in albedo, is rapidly initiated by the onset of the warm season (at higher latitudes) or the wet season (at lower latitudes). It can have noticeable impact on observable quantities such as near surface air temperature. The magnitude of the changes in land surface parameters during the seasonal green-up is generally much larger and more rapid than those associated with land use or land cover change. Proper observational or dynamic representation could help improve predictability during transitional seasons.

Vegetation responds to interannual variations in climate and becomes a source of further climate variations through land-atmosphere feedbacks. Figure 19

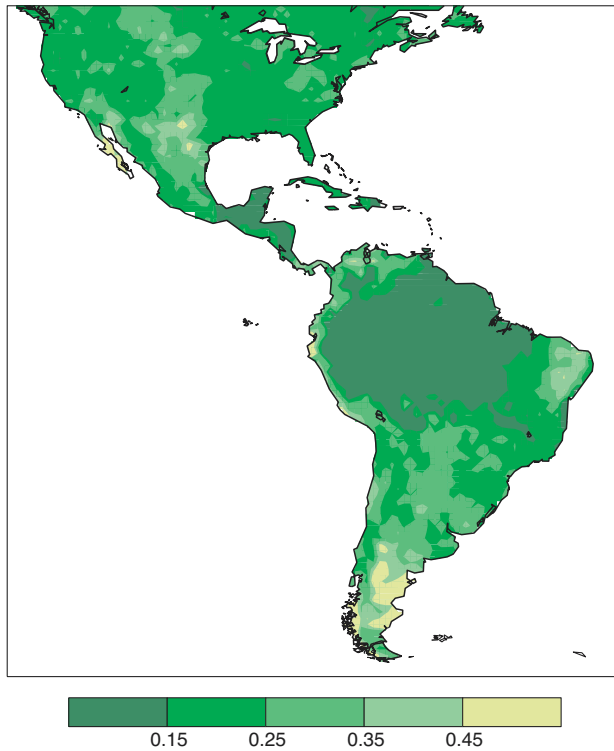


Figure 19. Interannual variability of leaf area index (LAI). The index is the ratio of the one half of the leaf area to the area of the ground surface.

shows that monthly anomalies of leaf area index (LAI) are most significant over the Great Plains (particularly toward the south), over the region of the North American monsoon, the Caribbean coast of South America, the Nordeste, from the Pampas to Patagonia, and along the western slopes of the Andes. Tropical forests change little except for trends associated with deforestation. Large swings in land surface characteristics can occur in regions of sparse vegetation and correspondingly impact evapotranspiration, providing long-term system memory. For example, one or more significant wet seasons in a semiarid region increases biomass productivity, and the added biomass provides fuel for fires (and a strong source of aerosols) in a subsequent dry year.

Changes in land use and land cover accrue over decades to centuries. Anthropogenic land use changes during the last century have been so widespread over North America that there is little land outside high latitudes that retains its natural vegetation cover. The rate of land use change in Central and South America is accelerating, especially in tropical forests and savannahs where logging, ranching, and farming are altering the landscape. These changes are likely supplemented by

land cover changes occurring in response to anthropogenic climate change. Recent assessments by the USGCRP suggest a mixed but wide-ranging set of climate changes that will invoke responses in both the natural distribution of biota and land use practices.

Linkage of the land surface to the atmospheric hydrological cycle promotes feedbacks involving radiation that may exacerbate anomalies; for example, a positive anomaly in shortwave radiation (perhaps due to reduced cloud cover) may increase surface temperatures and the Bowen ratio, hence decreasing humidity in the boundary layer and further suppressing cloudiness. Aerosols from dust, the smoke of natural and manmade fires, urban pollution, and natural forest emitters can alter the local and regional radiation balance and atmospheric chemistry in ways that are only beginning to be understood. Such effects may either enhance or diminish climate perturbations.

1.6 El Niño/Southern Oscillation

The aspects of the ENSO phenomenon relevant to the Pan American region are the processes that control the sea surface temperature and rainfall in the equatorial cold tongue/ITCZ region: the influence of ENSO on precipitation over the Americas, interactions between the seasonal march and the ENSO cycle, the effect of mean equatorial asymmetries on ENSO, the relation between warm episodes in the equatorial waveguide and El Niño events along the Ecuador and Peruvian coasts, teleconnections between ENSO and the Atlantic sector, and ENSO-like behavior in the Atlantic. Many of the more predictable regional climate anomalies associated with ENSO occur over the Americas, as summarized in Fig. 20. Most of these features can be explained on the basis of teleconnection patterns in the geopotential height and wind fields induced by differences in the distribution of deep convection over the Pacific sector during the warm and cold phases of the ENSO cycle.

The typical pattern of sea surface temperature anomalies associated with the ENSO cycle is shown in Fig. 21, together with the corresponding pattern of rainfall anomalies over the tropical Atlantic and Pacific. During warm episodes rainfall tends to be enhanced within the region of positive sea surface temperature anomalies, particularly along the outer margins of the equatorial dry zone (Figs. 1 and 2), and suppressed over much of the surrounding region. The enhancement or

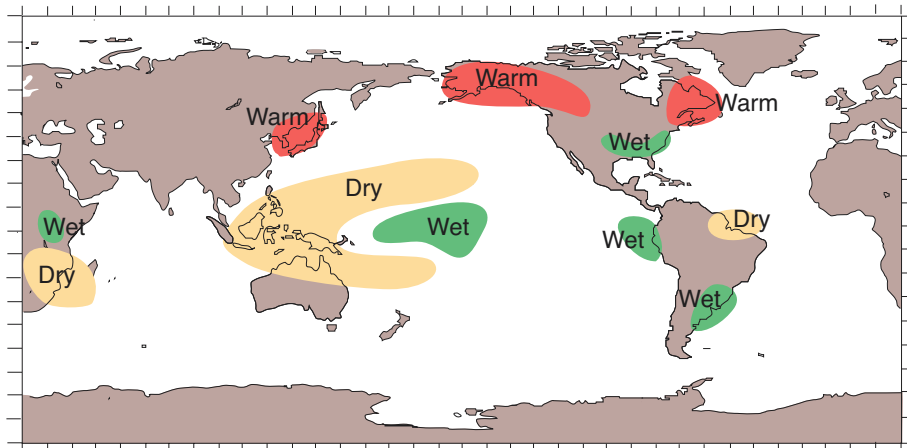
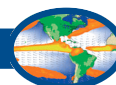


Figure 20. Summary of the major large-scale climate anomalies associated with the warm phase of the ENSO cycle during Northern Hemisphere winter.

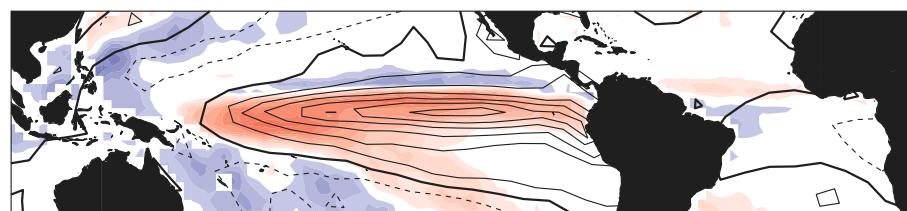


Figure 21. Sea surface temperature anomalies (contour interval 0.2°C) and ocean rainfall anomalies during a typical warm episode of the ENSO cycle. Enhanced rainfall, indicated by the red shading, is observed over the region of above-normal sea surface temperature, and reduced rainfall, indicated by the blue shading, is observed throughout much of the surrounding region and over the tropical Atlantic adjacent to Northeast Brazil.

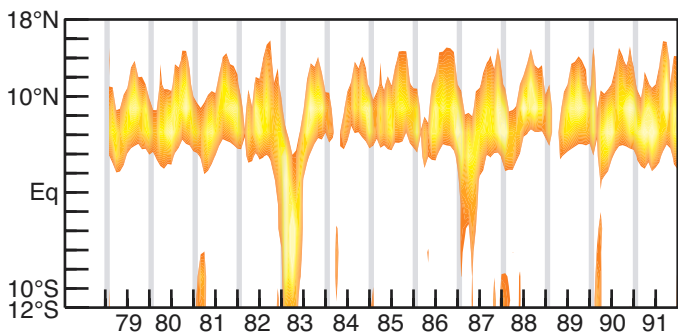


Figure 22. Time-latitude sections of the core of the heavy rainfall associated with the Pacific ITCZ, averaged over longitudes 180-110°W. Estimated rainfall amounts range from 20 cm per month for the orange up to ~50 cm per month for the yellow. Each year the ITCZ is closest to the equator from February through April. The rainy seasons of 1983 and 1987 fell within warm episodes of the ENSO cycle.

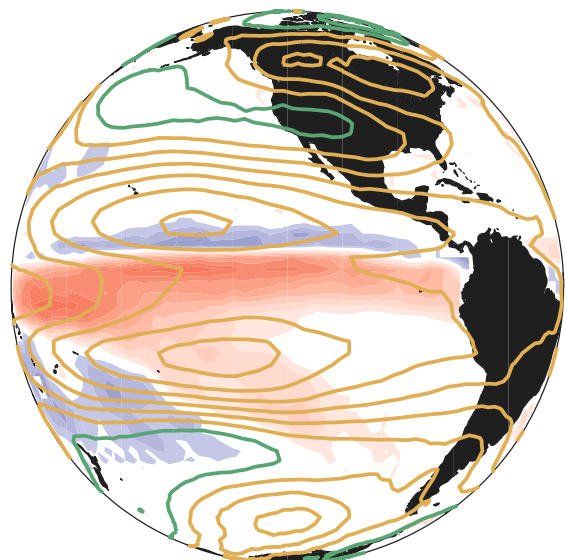


Figure 23. Anomalous rainfall observed during a typical warm episode of the ENSO cycle (colored shading repeated from Fig. 21) shown with the corresponding pattern of anomalies in mean tropospheric temperature (gold contour positive and green negative). The pair of temperature extrema straddling the equator in the eastern Pacific are warm anomalies, which correspond to anomalous anticyclonic gyres in the upper-tropospheric flow. These disturbances in the upper-level flow are responsible for the wide-ranging impacts of ENSO on the climate of the Americas.



suppression of rainfall tends to be most pronounced during the rainy season, as illustrated in Fig. 22. The ITCZ migrates southward toward the equator every year during the warm season (February-April), but penetrates deep into the equatorial zone only during warm episodes of the ENSO cycle.

The distribution of anomalous rainfall during a typical warm episode of the ENSO cycle is repeated in Fig. 23, this time superimposed on the corresponding anomalies in mean tropospheric temperature (a surrogate for the upper-tropospheric geopotential height field). The temperature pattern, which can be viewed as the planetary-scale response to the anomalies in the rainfall distribution, is characterized by a remarkable degree of equatorial symmetry. The pair of strong positive centers near 15° latitude, just east of the dateline, corresponds to the anticyclonic gyres in published studies based on the 200-mb wind field. The tight “packing” of the contours on the poleward flanks of these gyres is indicative of an enhanced meridional temperature gradient and a strengthening of the westerlies at the jet stream level, which favors an increased incidence of winter storms downstream over the southeastern United States (green patch in Fig. 20). These and other extratropical features such as the positive temperature anomalies over Canada (Figs. 20 and 23) were first noted by Sir Gilbert Walker over 60 years ago and they have been observed to recur during most of the warm episodes that have been recorded since that time.

The present generation of coupled models of the ENSO cycle has had success in predicting, out to several seasons in advance, the changes in amplitude and polarity of the typical (or “canonical” as it is sometimes called) pattern of sea surface temperature anomalies. In the simplest models, forecasts of an index of this pattern are then used as a basis for predicting the amplitude and polarity of the anomalous rainfall and circulation patterns in Figs. 20 and 23. Just as ENSO distorts the seasonal march in many areas of the world, rendering “forecasts” based on

climatology erroneous, so the departures from the canonical ENSO cycle that give each individual warm or cold episode its own peculiar character constitute a major source of error in current prediction models based on the canonical ENSO cycle. For example, the scientific community was caught off guard by the onset of the exceptionally strong 1982-1983 warm episode, which was preceded by a somewhat different sequence of events than any ENSO observed during the previous three decades. Indeed, there are times when anomalous ocean temperatures and winds in the equatorial Pacific bear so little resemblance to the “canonical” ENSO pattern that it is not even clear whether to classify them as “warm” or “cold.” Sea surface temperature anomalies in the tropical Atlantic tend to be rather weak, i.e., on the order of tenths of $^\circ\text{C}$, as opposed to values in excess of 1°C in the eastern Pacific. Within the Atlantic equatorial waveguide (near the node in the dipole pattern in Fig. 24) there is evidence of the signature of local ocean-atmosphere coupling analogous to that which occurs in association with ENSO, but the amplitudes are smaller. Less is known about the generation and maintenance of sea surface temperature anomalies off the equator.

The wintertime geopotential height field and sea surface temperature anomalies over the Caribbean and the tropical North Atlantic are linked to the Pacific North American (PNA) pattern. Evidently, when the PNA pattern is in positive polarity with a ridge over the Rockies, sea-level pressure tends to be above normal over the Sargasso Sea and the Gulf of Mexico, enhancing the pressure gradient that drives the tradewinds in this sector, leading to stronger surface winds and

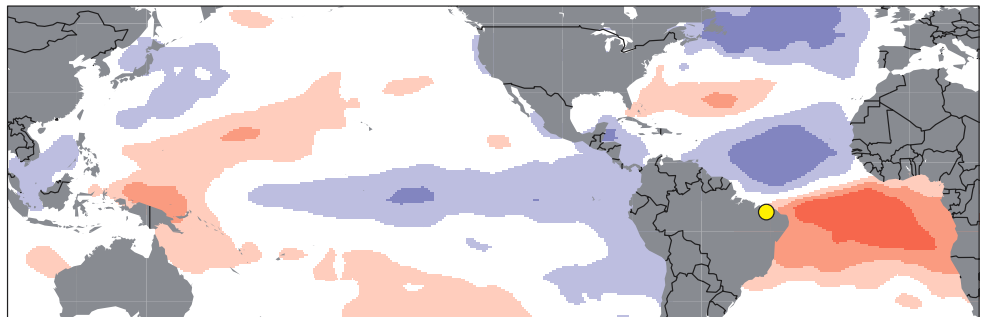
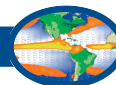


Figure 24. Correlation between average February-May precipitation in northeast Brazil (yellow dot) and sea surface temperature. Red (blue) shading indicates regions in which above-normal sea surface temperatures tend to be observed in conjunction with the above (below) normal rainfall in northeast Brazil. The strongest correlations are on the order of 0.7. Northeast Brazil rainfall tends to be more strongly correlated with Atlantic sea surface temperatures than with Pacific sea surface temperatures.



cooling of the sea surface. The North Atlantic tradewinds and the underlying sea surface temperature also exhibit interannual variability that appears to be independent of ENSO and are possibly linked to extratropical circulation anomalies over the North Atlantic sector. The persistence of sea surface temperature anomalies and their potential for feedback to the atmosphere in subsequent seasons depends on the depth to which they extend. Little is known about the subsurface structure of the off-equatorial ocean temperature anomalies in the tropical Atlantic.

ENSO also affects the climate of southeastern South America, including northeastern Argentina, Uruguay, and southern Brazil. Precipitation anomalies are consistently positive from November of an ENSO warm event through February of the following year and negative from July through December of a cold event year. There is some evidence that the ENSO connection between southeastern South America and the tropical Pacific is established through a wave train that extends from the tropical Pacific to South America. This wave train is called the Pacific South American (PSA) pattern, by analogy to the PNA teleconnection pattern over North America. The PSA has an equivalent barotropic structure and is excited by atmospheric convection over the tropical Pacific. The PSA is modulated by seasonal changes in the basic state flow that undergoes quasi-biennial changes not seen in the Northern Hemisphere.

1.7 Cold tongue/ITCZ complexes

With the exception of a few isolated regions of highly localized orographic forcing, the eastern Pacific ITCZ is responsible for the heaviest annual mean rainfall observed anywhere on Earth. The ITCZ appears as a continuous band of precipitation and surface convergence in monthly averaged maps, but is in fact made up of transient mesoscale and synoptic scale weather disturbances that obscure the ITCZ structure at an instant in time. Much of the rain falls from clouds whose tops do not show up as cold in infrared imagery as those associated with convection over and near the tropical land masses or over the “warm pool” region of the western Pacific. This is reminiscent of one of the major findings of the Global Atmospheric Research Program’s (GARP) Global Atlantic Tropical Experiment (GATE) 25 years ago. Vertical profiles of velocity and latent heat release in synoptic-scale disturbances in the Atlantic ITCZ region reach peak values 2–3 km above sea level, as compared to 5–10 km

in disturbances over the “warm pool” region of the tropical western Pacific (Fig. 25). Strong boundary-layer convergence evidently plays a critical role in organizing and maintaining the shallow but persistent convection in the ITCZs. Operational numerical weather prediction models and climate models have had difficulty in simulating the intensity of the ITCZ rainfall and the diversity of the convective heating profiles observed in different parts of the tropics. Existing model parameterizations of radiative transfer in clouds, cloud microphysics, and convection will need to be reconsidered in light of this problem.

In the season of coldest temperatures, the equatorial cold tongue is characterized by pronounced divergence in the surface wind field just north of the equator and weaker convergence in a band just south of it (Fig. 26). The ITCZ to the north of the equator appears as an intense and narrow band extending from near the coast of Central America to the central Pacific. The position and intensity of the divergent and convergent bands associated with the cold tongue/ITCZ complex are not simulated well in current operational prediction models. The reasons for these discrepancies are not well understood. The difficulty may be systematic errors in the simulated convective and radiative heating profiles or the inability of the

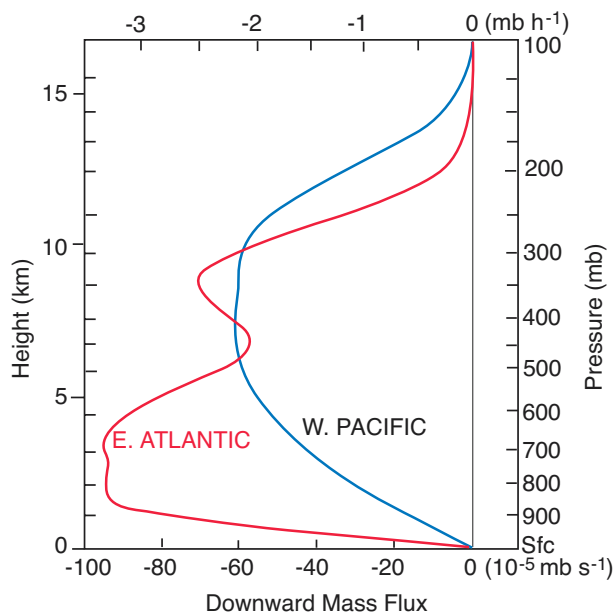


Figure 25. Contrasting vertical mass flux profiles in disturbed regions of the ITCZ in the eastern Atlantic and the “warm core” region of the western Pacific. In the ITCZ the low-level convergence (indicated by the large negative vertical derivative) is concentrated within the lowest 1.5 km, whereas in the western Pacific it is much weaker and extends all the way up to 5 km.

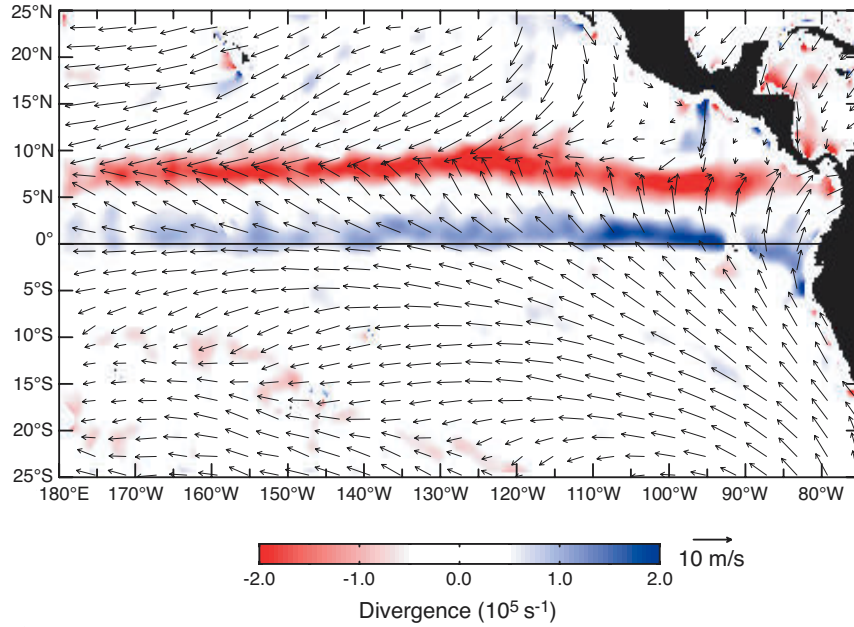
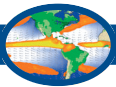


Figure 26. NASA QuikSCAT scatterometer 10-m vector wind averaged for November 1999 and the corresponding divergence field. Red and blue denote convergence and divergence, respectively.

models to properly simulate the mesoscale and synoptic scale weather disturbances that form the time-averaged ITCZ. In addition, the equatorial atmospheric boundary layer in the Atlantic and eastern Pacific, north of the equator, is characterized by strong and persistent backing of the wind with height from southerly at the surface to easterly at the top of the planetary boundary layer. Present difficulties in simulating the surface wind stress patterns over the eastern Pacific may be due in part to the inability of climate models to simulate the complex vertical structure of the atmospheric boundary layer in the cross-equatorial ITCZ inflow.

During the colder part of the year, vigorous tropical instability waves are frequently observed in the ocean along the sea surface temperature front to the north of the cold tongue in the eastern Pacific (clearly visible in the satellite imagery

shown in Fig. 27) and less frequently to the north of the Atlantic Ocean cold tongue. Similar oceanic disturbances can be seen along the southern edge of the Pacific cold tongue in Fig. 27. The Pacific Ocean disturbances appear to transport significant amounts of heat and momentum in the upper ocean. In the extreme eastern Pacific the northern edge of the equatorial cold tongue is often abrupt. Immediately to the north of this “equatorial front” is a region of strong air mass modification, where northward-moving air that has just crossed the equatorial cold tongue flows over much warmer surface waters. This transition is marked by an abrupt increase in surface wind speed and a decrease in relative humidity; as the

boundary layer becomes unstable and drier, faster-moving air is mixed downward toward the surface. Stratocumulus clouds form, analogous to those that develop when continental air flows over the Gulf Stream during wintertime. The distortions of the sea surface temperature front by tropical instability waves can produce distinct signatures in the air-sea heat exchange, stratocumulus cloud patterns, and surface wind fields.

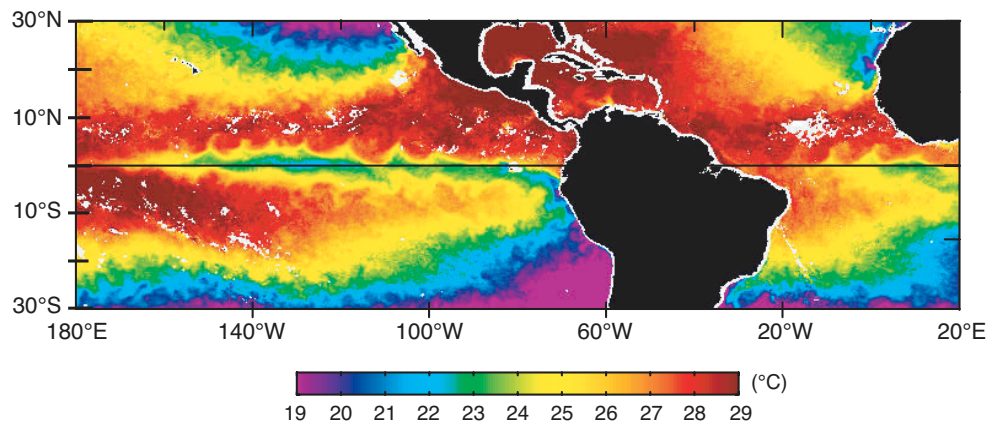


Figure 27. Three-day composite average maps of sea surface temperature for 11-13 July 1998, during a time of year when the equatorial Pacific and Atlantic are typically cool. The maps are based on measurements from a satellite microwave radiometer (TMI). White areas represent land or rain contamination. The sharp northern edge of the cold tongue is distorted by westward-propagating tropical instability waves, which originate in the ocean but produce a distinct signature in the fields of cloudiness and wind speed.



1.8 Stratus cloud decks

Oceanic boundary-layer cloud decks are extensive to the west of Peru and Chile in the Pacific, to the west of Angola in the Atlantic (Figs. 2 and 9), and off California and in the vicinity of the Azores. These cloud decks are highly reflective of solar radiation and hence produce both local and global cooling. The stratocumulus and cumulus rising into stratus, which make up these decks, are capped by strong inversions at heights between 500 and 1500 m. The stratus cloud decks are observed in regions of large-scale subsidence, and their variability is governed by the interplay among radiative transfer, boundary-layer turbulence, surface fluxes, cloud microphysics, and the thermodynamic conditions just above the inversion. They exhibit weekly, annual, and interannual variability in response to changes in sea surface temperature, winds, and the temperature of the overlying air. They also have a pronounced diurnal rhythm of nighttime thickening and daytime thinning due to the interplay between strong longwave cooling at cloud top and solar heating within the clouds. This diurnal variability is enhanced along the eastern edges of the cloud decks where land-sea differences affect the dynamics and thermodynamics of the boundary layer. Stratus decks are particularly variable along their western edge, where they transition from stratiform to tradewind cumulus as air flows equatorward in the trades. These transition zones have a potential for positive feedbacks between cloud amount and the underlying sea surface temperature: an increase in cloud amount tends to cool the ocean, and a cooler ocean leads to a shallower boundary layer, more stratiform clouds, and a larger fractional cloud amount. Drizzle is often observed in marine stratocumulus clouds and can have a substantial impact on their dynamics and macroscopic characteristics. The sensitivity of the drizzle processes to CCN aerosol characteristics couples these aerosols to the stability and extent of the stratus decks.

1.9 Subseasonal climate variability

U.S. CLIVAR research is also concerned with the frequency of occurrence of significant weather events such as hurricanes, flood, and drought over the course of a season. Subseasonal tropical rainfall variability is organized both on the smaller scales of local weather phenomena such as severe storms and sea breeze circulations as well as on the larger scales of intraseasonal phenomena. Intraseasonal fluctuations are clearly evi-

dent in the tropical planetary-scale sea-level pressure, wind, and precipitation fields.

Over the Pacific, the most prominent intraseasonal fluctuations are associated with the 30-60 day “Madden-Julian Oscillation” (MJO) that affects the atmospheric circulation throughout the global tropics and subtropics, and in particular, the wintertime jet stream and atmospheric circulation features over the north and south Pacific oceans and over western North America and southern South America. The MJO modulates storminess and temperatures over North and South America and hurricane activity in both the Pacific and Atlantic basins. It is characterized by an eastward progression of large regions of enhanced and suppressed tropical rainfall, usually first evident over the western Indian Ocean, and propagating over the very warm ocean waters of the western and central tropical Pacific. It generally becomes very nondescript as it moves over the cooler ocean waters of the eastern Pacific but reappears over the tropical Atlantic and Indian oceans.

Distinct patterns of lower- and upper-level atmospheric circulation anomalies are associated with the MJO. Madden-Julian Oscillation activity varies from year to year, with long periods of strong activity followed by periods in which the oscillation is weak or absent. Strong MJO activity is often observed during weak La Niña years or during ENSO-neutral years, while weak or absent MJO activity is typically associated with strong El Niño episodes.

The MJO impacts the wintertime atmospheric circulation over the North Pacific and western North America. It contributes to blocking activity (i.e., atmospheric circulation features that persist near the same location for several days or more) over the high latitudes of the North Pacific. The strongest impacts of intraseasonal variability on the U.S. occur during the winter months over the western states, which receive the bulk of its annual precipitation at this time. Storms are often accompanied by persistent atmospheric circulation features and last for several days or more. Of particular concern are extreme precipitation events linked to flooding. Extreme precipitation events can occur at all phases of the ENSO cycle, but the largest fraction of these events occurs during La Niña episodes and during ENSO-neutral winters.

During La Niña episodes much of the Pacific Northwest experiences increased storminess and pre-

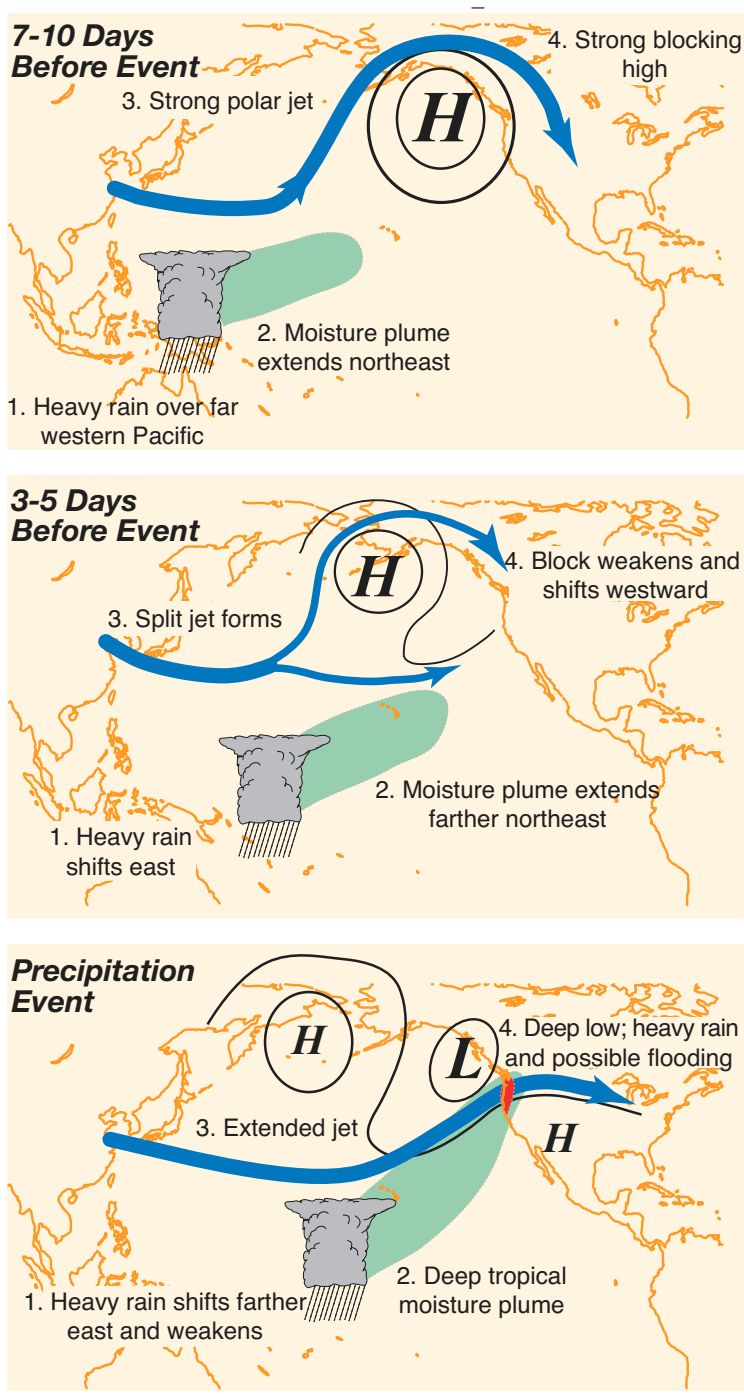


Figure 28. Typical wintertime weather anomalies preceding heavy precipitation events over the northwestern U.S.

precipitation, and more overall days with measurable precipitation. The risk of flooding in this region is greater during the weak La Niñas due to an increase in extreme precipitation events in the weaker episodes. In the tropical Pacific, winters with neutral-to-moderate cold episodes are often characterized by enhanced 30-60 day MJO activity and are a stronger link between the MJO

events and extreme west coast precipitation events (Fig. 28). A recent example is the winter of 1996-1997, which featured heavy flooding in California and in the Pacific Northwest (estimated damage costs of \$2-3 billion at the time of the event) and a very active MJO.

During the Northern Hemisphere summer months, low-frequency variability in the tropics is dominated by interannual variations associated with ENSO and by intraseasonal variations such as the MJO. The MJO can have a significant impact on regions that experience rainy seasons both during winter and summer seasons. For example, during the Northern Hemisphere summer, the MJO-related effects on the Indian summer monsoon are well documented. MJO-related effects on the North American summer monsoon also occur, though they are weaker. However, the relative influences of ENSO and the MJO on the summer precipitation regime of North America are not well understood. Statistical relationships between these modes and the frequency of occurrence of various kinds of significant weather events (e.g., floods, droughts, heat waves) are needed to obtain detailed information on the climatic signatures of these modes.

MJO-related impacts on the North American summer precipitation patterns are strongly linked to north-south adjustments of the precipitation pattern in the eastern tropical Pacific. A strong relationship between the leading mode of intraseasonal variability of the North American monsoon system, the MJO, and the points of origin of tropical cyclones is also present. Tropical cyclones occur throughout the Northern Hemisphere warm season (typically May-November) in both the Pacific and Atlantic basins, and there are periods of enhanced and suppressed activity within the season. There is evidence that the MJO modulates this activity (particularly for the strongest storms) by providing a large-scale environment that is favorable or unfavorable for development (Fig. 29). The strongest tropical cyclones tend to develop when the

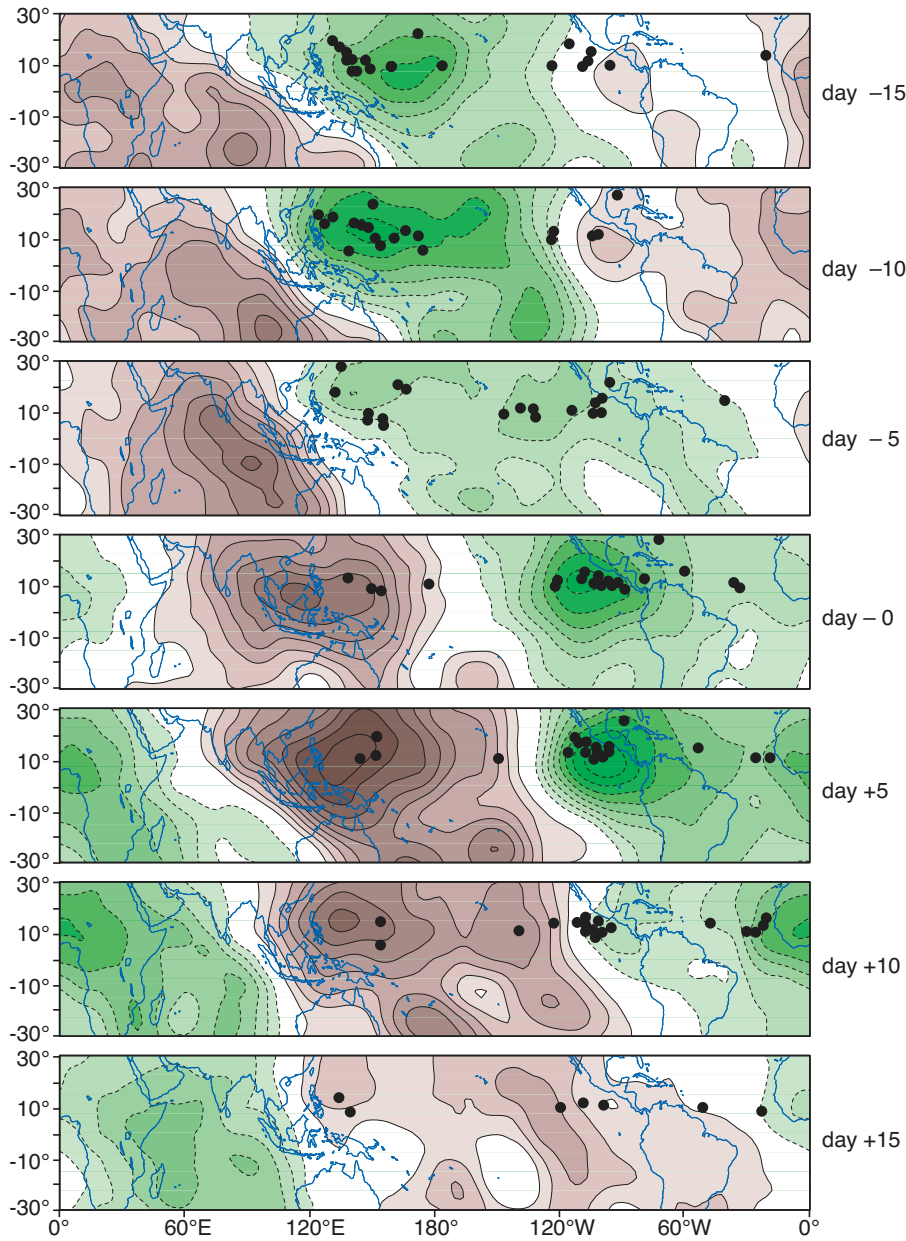


Figure 29. Composited evolution of 200 hPa velocity potential anomalies ($10^6 \text{ m}^2 \text{ s}^{-1}$) and points of origin of weather systems that developed into hurricanes or typhoons (\bullet). Brown indicates positive values while green indicates negative.

MJO favors enhanced precipitation. As the MJO progresses eastward, the favored region for tropical cyclone activity also shifts eastward from the western Pacific to the eastern Pacific and finally to the Atlantic basin. While this relationship appears robust, the MJO is one of many factors that contribute to the development of tropical cyclones. For example, it is well known that sea surface temperatures must be sufficiently warm and vertical wind shear must be sufficiently weak for tropical disturbances to form and persist.

America may therefore lead to improved prediction for the Northern Hemisphere. This is substantiated by evaluation of forecasts produced by the NCEP reanalysis model that shows that erroneous simulation of convection over tropical South America produces a southward shift of the subtropical jet over North America.

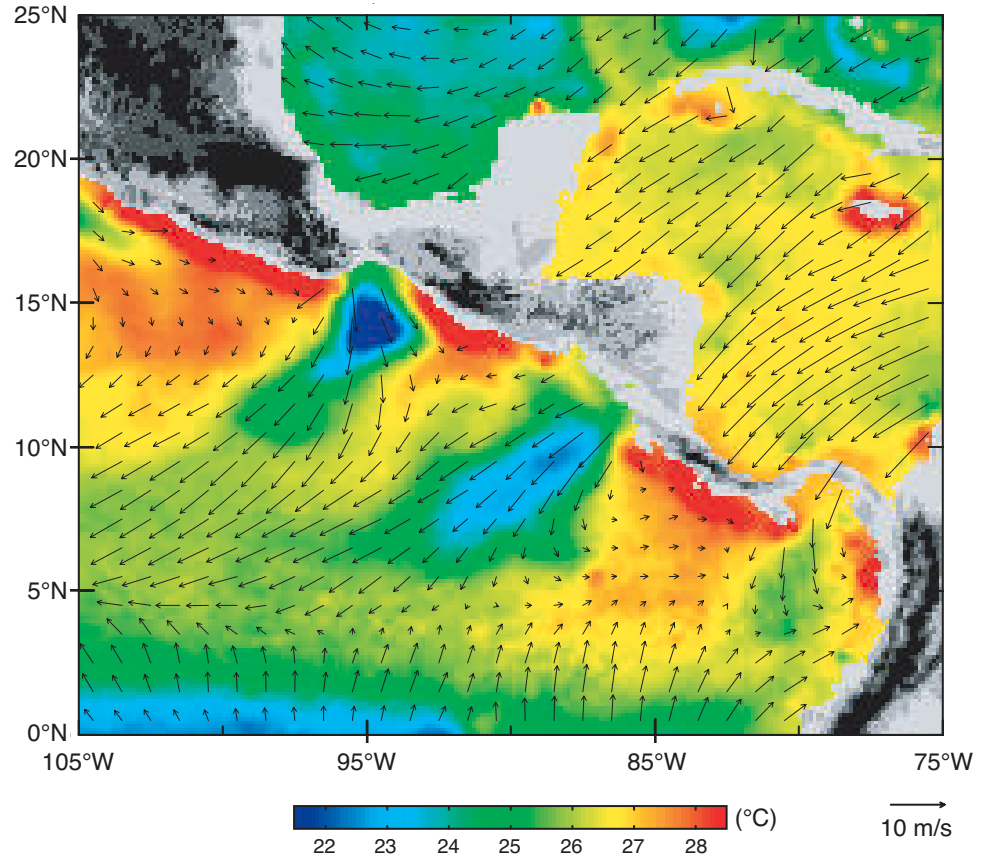
Over southwestern North America, mesoscale models have simulated many of the observed features of the North American monsoon, including southerly low-level flow over the Gulf of California, the di-

Over South America, circulation anomalies occur with 40-48 and 20-25 day periods during the austral summer. This modulation appears as a dipole of strong and weak convection as discussed in Section 1.4. The longest period is related to the MJO. The 200-hPa streamfunction exhibits a wave number 1 structure in the tropics and a wave train propagating downstream from the convective area in the tropical Pacific. The development of the SACZ-dipole pattern is also affected by the 20-25 day mode, which features meridional propagation of convection over South America from midlatitudes to the tropics. A wave train is found in the 200 hPa streamfunction extending from the central Pacific eastward to about 60°S and curving toward the northeast over South America.

When the SACZ is enhanced, these two modes become meridionally aligned over the continent and extend into the Inter-American Seas and the North Atlantic. This in turn may have an impact on (wintertime) precipitation over North America. Improvement of summer rainfall simulation over tropical South



Figure 30. Satellite measurements of surface wind and sea surface temperature averaged for January 2000. Dark shading over land indicates elevation in excess of 300 m. Strong offshore flow downstream of the gaps in the mountain ranges, with monthly mean wind speeds as high as 10 m/s, gives rise to local sea surface temperature minima, indicated by the blue shading and enhanced chlorophyll concentrations (Fig. 5).



urnal cycle of convection, and a low-level jet that develops over the northern end of the Gulf of California. One particularly important mesoscale feature that the models reproduce is a “gulf surge,” a low-level, northward surge of moist tropical air that often travels the entire length of the Gulf of California. Common characteristics of these disturbances include changes in surface weather (e.g., a rise in dewpoint temperature, a decrease in the diurnal temperature range, a windshift with an increased southerly wind component, and increased cloudiness and precipitation). Gulf surges appear to promote increased convective activity in northwestern Mexico and the southwestern U.S. and are related to the passage of Tropical Easterly Waves (TEWs) across western Mexico. One aspect of the connection between gulf surges and TEWs that has not been explored is the extent to which they might influence the interannual variability in the onset and intensity of the summer monsoon in this region. Sustained and enhanced in situ and satellite observations are required to examine the structure of the TEWs and Gulf of California surge events, their frequency of occurrence, and the temporal evolution of the moisture transport.

Wintertime cold air outbreaks along the eastern slopes of the Rockies often generate pressure surges that penetrate deep into Central America, creating strong pressure differences across the mountain ranges that form the Continental Divide. During such periods, strong to gale force winds blow across three pronounced gaps in the mountains: one across the Isthmus of Tehuantepec in southern Mexico, one across Lake Nicaragua, and one across Panama near the Canal Zone. Downstream of these gaps, tongues of strong winds extend 100 km or more into the Pacific, where they give rise to a succession of long-lived mesoscale eddies in the ocean circulation. The signature of the gap winds is also evident in the Coastal Zone Color Scanner imagery shown in Fig. 5 and in monthly mean wind fields (Fig. 30).

A remarkable amount of mesoscale structure is evident in the rainfall climatology (Fig. 14). The relationship of these features to the orography and coastal geometry becomes even more obvious when diurnal variations are taken into account (Fig. 31). These structures are related to terrain but in a manner that involves processes much more complex than orographically induced ascent and subsidence.

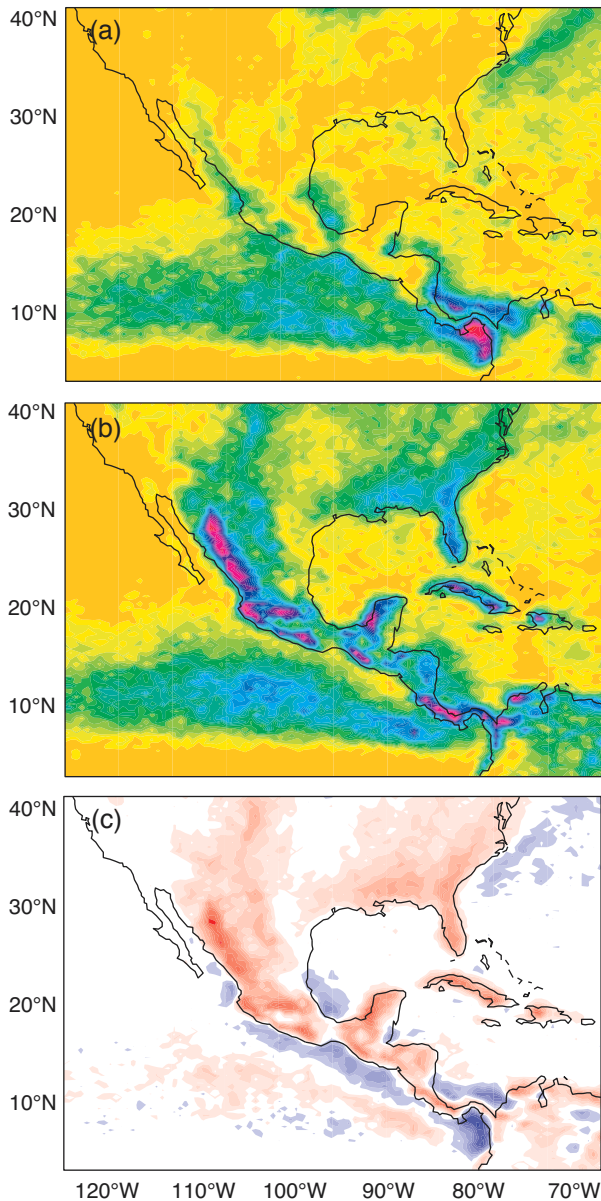


Figure 31. Frequency of deep convection as indicated by clouds with tops colder than -38°C at two different times of day during July. Around 5 AM local time (a) the highlands are cloud free and the offshore waters experience the highest frequency of convective clouds, whereas around 5 PM local time (b), convection tends to be concentrated over the high terrain and the compensating subsidence tends to keep offshore waters relatively cloud free. The difference between 5 PM minus 5 AM (c) shows even more clearly the complex influences of the mountain ranges and the shape of the coastline. It is interesting to note how at ~ 5 PM, the continental monsoon and the ITCZ are well separated, but at ~ 5 AM they appear to be nearly merged.

most strongly coupled to variations in continental rainfall in the tropical Atlantic and eastern Pacific oceans. It is continental, as opposed to national, because seasonal rainfall anomalies over the United States can only be understood in the context of the broader, continental scale pattern in which they are embedded.

The climate processes addressed by U.S. CLIVAR Pan American research are the same as those involved in assessing the effects of anthropogenic climate change. Anthropogenic changes in atmospheric gases and particulate composition modify the global energy balance. The practical consequences for people depend on how the climate system responds on regional scales to such global energy balance changes. Any regional response is likely to be tied to natural regional climate variations, and its modeling cannot be credible unless the significant natural climate variations are understood and included in the models addressing anthropogenic changes. Hence, U.S. CLIVAR research will increase the accuracy and credibility of regional projections of future anthropogenic climate change over the American continents.

Until recently, social and economic systems had usually been caught off guard by large seasonal climate anomalies and suffered losses or were unable to capitalize on favorable conditions. Better understanding of the sources of climate variability gained through focused research over the past decades has led to the development of routine seasonal climate prediction systems at several national and international centers in the Pan American Region such as the U.S. NCEP and the International Research Institute for Climate Prediction (IRI).

Figure 32 shows a selection of time series illustrating the large year-to-year variability of seasonal-mean rainfall. Features visible in these plots include the anomalous summer of 1993, marked by disastrous floods in the central U.S. and drought in the southeast,

2. Practical and Scientific Motivation for Pan American Climate Research

U.S. CLIVAR promotes an improved understanding of the processes that control the distribution of rainfall over the Americas and applies that knowledge to improve the models used for climate prediction on seasonal and longer time scales. More accurate and detailed information concerning the statistical probabilities of various rainfall scenarios are required for planning such activities as agriculture and providing water resources. The focus of Pan American research is regional, rather than global, because large-scale sea surface temperature variations are more clearly defined and

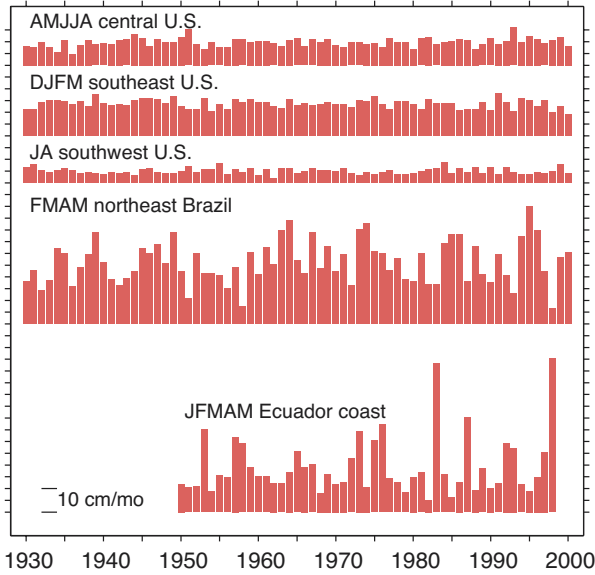
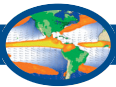


Figure 32. Time series of warm-season rainfall over selected regions: U.S. Great Plains; southeast U.S.; Arizona; Ceara, Brazil; and Guayaquil, Ecuador. Average months as indicated.

and the summers of 1988 and 1991 in which the farmers in the central U.S. suffered major drought-related crop losses. Longer time scale features, such as the legendary “dust bowl” epoch in the central U.S. in the 1930s, are also evident. In semiarid regions, such as parts of Arizona and northeast Brazil, the interannual variability tends to be even larger in relation to the seasonal-mean rainfall, rendering agriculture a high-risk venture.

Following the success of TOGA, government agencies in Peru (Lagos and Buizer 1992) and Brazil have been incorporating El Niño predictions into their ag-

	1987	1992	1993	1994
Grain production	15	82	31	170
Rainfall	70	70	41	105

Table 1. Grain production and growing season rainfall in the state of Ceara in northeast Brazil, for selected years, both expressed as percentages of the long-term mean.

ricultural planning. The ENSO phenomenon is the major source and best understood aspect of interannual global climate variability. Benefits of the forecasts are listed in Table 1, which shows grain production for a number of recent years in the state of Ceara in northeast Brazil and corresponding rainfall totals over the state, both expressed as percentages of normal. The moderately severe drought conditions that prevailed in 1987 drastically reduced grain production that year, but similar drought conditions in 1992, after the advent of climate prediction, only slightly reduced agricultural production. Even the much more severe drought of the following year had a less adverse impact on grain production than the 1987 drought.

Major ENSO warm events, such as the 1982-1983 and 1997-1998 events, present the best opportunity for assessing the range of impacts to be expected from climate variability. The impacts of coherent climate variability during major ENSO events stand out against the background of normal weather variability. A wide range of social and economic sectors were affected by the 1997-1998 El Niño (Fig. 33). These sectors included agriculture, energy, water resources, health, ecosystems, tourism, and social systems. Regionally they were fo-

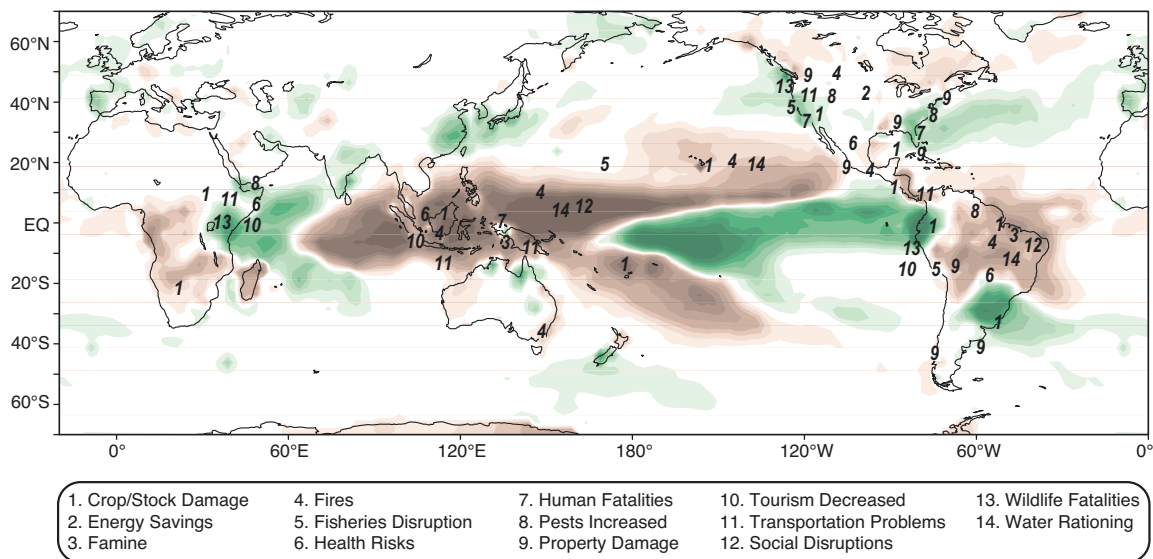


Figure 33. Nature of global El Niño impacts during 1997-1998. Brown indicates dry regions while green indicates wet.

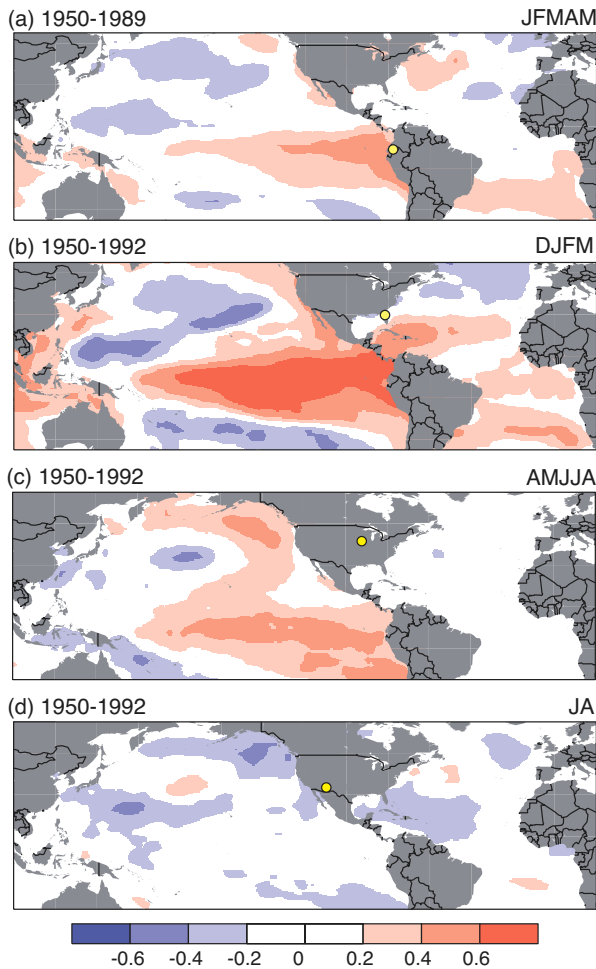


Figure 34. Simultaneous linear correlations between seasonal-mean rainfall in the indicated region (yellow dot) and Pacific and Atlantic sea surface temperature anomalies. Averaging months and periods of record as indicated. Precipitation time series used are shown in Fig. 32. See also Fig. 24.

cused in the global tropics/subtropics and in midlatitudes in the Americas. Seasonal forecasts for temperature and rainfall were available for the U.S., and some use of these was made for disaster mitigation and economic benefit. Mitigation actions were also taken in other countries with great success. A number of institutions make routine forecasts with lead times by using statistical and dynamical tools for SST variations in the tropical Pacific. NCEP and the IRI also make routine seasonal temperature and rainfall forecasts for continental areas.

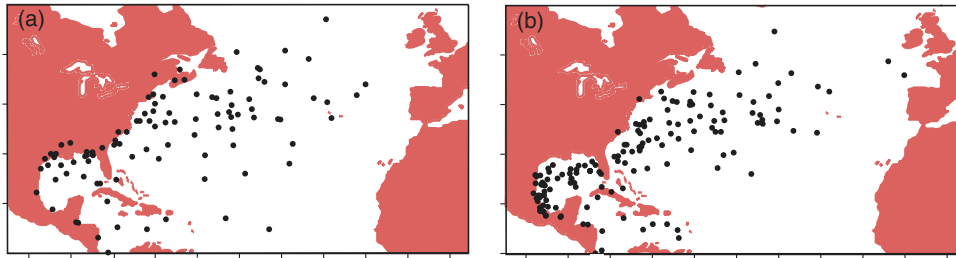
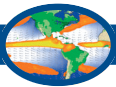
Empirical studies have identified a number of significant relationships between tropical sea surface temperature anomalies and concurrent or subsequent rainfall anomalies over the Americas (Figs. 24 and 34). Rainfall on the coastal plain of Ecuador and northern Peru is positively correlated with sea surface temperature in

the equatorial Pacific. The same distinctive “El Niño signature” is apparent with varying degrees of strength in several other correlation maps. Tropical Atlantic sea surface temperature signatures are also apparent in several of the patterns, particularly for February–May rainfall in northeast Brazil.

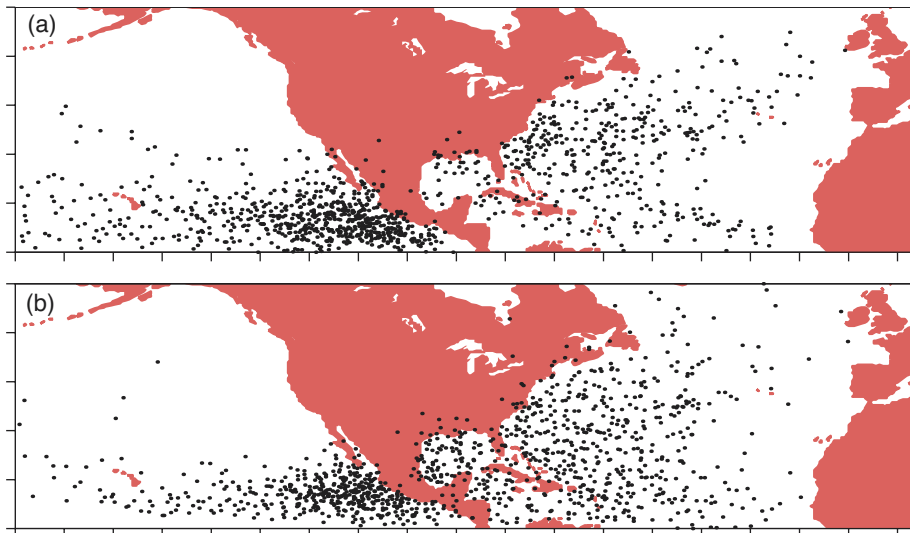
Significant spatial correlations do not alone constitute proof that sea surface temperature anomalies influence rainfall; inference of causality on the basis of empirical evidence alone is fraught with ambiguity. However, they suggest modeling experiments are required to establish causality. The effects of ENSO on rainfall in Ecuador, as well as in more remote regions such as the southeastern United States have in fact been verified by numerous experiments with atmospheric general circulation models (AGCMs), and the dynamical mechanisms that give rise to the remote response are reasonably well understood. Sea surface temperature anomalies in the tropical Atlantic have likewise been shown to influence northeast Brazil rainfall. The extratropical response to tropical sea surface temperature anomalies is strongest during the cold season. Hence, most AGCM investigations have been based on wintertime conditions.

Equatorial sea surface temperature anomalies associated with ENSO may influence warm-season rainfall over the Americas. Still the correlation pattern for summer rainfall over the U.S. Great Plains in Fig. 34 remains difficult to interpret. Are the North Pacific features in the sea surface temperature correlation pattern by the same atmospheric circulation anomalies that are responsible for the rainfall anomalies? Is the hint of an ENSO signature in the pattern indicative of a causal relationship? The answers to such questions must take into account the positive or negative feedbacks by the land surface in modulating the response. In addition, anomalies in soil moisture, vegetation characteristics, or changes in land use and land cover can act alone to alter climate. The soil moisture feedback to precipitation anomalies is generally positive and could potentially exacerbate extremes. The vegetation feedbacks may help to shift marginal zones from one climate regime to another. Such a bipolar mode may operate in sub-Saharan Africa, and large swings in climate may be the norm for western North America as well.

Statistics of significant weather events may be predictable a season or more in advance. The ENSO cycle may exert a far-reaching influence on summertime climate in the Pan American domain through its control



◀ **Figure 35.** Hurricane positions on the last day that they exhibit hurricane-force winds during the (a) 25 warmest and (b) 25 coldest years in terms of sea surface temperature in the equatorial cold tongue region (6°N-6°S, 180-90°W) based on the period of record (1886-2000).



◀ **Figure 36.** Daily hurricane and tropical cyclone positions during the (a) 10 warmest and (b) 10 coldest years in terms of sea surface temperature in the equatorial cold tongue regions based on the period of record (1949-2000).

of hurricane frequency and in the partitioning of the storms between the Caribbean/Gulf of Mexico and the eastern Pacific. Figure 35 shows the position of Atlantic storms on the last day that they exhibited hurricane-force winds for two sets of years, classified on the basis of an index of equatorial Pacific sea surface temperature. More than twice as many storms enter the Gulf of Mexico and make landfall along its coastline during the cold years than during the warm. Figure 36 shows analogous warm- versus cold-year composites but for hurricane and tropical storm days. Warm years of the ENSO cycle are characterized by more Pacific storm days in general, and more of the storms reach northwestern Mexico and Hawaii before they dissipate.

3. Implementation Strategy

U.S. CLIVAR Pan American research will require a broad range of activities to achieve its objectives. Empirical and modeling studies, as well as the development and analysis of historical datasets, will contribute to a better understanding and simulation of the phenomena that control the annual march of seasonal rainfall patterns and their variability on seasonal-to-decadal time scales. U.S. CLIVAR will make a major

contribution to improving the climate observing system in the oceans and seas adjacent to the Americas and will collaborate with CLIVAR VAMOS and with national and international agencies and organizations to improve the quality and coverage of atmospheric climate observations. Three field programs, NAME, MESA, and EPIC, will improve the understanding of key climate processes that are presently hindering advances in climate simulation and prediction over the Americas.

- ◆ Informal groups of observers and theoreticians will work together to understand and simulate key phenomena and processes and hence to accelerate progress.

U.S. CLIVAR and GEWEX are complementary programs in the Pan American region. U.S. CLIVAR emphasizes the planetary-scale context and the variability of the weather systems that produce rain on seasonal and longer time scales while GEWEX emphasizes land-atmosphere interaction on intraseasonal-to-interannual time scales. Mesoscale modeling of continental and oceanic precipitation in a climate context is a common element of both programs. U.S. GEWEX projects fo-



cus on North American rainfall and the Brazil/NASA-led LBA hydrometeorology program focuses on rainfall in the Amazon basin. A NOAA PACS/GCIP research initiative focuses on the seasonal-to-interannual variability of warm-season rainfall, surface air temperature, and the hydrologic cycle over North America.

- ◆ NAME and MESA will be developed jointly with GEWEX and will collaborate with CLIVAR Seasonal-to-Interannual Modeling and Prediction (SIMAP), Global Land Atmosphere System Study (GLASS), and the International Satellite Land Surface Climatology Project (ISLSCP)-Global Soil Wetness Project (GSWP).

3.1 Understanding and simulating Pan American climate variability

Empirical and modeling studies of coupled climate processes are central to U.S. CLIVAR's implementation strategy for the Pan American region. The regional distribution of precipitation over the Americas depends on small-scale phenomena such as the low-level jets over the continents, the mesoscale convective systems that form the highly persistent ITCZ, the equatorial cold tongues with their shallow oceanic mixed layers, and the marine boundary-layer cloud decks in the eastern Pacific. It also involves complex processes that result in the exchange of heat, moisture, momentum, and chemical constituents between the land surface, ocean, and atmosphere.

- ◆ Understanding Pan American phenomena requires major advances in the understanding of large-scale ocean-atmosphere-land interaction and climate modeling.

Improved historical datasets and climate reanalyses will be used to understand the complex mechanisms that govern Pan American climate variability and to formulate hypotheses to be tested with climate models. Descriptive and diagnostic studies of ocean-atmosphere-land coupling will provide context and guidance for the design of NAME and MESA field studies. Continued efforts to build a climate observing system over land, especially in Latin America, will be essential to support empirical and modeling studies addressing these problems.

Fully coupled ocean-atmosphere-land models will be required to study the role of land surface processes

in climate variability. Simulating such a wide range of phenomena and processes provides a major stimulus for the development of high-resolution global climate models that exploit increasingly powerful supercomputers. Modeling strategies will evolve over the CLIVAR period as the scientific objectives of the program are advanced. Initially, the emphasis in the Pan American region is being placed on modeling the seasonally varying mean climate over the tropical Americas and adjacent oceans, including phenomena such as sea breezes and mountain-valley winds. These studies will examine the influence of mesoscale atmospheric features on the planetary and synoptic scale climatology over land and adjacent waters, as well as the coupling between the ocean and atmosphere in the eastern Pacific cold tongue/ITCZ complex. A limited amount of high-resolution modeling will be required for the understanding and synthesis of observations from EPIC, NAME, and MESA. These studies should pave the way for addressing the influence of the slowly varying planetary-scale interannual fluctuations, such as the ENSO phenomenon, on the mesoscale atmospheric circulation and precipitation patterns, and the frequency and distribution of significant weather events. The research will likely first consider the tropical portion of the Pan American domain, where the impacts are most direct, and expand to address summer conditions in the extratropics.

3.2 Atmospheric response to boundary conditions

The ENSO cycle modulates rainfall over much of the United States, especially for the cold season and southern states. The strength and dependability of possible warm-season links are not yet well known. Hence, U.S. CLIVAR will conduct (a) statistical studies documenting relationships between anomalous boundary forcing and climate anomalies over the Americas and (b) diagnostic studies elucidating the physical and dynamical mechanisms through which these links occur. Anomalous boundary forcing includes both sea surface temperature and land surface processes, and climate anomalies refer not only to mean temperature and rainfall but also to the frequency of droughts, floods, and severe thunderstorm outbreaks and to the tropical and extratropical storm tracks.

- ◆ Empirical studies, complemented with numerical experimentation, will examine the complex interactions between SSTs, land processes, their effects on rainfall anomalies, and resulting surface wind systems.



Inference of causal relationships based on empirical evidence is often difficult because the anomalous surface wind field associated with the rainfall anomalies may induce sea surface temperature anomalies of its own, and anomalous boundary conditions in a number of different regions are often interrelated by way of planetary-scale atmospheric teleconnections. For this reason, empirical studies of the atmospheric response to anomalous boundary forcing need to be complemented by a program of experimentation with atmospheric general circulation models.

AGCMs will be used to explore the relative contributions of oceanic and land processes to the determination of the seasonal cycle of precipitation; for example, modifications of the prescribed seasonality of the sea surface temperatures or of the seasonal cycle of solar heating or of other model parameters can be used. Initial studies suggest that precipitation in the eastern Amazon is more controlled by oceanic conditions while the western Amazon is more influenced by the seasonality of land solar heating. The AGCM experiments, together with detailed observations of regional weather phenomena can show how the slowly evolving planetary-scale atmospheric response to boundary forcing modulates the more intermittent, higher frequency synoptic and sub-synoptic phenomena that are responsible for the individual episodes of heavy rainfall and significant weather, e.g., flare-ups in the ITCZ and the SACZ, migrating frontal systems, and higher latitude-blocking events associated with wintertime cold air outbreaks. Although deterministic prediction of phenomena such as these is not feasible on seasonal and longer time scales, realistic models can potentially provide more accurate and detailed information concerning their frequency or likelihood of occurrence than empirical evidence alone.

AGCM simulations can also provide insights into the physical mechanisms responsible for the remote links between anomalous conditions at Earth's surface and regional climate variations. These investigations have traditionally compared simulations where the model is forced with different prescribed sea surface temperatures, the distribution of which is often motivated by empirical studies. The observed correlation pattern in Fig. 24 indicates that monsoon rainfall anomalies over northeast Brazil are positively correlated with sea surface temperature anomalies over the tropical south Atlantic and negatively correlated with sea surface temperature anomalies over the tropical north

Atlantic. AGCM simulations with sea surface temperature anomalies prescribed in accordance with this pattern yield rainfall anomalies of the observed sign, relative to the "control run" with climatological mean sea surface temperature. The consistency between the model simulations and the observations supports the inference that the sea surface temperature anomalies contribute to the anomalous rainfall. In a similar manner, AGCM experiments can examine the hypothesis that sea surface temperature anomalies associated with El Niño are capable of inducing rainfall anomalies over northeast Brazil and other regions of the Americas, independently of the anomalies in the Atlantic.

3.3 Coupling between land and ocean

Empirical and modeling studies are needed to explore the mechanisms that link the oceanic climate variability to that over land in the Pan American region. Do land surface processes simply respond to signals largely determined externally by coupled ocean-atmosphere interaction, or do they actively determine such climatic features as seasonal precipitation patterns over land? With prescribed atmospheric forcing, land may respond in a rather deterministic fashion. However, feedbacks involving the ocean and atmosphere may introduce stochastic or chaotic behavior into the climate system over land system.

- ◆ Accurate representation of land surface effects in climate models will be required to study the subtle mechanisms that couple climate variability over the ocean and land during the warm season.

The physical parameters determined by land surface schemes are the net radiation absorbed by the surface, how that energy is partitioned between latent and sensible heat, conductive heat storage, and the radiative temperatures of the land surface and boundary-layer air that are required for energy balance. Vegetation is a major factor in the surface energy and water balance. Also significant is the vertical movement of water and heat within the soil column. In the present generation of land surface schemes, observational data on the horizontal distribution of vegetation types, properties, and soil characteristics are used as model parameters. Vegetation characteristics affect basic properties such as albedo and roughness length. Soil properties affect the partitioning of rainfall between runoff and infiltration, as well as the radiative, thermal, and water-holding capacities of the land.



Analogous to the initial efforts to represent the effects of clouds in climate models, parameterizations of the energy and water conservation requirements of the land surface were first introduced with very simple schemes. More complex schemes are now included in most operational forecast and data assimilation systems. An explicit representation of vegetation and its role in the hydrological cycle has been introduced, along with more detailed treatments of soil moisture, snow, runoff, and river routing.

In addition, improvements in the representation of air-sea interaction processes will also be required for understanding the coupling between land and ocean. As part of the NAME, MESA, and EPIC field programs, U.S. CLIVAR researchers will seek to improve the understanding and simulation of the mechanisms that couple the annual march and variability of the cold tongue/ITCZ complexes and the southeastern Pacific stratus decks to the monsoon precipitation and circulation over land.

3.4 Seasonally varying mean climate

Regional rainfall anomalies over the Americas involve the intensification, weakening, or subtle displacements in positions of seasonally varying, climatological-mean features.

- ◆ U.S. CLIVAR Pan American research will study the annual march of phenomena that are crucial for organizing seasonal rainfall patterns, i.e., the monsoons, the oceanic ITCZs, the tropical and extratropical storm track, and especially the contribution of land surface processes.

The synoptic climatology of rainfall and significant weather events over the Americas is in need of further elaboration, particularly for the warm season. Topography over the Americas gives rise to a number of distinctive local features in the synoptic climatology such as low-level jets with moist, poleward flow to the east of the Rockies and Andes, disruption of the northeast trade winds by Mexico and Central American mountain ranges, and strong diurnal variations in rainfall patterns. Informal groups of U.S. CLIVAR investigators will focus on improving understanding and simulation of these important contributors to precipitation patterns over the Pan American region. Empirical studies that define and elucidate the fundamental characteristics of these features will be complemented by ef-

forts to simulate the observed features with high-resolution regional climate models.

Mesoscale processes affect the distribution of continental-scale precipitation and its variability on seasonal and longer time scales. Along the coasts and over the mountainous terrain of the Americas, the simulated rainfall in the AGCMs and coupled general circulation models (GCMs) cannot be compared directly with the station data because the weather systems and the topographic features responsible for the observed rainfall patterns have length scales almost an order of magnitude smaller than those resolved by the GCM grids currently in use. The AGCM and coupled GCM simulations are particularly poor in summer, when mesoscale convective systems organize the precipitation over the Americas, and in the ITCZs over the eastern Pacific and western Atlantic oceans. Consequently, seasonal precipitation fields produced by assimilation of climatological data into state-of-the-art climate models do not agree well with independent precipitation data, especially over the data-sparse regions of Mexico, Central America, and South America.

- ◆ Improvement of simulations of seasonally varying mean features and their variability depend both on empirical and modeling studies and on the development of improved datasets and climate analysis methods.

Many aspects of the detailed distribution of rainfall over the Americas and in the oceanic ITCZs can be understood without resolving mesoscale processes over the entire globe. High-resolution regional models have demonstrated a useful capability to “downscale” the coarse resolution information from global climate models to provide more accurate and detailed descriptions of regional precipitation. Appropriate numerical methods and strategies for these variable resolution models need to be addressed. Advances in supercomputing technology may make it feasible by the end of CLIVAR to resolve mesoscale processes within a global climate model.

3.5 Evolution of tropical sea surface temperature anomalies

Prediction of seasonal rainfall anomalies requires accurate prediction of sea surface temperature anomalies. U.S. CLIVAR will provide unprecedented observations of upper-ocean structure from the eastern tropi-



cal Pacific through the Caribbean Sea and Gulf of Mexico into the tropical Atlantic Ocean. The oceanic regions in the Pan American sector are subject to the ENSO phenomenon, modulation by ENSO, and variability on decadal-to-centennial time scales. Of high interest to the Pan American program is whether the long-term changes originating in the Pacific should be viewed as deterministic fluctuations in the coupled climate system or whether they are merely a reflection of sampling variability associated with the ENSO cycle. Empirical studies are needed to determine how long-term variability affects the relationship between ENSO and the Pan American monsoon system and to determine whether the effects of long-term variability are potentially predictable or at least subject to real-time assessment. Also of interest are the processes that determine the evolution of the more subtle sea surface temperature anomalies in the tropical Atlantic and their impact on the South American monsoon system. Tropical Atlantic variability shows evidence of organization on a space scale comparable to the width of the basin and on time scales longer than the characteristic thermal damping time of the mixed layer.

4. Field Studies

U.S. CLIVAR will carry out field programs to observe and understand key climate processes that are presently hindering advances in climate simulation and prediction over the Americas. The framework for Pan American CLIVAR field studies is built on three major initiatives: North American Monsoon Experiment (NAME), Monsoon Experiment South America (MESA), and Eastern Pacific Investigation of Climate Processes in the Coupled Ocean-Atmosphere System (EPIC). The success of NAME, MESA, and EPIC depends on U.S. CLIVAR's unprecedented observations of upper-ocean structure and variability over the Atlantic and eastern Pacific oceans, including the western hemisphere warm-pool region from the eastern tropical Pacific through the Caribbean Sea and Gulf of Mexico into the tropical Atlantic Ocean.

NAME supports Pan American CLIVAR scientific objectives by better defining the structure and dynamics of the monsoon in the data-sparse regions of the southwestern United States and northwestern Mexico through intensive field campaigns. NAME will synthesize these observations to validate and improve simulations of the North American monsoon variability using coupled ocean-atmosphere-land models. MESA

seeks to describe and understand several key components of the seasonally varying climate over South America that have yet to be adequately observed, including the low-level jet on the eastern slopes of the Andes and the interaction of the monsoon over the Andean highlands with circulation over the southeastern Pacific. In addition, enhanced climate monitoring, as part of MESA, will support empirical and modeling studies of ocean-atmosphere-land interactions involving the Amazon basin and southeastern South America. Through enhanced climate monitoring and intensive observational campaigns, EPIC seeks a better understanding and more realistic simulation of the cold tongue/ITCZ complex in the eastern Pacific and the processes that are responsible for the structure and variability of the extensive boundary-layer cloud decks in the southeastern Pacific. The results of EPIC are expected to improve the performance of coupled ocean-atmosphere models over the eastern Pacific and result in improved short-term climate analysis and prediction systems for the Americas.

NAME and MESA are joint initiatives of CLIVAR and GEWEX, while EPIC is primarily a CLIVAR initiative. NAME is being planned as a major U.S. national contribution to VAMOS. The Pan American panel will implement NAME through a science working group in collaboration with U.S. GEWEX investigators. U.S. participation in MESA is being planned by an informal group of U.S. scientists who are collaborating with international CLIVAR and GEWEX investigators. The first phase of EPIC has been implemented by PACS and the EPIC 2001 Science Working Group, while the second phase is being planned by the U.S. CLIVAR Pacific and Pan American sector implementation panels. NAME and MESA are major components of the international CLIVAR VAMOS program that is being developed by VAMOS scientists and agencies in both North and South America. Elements of the U.S. EPIC initiative are included in VAMOS implementation plans for NAME and MESA.

4.1 North American Monsoon Experiment (NAME)

NAME focuses on determining the sources and limits of predictability of warm-season precipitation over North America, with emphasis on seasonal-to-interannual time scales. It is a major nationally planned study. U.S. CLIVAR participation in NAME will be planned by the Pan American panel and implemented by the NAME Science Working Group.



The principal scientific objectives of NAME are to promote a better understanding and more realistic simulation of

1. the evolution of the North American monsoon system and its variability.
2. the response of the warm-season atmospheric circulation and precipitation patterns over North America to slowly varying, potentially predictable surface boundary conditions (e.g., SST, soil moisture, and vegetation).
3. feedbacks between land surface processes and precipitation on seasonal-to-interannual time scales.
4. the diurnal heating cycle and its relationship to the seasonally varying mean climate.
5. intraseasonal aspects of the monsoon.

Achieving these objectives will require improved empirical and modeling studies of the monsoon system and its variability, sustained observations of the

atmosphere, ocean, and land and enhanced observations over portions of the core monsoon region, analysis products (i.e., the combination of the observations and numerical models through data assimilation), and coupled model runs with various combinations of the relevant boundary-forcing parameters.

NAME will link CLIVAR-led programs, which have an emphasis on ocean-atmosphere interactions, and GEWEX-led programs, which have an emphasis on land-atmosphere interactions and ground hydrology, in order to determine the relative importance of the coupled interactions between the ocean, land, and atmosphere as they relate to the monsoon. NAME will integrate the work of GEWEX/GAPP, which continues and expands GCIP efforts, with a NOAA PACS/GCIP research initiative on the seasonal-to-interannual variability of warm-season precipitation. In addition, NAME will also make a major contribution to CLIVAR/VAMOS, which is coordinating international field programs and dataset development efforts as well as empirical and modeling research on the American monsoons. Other anticipated benefits of NAME include the following: joint international experience in the exploitation of in situ data and new satellite sensors measuring atmospheric, surface, and hydrological parameters over the Americas; joint international experience in assessing the capabilities and limitations of assimilated data products for capturing these parameters; advancements in coupled model development over land and ocean areas; advancements in the development of the climate observing system; and the production of consistent datasets over North America to verify numerical model products and remote sensing data.

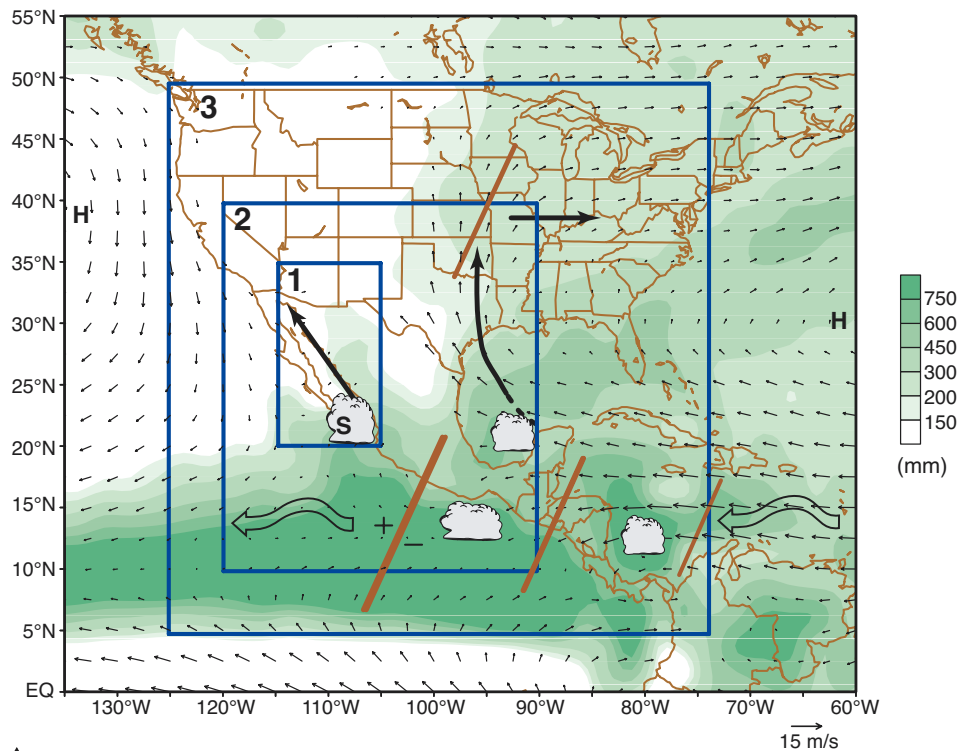


Figure 37. Schematic figure illustrating the implementation plan for the North American Monsoon Experiment (NAME). Analytic, diagnostic, and model development activities will be organized using a multiscale approach. NAME includes specific research objectives addressing mesoscale (Tier 1), regional scale (Tier 2), and continental scale (Tier 3) phenomena. The N-S arrows are the Gulf of California and Great Plains low-level jets. Squiggly arrows represent tropical easterly waves (TEW) and angled lines show the intensification of a TEW as it moves westward. The angled line over the Central Plains indicates a midlatitude disturbance that is propagating eastward, as indicated by the arrow. "S" indicates the origin of a Gulf of California moisture surge, and the "H" indicates the locations of subtropical high pressure systems, specifically the Bermuda high in the Atlantic and the eastern Pacific subtropical high. Shading indicates July-September average rainfall (1979-1995).

and the production of consistent datasets over North America to verify numerical model products and remote sensing data.

The NAME objectives will be addressed by a mix

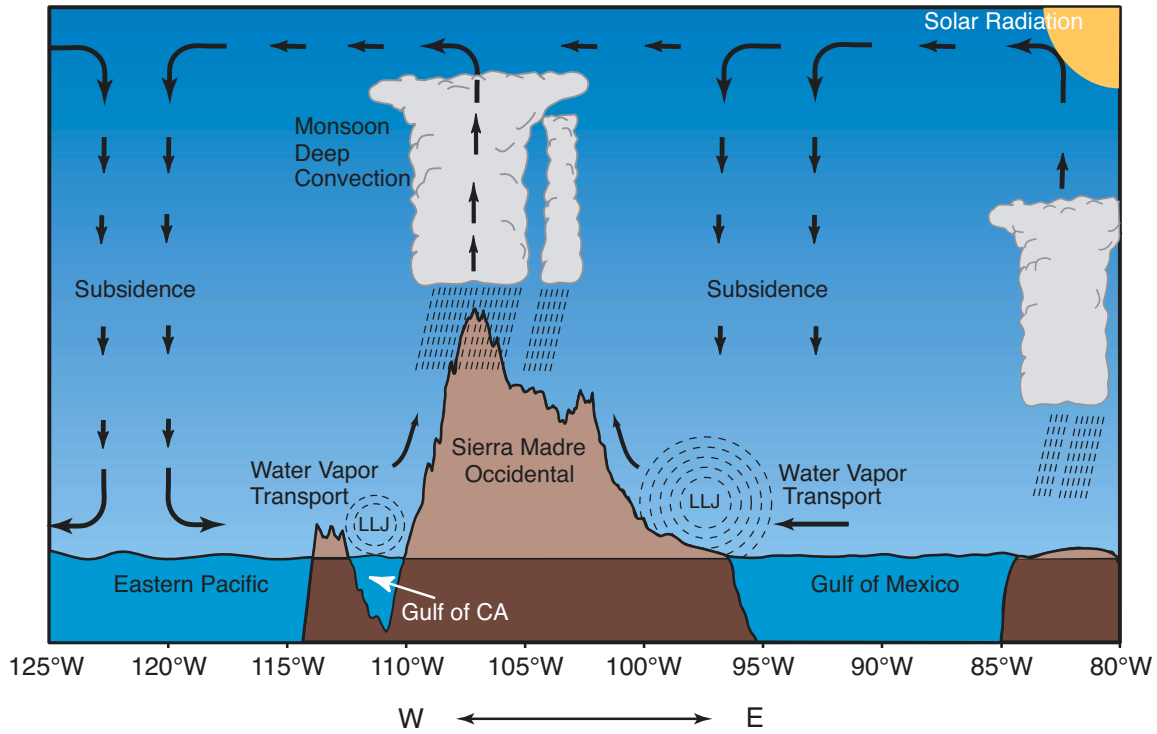


Figure 38. Schematic vertical (longitude-pressure) cross section through the North American monsoon system at 27.5°N illustrating processes and phenomena that contribute to the budgets of heat and water in the core monsoon region.

of diagnostic, modeling, and prediction studies, with enhanced observations. This research activity will necessarily be diverse because it seeks to answer scientific questions relating to several different coupled processes and phenomena. NAME will include focused activities in the core monsoon region, on the regional and continental scales, which for convenience are referred to as Tier I, Tier II, and Tier III respectively (Fig. 37). Each tier has a specific research focus aimed at improving warm-season precipitation prediction, and activities related to each tier will proceed concurrently.

Tier I focuses on key aspects of the low-level circulation and precipitation patterns in the core monsoon region (Fig. 38). The goal of activities in this region is improved monitoring and modeling of the coupling between the sea breeze/land breeze and mountain/valley circulations. This coupling is intimately related to the diurnal cycle of moisture and convection in the core monsoon region, so a better understanding of it is viewed as a fundamental step toward improved warm-season precipitation prediction. Some principal scientific questions follow: How is the coupling between the sea breeze/land breeze and mountain/valley circulations along the Gulf of California related to the diurnal cycle

of moisture and convection? What role does the Gulf of California low-level jet play in the summer precipitation and hydrology of southwestern North America? What are the dominant sources of precipitable moisture for monsoon precipitation over southwestern North America? What are the relative roles of local variations in sea surface temperature and land-surface parameters (topography, soil moisture, and vegetation cover) in modulating warm-season precipitation in this region? What are the effects of aerosol loading from dust, smoke, and anthropogenic emissions on precipitation in the core monsoon region?

Tier II focuses on regional-scale features over southwestern North America and the warm-pool region to the southwest of Mexico. The goal of activities in this region is an improved description and understanding of intraseasonal aspects of the monsoon. A field study focusing on intraseasonal variability might address the following questions: How important are interactions between Tropical Easterly Waves (TEWs) and Gulf of California moisture surges in the prediction of monsoon precipitation? What is the nature of the relationship between the MJO, tropical cyclone activity, and monsoon precipitation? What summer precipitation forecast skills, in addition to those already

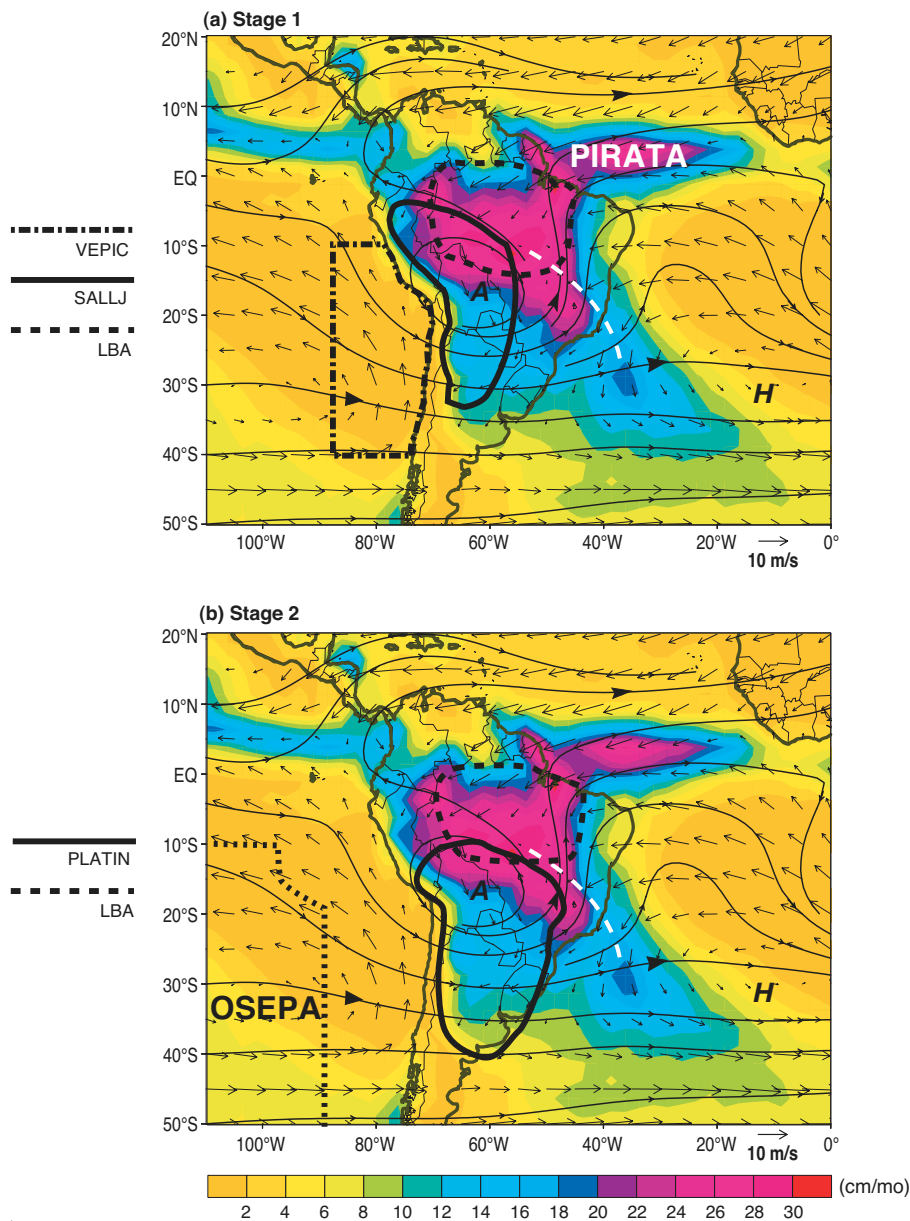


Figure 39. The implementation plan for MESA (Monsoon Experiment South America) will have two stages conducted in sequence. (a) Stage 1, a field study leading to a better description and understanding of the role of the South American low-level jet (SALLJ) in climate variability, and study of ocean-atmosphere-land interactions in the region of the southeastern Pacific Ocean and western South America, VAMOS EPIC (VEPIC). Dashed white line indicates the mean position of the SACZ. (b) Stage 2, a study of the hydroclimatology of the La Plata River basin. LBA (Large-scale Biosphere-Atmosphere in Amazonia) is a GEWEX program focusing on the water and energy budgets of the Amazon River basin. PIRATA (Pilot Research Moored Array in the Tropical Atlantic) and OSEPA (proposed Ocean Southeast Pacific Array) are moored buoy arrays designed for enhanced ocean-atmosphere climate monitoring. Shading indicates December-February mean rainfall and 200 hPa streamlines (1979-1995).

gleaned from ENSO, will arise from an ability to forecast MJO activity over a season? What is the physical setting for the bimodal distribution (i.e., wet-dry-wet) in warm-season precipitation over Mexico and Central America, and what factors influence the interannual variability of the pattern?

cidental (wind, surface temperature, sea-level pressure from automated weather stations), research aircraft flights, and other ground-based elements (915-MHz wind profilers, radars). The overall philosophy for observing-system enhancements will be to augment pre-existing routine observing systems over the region of

Tier III focuses on aspects of the continental-scale monsoon circulation. Here the goal is an improved description and understanding of spatial/temporal links between warm-season precipitation, circulation parameters, and the dominant boundary-forcing parameters. A field study focusing on the continental-scale monsoon might address the following questions: How is the evolution of the warm-season precipitation regime over North America related to the seasonal evolution of the boundary conditions? What are the interrelationships between year-to-year variations in the boundary conditions, the atmospheric circulation, and the continental hydrologic regime? What are the links, if any, between the strength of the summer monsoon in southwestern North America and summertime precipitation over the central United States? What are the relationships between the statistical frequency and magnitude of extreme events (e.g., floods, droughts, hurricanes) and climate variability on intraseasonal-to-interannual time scales?

Elements of the field study may include special soundings (rawinsondes, pilot balloons), improvements to the raingauge network (both simple and digital recording raingauges), transects from the Gulf of California to the Sierra Madre Occ-



interest with special observations that will adequately describe the features of interest. Regional mesoscale models and regional data assimilation systems will be used to guide enhanced monitoring activities. These studies will be carried out in tandem with land surface model experiments and land data assimilation experiments and will benefit from multi-year regional re-analyses and retrospective soil moisture analyses.

The enhanced monitoring activities should operate for at least 4 summer months (June-September) to coincide with the peak monsoon season. During this period there would be a number of intensive observing periods (IOP), each lasting 2-5 days, in order to describe some aspects of the regional low-level circulation in greater detail than can be provided by twice-daily soundings. The timing of the enhanced monitoring activities would be coordinated with other field studies such as EPIC, American Low-Level Jets (ALLS), and CEOP.

4.2 Monsoon Experiment South America (MESA)

MESA is an internationally coordinated process study to improve prediction of the monsoon and its variability over South America, with emphasis on warm-season precipitation. MESA is a joint project of CLIVAR VAMOS and GEWEX. Several key components of the South American monsoon system have yet to be adequately described and understood. South American climate has a unique character that is influenced by the characteristics of both the land surface and the adjacent waters (the eastern Pacific Ocean, the Gulf of Mexico and the Caribbean, and the north and south Atlantic oceans).

The principal objectives of MESA are

1. a better understanding of the key components of the American monsoon systems and their variability.
2. a better understanding of the role of those systems in the global water cycle.
3. improved observational datasets.
4. improved simulation and monthly to seasonal prediction of the monsoon and regional water resources.

The sparse network of conventional weather observations over South America has forced investigators to rely heavily on coarse resolution numerical analyses and satellite data for studies related to the climate of

South America. There is a significant disparity between North and South America in both the sampling density of conventional weather observing systems and the number of past field experiments that are relevant to CLIVAR objectives. MESA therefore places strong emphasis on achieving an improved description and understanding of basic climatological features of the South American monsoon.

MESA investigators will conduct enhanced monitoring and intensive observations of the low-level jet on the eastern slopes of the Andes and its role in determining the seasonal rainfall patterns over the La Plata River basin. Plans are being developed in collaboration with EPIC investigators to study the mechanisms that link the seasonal varying structure of the ocean and atmosphere over the southeastern Pacific to the South American monsoon. In addition, CLIVAR and GEWEX LBA investigators will collaborate to better understand ocean-atmosphere-land interactions between the Amazon basin and the tropical Atlantic regions. MESA benefits from recent field experiments (such as LBA and campaigns over the Altiplano) that have begun to shed light on land-atmosphere interactions in South America. MESA will also benefit from the CLIVAR enhancements of the ocean observing system, including the PIRATA array in the tropical Atlantic and a proposed array of moored buoys in the eastern Pacific (OSEPA).

The MESA implementation plan calls for two stages conducted in sequence (Fig. 39). MESA's Stage 1 comprises the component of the ALLS program that focuses on the moisture corridor between the Andes and the Brazilian Altiplano. The main objective of this component is to better understand the role of moisture transports, their variability, and links to remote and local climate anomalies of the South American low-level jet (SALLJ). Scientists from Argentina, Brazil, Chile, and the U.S. have developed a field program on SALLJ under the auspices of VAMOS. Scientists from Bolivia and Paraguay are expected to participate in the campaign, which is planned for 2002-2005. Stage 1 includes a VAMOS EPIC component (VEPIC) focusing on ocean-atmosphere-land processes centered on the coast of Chile and Peru. VEPIC will implement the international collaboration for EPIC Phase II, tentatively scheduled for 2003-2005. Stage 2 will be a study of the hydroclimatology of the La Plata River Basin (PLATIN). Here the goal is an improved description and understanding of spatial and temporal links between precipitation and streamflow. Scientists from Argentina, Brazil, Uruguay,



and the U.S. have written a document preparatory to a field campaign. The tentative dates for PLATIN are 2005-2010. The participation of the U.S. in MESA will be planned by individual investigators and reviewed by the Pan American panel. Proposed U.S. CLIVAR commitments to international efforts will be prepared by the panel for approval by the Scientific Steering Committee (SSC).

4.3 Eastern Pacific Investigation of Climate Processes in the Coupled Ocean-Atmosphere System (EPIC)

EPIC is a process study to improve the description and understanding of the cold tongue/ITCZ complex (CTIC) and boundary-layer cloud deck regions. It focuses on investigating the key physical processes that must be parameterized for successful CTIC and stratus deck simulation with dynamical ocean-atmosphere models. EPIC pilot studies funded by the NOAA PACS program have already been conducted in the equatorial Pacific at 125°W, where the prevailing September-October surface winds are easterly. EPIC is presently studying the ocean-atmosphere coupling in the monsoonal regime further to the east, where southerly surface winds prevail at the equator in September-October, while maintaining interest in the eastern central Pacific and the oceanographic processes associated with the western part of the cold tongue. EPIC investigators are also studying air-sea interaction in the stratus deck region off the coasts of Peru and Chile. U.S. EPIC efforts are a contribution to the international CLIVAR VAMOS program and are a focus of U.S. CLIVAR Pacific and Pan American climate research. These studies of the ocean mixed layer, the atmospheric planetary boundary-layer structure, and the interfacial fluxes in the cold tongue/ITCZ complexes, based on pilot observations, existing marine surface observations, and satellite data, provide the large-scale context for more intensive EPIC field campaigns.

The scientific objectives of EPIC are

1. to observe and understand the ocean-atmosphere processes responsible for the structure and evolution of the large-scale heating gradients in the equatorial and northeastern Pacific portions of the cold tongue/ITCZ complex.
2. to observe and understand the dynamical, radiative, and microphysical properties of the extensive boundary-layer cloud decks in the southeasterly tradewind and cross-equatorial flow regime, their interactions with the ocean below, and the evolution of the upper ocean under the stratus decks.

To accomplish these objectives, enhanced monitoring and empirical studies were initiated by the NOAA PACS program during 1999-2004 to carry on some elements from the pilot studies, initiate new elements, and provide the spatial and temporal context for EPIC. The intensive observation phase of a process study called EPIC 2001 took place in September-October and consisted of a CTIC component and an exploratory stratus deck component. An intensive observational program in the southeastern Pacific stratus deck regime will be planned by the Pan American and Pacific sector implementation panels on the basis of EPIC-enhanced monitoring activities, the exploratory observations of the stratus decks, and the underlying ocean collected during EPIC 2001. This project will be internationally coordinated with VAMOS investigator activities in South America. EPIC data analysis and modeling in which results from the enhanced climate monitoring and intensive observations are synthesized will be used for coupled model validation and improvement.

4.3.1 Pilot field studies

EPIC field studies completed and already underway have focused primarily on the cold tongue/ITCZ complex in the eastern Pacific, which dominates the interannual variability of the coupled climate system, and the stratus cloud deck off the coast of Peru. Within the eastern Pacific cold tongue region there exist two rather different regimes that prevail within different ranges of longitude that will be labeled as the “easterly regime” and “southerly regime” on the basis of the direction of the prevailing winds along the equator as illustrated in Fig. 40. The dividing line, near 110°W, corresponds to the ridge in the equatorial sea-level pressure profile.

Westward of 110°W, the zonal pressure gradient along the equator drives easterly surface winds that comprise the lower branch of the Walker Circulation. The easterlies induce a distinctive, equatorially symmetric upwelling signature in the sea surface temperature pattern: a reflection of surface Ekman divergence, partially balanced by an opposing geostrophic convergence due to the eastward-directed pressure gradient force that sets up in response to these winds. The divergence represents the upper branch of a pair of wind-driven circulation cells in the meridional plane, symmetric about the equator, whose convergent, lower branch is at the depth of the thermocline and the core of the Equatorial Undercurrent. The strongest and most



coherent sea surface temperature fluctuations that occur in association with the ENSO cycle lie within this easterly regime. Seasonal variations are also observed, but they are weaker than those in the southerly regime farther to the east. Eastward of 110°W the strong equatorial asymmetry in the American coastline induces northward cross-equatorial flow in the atmospheric planetary boundary layer, whose curvature is in cyclostrophic balance with the zonal sea-level pressure gradient along the equator. The cold tongue, centered near 1°S, cannot be interpreted as an equatorial upwelling signature induced by westerly wind stress, since the zonal wind at these longitudes is quite weak. It may simply be the surface signature of the ridge in the thermocline above the equatorial undercurrent, rendered visible in the sea surface temperature pattern by wind-driven entrainment. Alternatively, it could be a manifestation of upwelling south of the equator induced by

the southerly surface winds, or it might be the signature of the plume of the cold water upwelled along the coast of Peru.

The observed distribution of rainfall and cloud types, together with the prevailing cross-equatorial southerly surface winds depicted schematically in Fig. 41, suggests that this southerly regime is characterized by a thermally direct time-mean meridional circula-

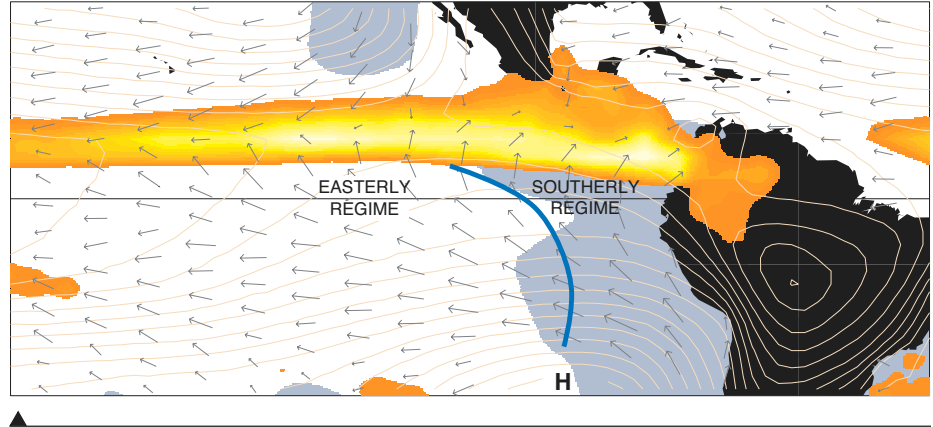


Figure 40. Equatorial wind regimes as defined in the text, superimposed on the average September-October climatology. Surface vector wind, rainfall, and stratus cloud sources and plotting conventions as in Fig. 2. The contours indicate sea-level pressure (contour interval 1 mb). The heavy line depicts the “ridge line” in the sea-level pressure field, i.e., the highest pressure at each latitude.

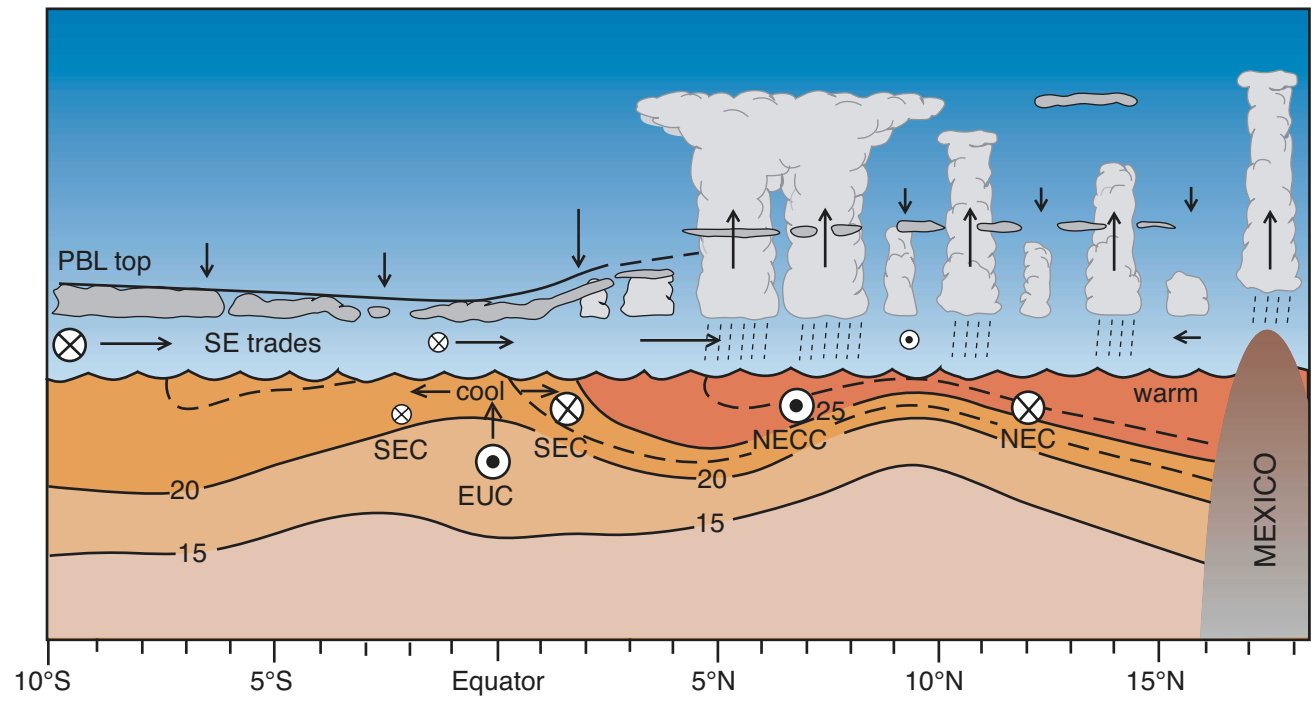


Figure 41. Idealized cross section through the cold tongue/ITCZ complex in the monsoonal regime showing the atmospheric meridional circulation, atmospheric boundary-layer depth, and the oceanic thermal structure. SEC refers to the South Equatorial Current, NECC to the North Equatorial Countercurrent, and EUC to the Equatorial Undercurrent. The heavy twin-column cloud denotes the position of the ITCZ. Encircled x's (dots) denote westward (eastward) flowing winds or currents.



tion. Subsidence and extensive stratiform cloudiness prevail to the south of the equator where sea surface temperature is remarkably cold considering the latitude, and ascent and deep convection occur over the warm pool to the north. Much of the meridional contrast in sea surface temperature is concentrated in a rather strong “equatorial front,” which usually lies near 2°N, and most of the rainfall is concentrated in the ITCZ, which migrates seasonally between 6° and 12°N.

The equatorial asymmetries of wind, rain, and temperature are strongest during the boreal summer and early autumn, when the ITCZ at these longitudes is particularly broad and active and merges with the monsoonal precipitation over Central America. The southern limit of the rain area, characterized by strong low-level southerly inflow, appears to be an integral part of the ITCZ, whereas the northern limit appears to be related to the land-sea geometry that determines the outline of the monsoonal rainfall. The extent of the stratus cloud deck west of the Peruvian coast is also greatest during the boreal late summer and early autumn when the northward flow across the equator is strongest.

The northward cross-equatorial flow, which is believed to be quite shallow, exhibits strong diffuence as it crosses the equatorial cold tongue, and it is subject to strong air mass modification as it passes over the warmer waters to the north of the equatorial front. Stratocumulus cloud streets aligned with the flow, analogous to those that develop in polar air masses advected over the Gulf Stream, are often observed downstream of the front. The front and the atmospheric features associated with it migrate northward and southward with the passage of westward-propagating, 20-day period, 1000-km wavelength tropical instability waves, whose signature is clearly evident in the sea surface temperature image shown in Fig. 27.

The degree to which this seasonally varying meridional circulation and the associated clouds and rainfall influences the sea surface temperature distribution and the structure of temperature and salinity in the ocean mixed layer near the equatorial cold tongue is not known. It has been suggested that the strengthening of this northward flow around May of each year that occurs in association with the northward migration of the monsoonal rain area over the Americas might be responsible for the pronounced strengthening of the cold tongue at this time, but ocean models,

at least as currently formulated, exhibit only a weak response to this seasonally dependent forcing.

Sea surface temperature and mixed-layer structure within the southerly regime are determined by a subtle interplay among a number of competing processes that may be affected, to varying degrees, by the meridional circulation: northwestward advection of cold water that has upwelled along the South American coast, the input of solar energy which may be highly sensitive to the fractional coverage of stratus clouds, local wind-driven upwelling and entrainment, and southward transport of heat by tropical instability waves. Coupled ocean-atmosphere models fail to capture the strength of this southerly regime.

4.3.2 Enhanced monitoring for EPIC

EPIC-enhanced ocean and atmosphere monitoring in the southerly regime of the tropical eastern Pacific builds upon the TOGA observing system, a collection of sparse in situ observations from research and voluntary observing ships and island stations anchored by the Tropical Atmosphere Ocean (TAO) array of moored buoys. In the cold tongue/ITCZ complex, monitoring will be focused along 95°W, the easternmost TAO line. In the stratus deck region, monitoring is centered at 85°W, 18°S. The EPIC-enhanced monitoring period is nominally 1999-2004. It is expected that these data will lead to improved climatologies of this region and will set the context for more intensive field activities.

Atmospheric monitoring

With nearly 70 buoys arranged along 10 lines, the TAO array forms the basic observing framework for monitoring surface wind, temperature, relative humidity, and subsurface ocean temperature in the tropical Pacific. As part of EPIC-enhanced monitoring, the easternmost TAO line at 95°W has been enhanced with additional moorings at 3.5°N, 10°N, and 12°N, and with additional sensors, including shortwave and longwave radiometers, rain gauges, barometric pressure, thermistors, conductivity sensors, and current meters. Daily averages of nearly all quantities are telemetered to the Pacific Marine Environmental Laboratory (PMEL) via Service Argos and are made available within one day at PMEL-maintained ftp databases. High-resolution data will be made available in delay mode via PMEL and national archives.



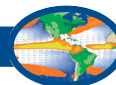
These enhancements will enable the determination of the net surface heat, moisture, and momentum flux at the 10 sites along 95°W. With the southernmost site at 8°S, 95°W and the northernmost site at 12°N, 95°W, the picket fence extends from the stratus deck region, through the cold tongue, and to the north of the ITCZ monsoon trough. Surface heat flux products currently available for this region show discrepancies in both phase and magnitude of the seasonal climatologies. At 0°, 110°W the seasonal climatologies can vary by as much 80 W m⁻², although for most products the differences are closer to 20–40 W m⁻². For climate prediction, flux estimates must be accurate to 10 W m⁻². Ultimately, determination of the optimal flux product will be made based on comparisons with direct measurements and on which product succeeds best in closing the heat budgets. The long time series of flux measurements from buoys will provide a benchmark by which products can be measured. These enhancements will help elucidate the nature of the surface meteorological variability, and the degree and means by which the ocean and atmosphere are coupled in the southerly regime of the eastern tropical Pacific. The cold tongue/ITCZ system is clearly coupled on seasonal and longer time scales. However, even on weekly time scales, TAO wind and sea surface temperature show tight correlation patterns. Recent QuikSCAT scatterometer wind stress and sea surface temperature measurements indicate that coupling occurs on tropical instability wave time and space scales. In situ time series from the buoys will help diagnose the mechanism by which the coupling occurs.

The persistent stratus clouds off the Peruvian coast are believed to play an important role in the strong equatorial asymmetry in sea surface temperature and surface winds in the eastern Pacific. Atmospheric and coupled GCMs have difficulty simulating the extent and properties of these clouds and their interactions with the underlying sea surface temperature field. Thus, a well-instrumented air-sea interaction buoy has been deployed at 20°S, 8°W in the persistent stratus cloud deck region west of Peru and Chile for three years. The site was chosen because it is representative of the stratus region and was near the position occupied by a NOAA NDBC buoy from 1985–1995, which will provide some historical context. The mooring will provide, with good vertical and temporal resolution, upper-ocean velocity, temperature, and salinity profiles and will collect a complete set of surface meteorological time series, allowing computation of the air-sea fluxes of momentum, heat, and fresh water. Surface meteorologi-

cal data will be telemetered, enabling near real-time analysis and data assimilation.

Computation of the sensible and latent heat fluxes from buoy data will rely on a bulk algorithm. The TOGA Coupled Ocean-Atmosphere Response Experiment (COARE) algorithm was developed for the western Pacific warm pool. In order to have the required 10 W m⁻² accuracy, the bulk algorithm must be validated, and possibly tuned, for the stratocumulus conditions of the eastern Pacific southerly regime. While marine stratocumulus clouds have been extensively studied in the past, almost no data exists on clouds or air-sea fluxes in this region. Thus, cloud and marine boundary-layer measurements will be made aboard the TAO tender (NOAA Ship *Ka'imimoana* or NOAA Ship *Ron Brown*), which services the 95°W and 110°W TAO lines every 6 months. The instrument package consists of a cloud ceilometer, an S-band cloud/precipitation Doppler radar, a water vapor/liquid microwave radiometer, and an automated air-sea flux package including a sonic anemometer, a pair of pyranometers, a pair of pyrgeometers, slow air temperature and humidity sensors, and a ship-motion package to make the necessary corrections to calculate directly the co-variances for turbulent fluxes. This set of instruments will allow computation of low cloud statistics (integrated liquid water content, cloud base height, and fraction) and the complete surface energy budget of the oceanic and atmospheric boundary layers. The cloud statistics will help improve cloud models and satellite retrieval methods. When combined with measurements of downward longwave and shortwave radiative fluxes, the cloud measurements will allow computation of cloud infrared and visible optical thicknesses plus the surface cloud radiative forcing, a key diagnostic variable in climate models.

The TAO tender will also be used to launch radiosondes to monitor the tropospheric structure, in particular the atmospheric boundary layer (ABL) along 95°W and 110°W on 6-month intervals. These observations will be used to examine the ABL and its relationships to the underlying sea surface temperature and the background, large-scale atmospheric flow. Higher temporal resolution will be provided at island stations. However, at present the operational upper-air sounding network is extremely sparse. At the beginning of U.S. CLIVAR, the only operational upper-air soundings in the eastern Pacific were made at Baltra in the Galapagos Islands. This site, together with a 915-mHz



wind profiler on Santa Cristobal Island, has been operating for only a few years. It has been an early priority of U.S. CLIVAR to expand routine soundings to the few available islands in the eastern Pacific. Only three islands, Clipperton (10°N, 109°W), Cocos (6°N, 87°W), and Malpelo (4°N, 82°W), are currently uninhabited or sparsely inhabited. The ITCZ passes over all of the islands and during northern summer Cocos and Malpelo are in monsoonal southwesterly flow, well to the south of the mean surface confluence line.

The sounding network on the periphery of the eastern Pacific is also in need of improvement. Several of the sounding sites are seriously affected by local topography (Guatemala City, Guatemala; San Jose, Costa Rica; and Bogota, Colombia), and it may be feasible to improve the specification of the lower-tropospheric wind and even thermodynamic fields through the establishment of judiciously situated pilot balloon soundings. Cooperation with the respective countries in Latin America will be needed for effective implementation of this type of network. A pilot monitoring effort (PACS-SONET) has begun the placement of an upper-air sounding station on Cocos Island and pilot balloon wind observing stations in data-sparse areas of Mexico, Central America, and northwestern South America (Fig. 42).



Figure 42. PACS-SONET upper-air stations for enhanced climate monitoring.

The expansion of routine soundings discussed above can provide frequent observations with limited spatial coverage and infrequent observations with good meridional coverage along 95°W and 110°W. Improved sampling may be possible using commercial ships as a vehicle for portable sounding systems, similar to what is done on the TAO tender. An attempt will be made to determine whether there are suitable ships that traverse the Pan American area of highest priority, east of 120°–130°W. The feasibility of using other ships, including those in commercial fishing fleets, will also be explored. Another possibility for obtaining routine observations would be to make long-ranging dropwindsonde aircraft flights or unmanned flights over the eastern Pacific at periodic intervals to investigate the dynamics of the ITCZ and related tropical circulations. Aircraft such as the NOAA G-IV, which is able to provide soundings over a large region in one flight at a cost of roughly \$30K per mission, could fulfill this role. Recent technological innovations in unmanned aircraft offer the hope of sampling the atmosphere over much of the depth of the troposphere, with ranges up to 7000 km. The data provided by the manned and unmanned aircraft soundings might be viewed as complementing the land- and island-based observations. They would provide comprehensive “snapshots” of the full three-dimensional circulation several times a year, while the surface-based observations would provide time continuity. The most efficient mix of observational platforms for monitoring tropospheric structure over the eastern Pacific has not yet been determined.

Ocean monitoring

As with the atmospheric monitoring, the TAO array forms the basic framework of tropical ocean monitoring for EPIC. Standard ocean TAO measurements include sea surface temperature and subsurface temperature at 10 depths with 20–200 m vertical resolution. This vertical resolution, however, is not sufficient for monitoring variability within the mixed layer, the site of active ocean-atmospheric interactions. Thus as part of the EPIC-enhanced monitoring program, the 10 enhanced 95°W TAO moorings (at 8°S, 5°S, 2°S, 0°, 2°N, 3.5°N, 5°N, 8°N, 10°N, and 12°N) have additional sensors to monitor the upper-ocean temperature, salinity, and surface currents. These TAO ocean measurements, together with the surface heat, moisture, and momentum flux enhancements, form a complementary coupled ocean-atmosphere observing system for the cold tongue/ITCZ complex in the southerly regime of



the eastern tropical Pacific. Although zonal gradients and thus the effects of zonal advection are not well resolved, the local response to the surface wind and buoyancy forcing can be evaluated at each of the 10 95°W moorings. Understanding the relationship between the meridional gradients in the surface forcing and sea surface temperature is a major objective of this study. The Pan American region is characterized by large meridional gradients not only in the heating and sea surface temperature fields but also in the rainfall and salinity fields. Conductivity Temperature Depth (CTD) measurements taken from the TAO tender along 95°W show surface salinity as low as 33.5 psu near 5°-8°N associated with the ITCZ, while south of 5°S, the surface salinity is higher than 35 psu. Salinity is an important variable not only because it is a rough indicator of rainfall patterns but also because it affects the buoyancy of the water column. Thus salinity can affect sea surface temperature through its influence on vertical mixing, penetrative radiation, and dynamic height (and thus ocean currents and advection). It is expected that the freshwater influence within the ITCZ plays an important role in maintaining the warm sea surface temperatures despite the shallow thermocline in the region.

In the stratus region, the air-sea interaction buoy at 18°S, 85°W will monitor the upper temperature, salinity, and current profile with high temporal and vertical resolution. Ocean measurements also will include a floating sea surface temperature sensor at 5-cm depth. These data will be used to analyze the temporal evolution of the surface forcing and upper-ocean structure on time scales from minutes to seasonal and possible feedback mechanisms that link that evolution of the atmospheric and oceanic boundary layers in the stratus region. Understanding and properly parameterizing the coupling mechanism in the stratus region is crucial for simulating the observed climatic asymmetries in the Pan American region.

Circulation in the Pan American region is fully three dimensional with strong upwelling near the equator and relatively shallow zonal currents associated with the Equatorial Undercurrent, South Equatorial Current, the North Equatorial Countercurrent, and the North Equatorial Current, all of which are in some way affected by the nearby continental boundaries. Understanding the three-dimensional circulation is critical for determining the interhemispheric transfers and the pathways of water as they enter and exit the equatorial current system. At present, this complex oceanic circu-

lation is not adequately monitored. As part of the ENSO observing system, the horizontal currents have been monitored at 0°, 110°W by an Acoustic Doppler Current Profiler (ADCP) and/or current meters since 1980, providing one of the longest time series of currents available. The enhanced moorings along 95°W also have a very sparse array of current meters. However, with only 1-2 current meters per mooring, this array does not adequately resolve the vertical shear. Argo floats and surface drifters will be relied on to provide information on the large-scale circulation patterns. Shipboard ADCP measurements from the TAO tender provide excellent meridional resolution of the current structure, but only every 6 months. Large-scale geostrophic current fields can also be computed from dynamic height estimates from TAO moorings, CTDs, and XBTs, and from the Ocean Topography Experiment (TOPEX) satellite sea-level height measurements. However, none of these monitoring systems is able to measure the equatorial upwelling that is crucial for understanding the dynamics and variability of the cold tongue. Likewise, while the large-scale current structures may be resolved, the rich variability and interactions associated with the large horizontal and vertical shears between the current structures are not well resolved. Feasibility studies based on historical data and numerical and theoretical models may lead to an improved strategy for monitoring the critical components of this three-dimensional ocean circulation and for designing a plan to monitor them.

4.3.3 EPIC 2001: An intensive observing period

In addition to the expanded monitoring discussed in the previous section, Pan American CLIVAR investigators have conducted a short-term field study, called EPIC 2001, which was designed to improve understanding and modeling of seasonal-to-decadal climate variability within the eastern tropical Pacific. The experiment consisted of four components, focusing on (1) ITCZ/warm-pool phenomena, (2) cross-equatorial inflow into the ITCZ, (3) upper-ocean structure and mixing in the ITCZ/warm pool, and (4) an exploratory study of boundary-layer cloud properties in the southeasterly tradewind regime. Each component will be coordinated to share resources and create a dataset with added value. The field phase, involving intensive shipboard atmospheric and oceanic boundary-layer measurements and aircraft surveys, was carried out during September-October 2001. Taking advantage of the enhanced monitoring already in place along 95°W, the fieldwork for the first three were focused along 95°W,



particularly near 10°N. The analysis and modeling phase is underway.

5. Modeling Issues

Numerical modeling in U.S. CLIVAR Pan American research addresses the overall goal of extending the scope and improving the skill of operational climate prediction over the Americas on time scales of a season and longer. A broad-based program of experimentation with a hierarchy of models will contribute to the pursuit of all three Pan American scientific objectives. Simulation of boundary-forced rainfall anomalies and the frequency of occurrence of significant weather events over the Americas addresses the potential predictability of the atmosphere, given perfect knowledge of the boundary conditions, while the simulation of quantities such as sea surface temperature, soil moisture, snow cover, and vegetation addresses the predictability of the boundary conditions. Improved representation of coupling between atmosphere and land surface processes developed by GEWEX investigators will be required for understanding and simulating modes of climate variability that depend significantly on land surface “memory.” Simulation of the seasonally varying mean precipitation and other aspects of climate over the Americas and the adjacent oceans as an initial value problem with coupled GCMs provides an incisive test of current understanding of the coupled ocean-atmosphere-land system, as reflected in the design of the models. Of particular importance is the simulation of the structure of the cold tongue/ITCZ complex and the monsoonal precipitation patterns over the land, which play a central role in the coupling between the tropical atmosphere, the ocean, and land surface processes on seasonal and longer time scales.

U.S. CLIVAR will emphasize the use of fully coupled ocean-atmosphere-land models to study the role of land surface processes in climate variability. A limited amount of high-resolution modeling will be required for the understanding and synthesis of observations from the field studies described in Section 4. The challenge of simulating phenomena that determine the regional distribution of precipitation over the Americas, such as the low-level jets over the continents, the mesoscale convective systems that form the highly persistent ITCZ, the equatorial cold tongues with their shallow oceanic mixed layers, and the marine boundary-layer cloud decks in the eastern Pacific, provides a major stimulus for the development of high-resolution

global climate models that exploit increasingly powerful supercomputers. Understanding Pan American climate phenomena in the context of the atmospheric and oceanic general circulation and simulating them realistically will require major advances in the understanding of large-scale ocean-atmosphere-land interaction and state-of-the-art climate modeling.

5.1 Atmospheric general circulation models (AGCMs)

AGCM simulations forced with climatological-mean boundary conditions exhibit systematic biases in regions of interest to U.S. CLIVAR, e.g., an underestimation of wind stress in the equatorial belt. Increasing the horizontal resolution may alleviate this problem by increasing the poleward eddy momentum flux, and it may, at the same time, provide a better representation of topographic effects on the low-level flow. The Andes, for example, may help determine the prevailing along-shore surface winds off Peru and the associated oceanic upwelling in that region. Models also underestimate the coverage of oceanic stratus clouds, hence their reflection of solar energy and the consequences for the atmospheric planetary boundary layer and the ocean mixed layer believed to be responsible for much of the equatorial asymmetry of sea surface temperature in the tropical Atlantic and eastern Pacific. These well-defined biases within the Pan American region serve to highlight basic deficiencies in the atmospheric models that need to be corrected in order to pave the way for the development of realistic coupled models.

5.2 Mesoscale atmospheric models

Mesoscale processes affect the distribution of continental-scale precipitation and its variability on seasonal and longer time scales. Along the coasts and over the mountainous terrain of the Americas, the simulated rainfall in the AGCMs and coupled GCMs cannot be compared directly with the station data because the weather systems and the topographic features responsible for the observed rainfall patterns have length scales almost an order of magnitude smaller than those resolved by the GCM grids currently in use. The AGCM and coupled GCM simulations are particularly poor in summer, when mesoscale convective systems organize the precipitation over the Pan American region.

Many aspects of the detailed distribution of rainfall over the Americas and in the oceanic ITCZs can be



understood without resolving mesoscale processes over the entire globe. High-resolution regional models have demonstrated a useful capability to “downscale” the coarse resolution information from global climate models to provide more accurate and detailed descriptions of regional precipitation. However, much work remains to determine the most appropriate numerical methods and modeling strategies. Furthermore, advances in supercomputing technology may make it feasible to resolve mesoscale processes over the globe during the next 10 years, making it unnecessary to deal with the practical problems of variable spatial resolution. In the meantime, a number of technical issues remain for the use of mesoscale models in climate research. What horizontal and vertical resolutions are required for a nested model to adequately simulate seasonal and interannual variations in summertime rainfall? How sensitive are the simulations to the techniques employed to nest the mesoscale models in global models? Very little has yet been done to apply variable resolution methods developed in other disciplines that would allow a global model to increase its resolution where it is needed or other approaches, such as a “window model,” in which the large-scale flow is simulated directly at a lower resolution, while the selected region is examined at higher resolution through the use of a perturbation model that has essentially the same physics and model dynamical structure.

5.3 Modeling the effects of the land surface

Modeling the role of the land surface, as a lower boundary condition for atmospheric models, requires theoretical and observational exploration of the processes involved, modeling sensitivity studies to determine the relative importance of different processes, and numerical implementation of the improved understanding. Analogous to efforts to represent the effects of clouds in climate models, the energy and water conservation requirements of the land boundary conditions were first introduced with very simple schemes. More complex schemes are now included in most operational forecast and data assimilation systems. An explicit representation of vegetation and its role in the hydrological cycle has been introduced, along with more detailed treatments of soil moisture, snow, runoff, and river routing. With application of prescribed atmospheric forcing, land may respond in a rather deterministic fashion, but when coupled to AGCMs, the feedbacks can result in nonlinear responses to perturbations that are quite different than what one finds integrating

either model separately. Enhanced or reduced sensitivities can result; multiple equilibria may be attained.

The physical parameters that a land scheme determines are the net radiation absorbed by the surface, how that energy is partitioned between latent and sensible heat, conductive heat storage, and what is the difference in temperature between the surface and the near-surface air required for net radiation to be balanced by these other fluxes. Vegetation is a major determinant of all these factors. Also significant is the vertical movement of water and heat within the soil column. In the present generation of land surface schemes, observational data on the horizontal distribution of vegetation types, properties, and soil characteristics are used as model parameters. Vegetation characteristics affect basic properties such as albedo and roughness length. Soil properties affect the partitioning of rainfall between runoff and infiltration, as well as the radiative, thermal, and water holding capacities of the land. Improvements in such information, either from observations or as interactive components of the model, should allow for more realistic simulations of climate and its variability.

5.4 Ocean General Circulation Models (OGCMs)

The processes that determine the annual march of sea surface temperature in the eastern equatorial Pacific Ocean are only partly known, yet this is a crucial facet of the climatology in the Pan American domain, particularly with respect to the annual march of the ITCZ and the northwestward shift of the American monsoon from equatorial South America to Central America and Mexico in boreal summer. Although the annual march is largely a reflection of coupled air-sea interactions, there remain a number of important questions concerning the processes that contribute to sea surface temperature variability in this region that could be addressed in the context of OGCM experiments in which the ocean is forced by specified atmospheric fluxes. As the important components of the ocean response become better understood, improvement of coupled models will be expedited.

The mechanisms that control the annual march of sea surface temperature in the monsoon regime of the eastern tropical Pacific appear to be fundamentally different from those in the tradewind regime of the central Pacific, upon which much of the prior OGCM development effort has been focused. In the central Pa-



cific, where interannual variability associated with El Niño is dominant over the seasonal cycle, the forcing is mainly in the form of zonal wind variations. Further east, where the meridional winds are strong, the seasonal cycle is the dominant signal. The sea surface temperature variations associated with that cycle differ significantly from those associated with El Niño in not being correlated with vertical movements of the thermocline. This attests to the importance, on annual time scales, of other processes such as insolation and other surface fluxes, upwelling, horizontal advection, and vertical mixing in the heat balance. Vertical mixing influences sea surface temperature not only by entraining cold water into the upper layer but also by affecting the depth over which the surface heat and momentum fluxes are distributed. The depth of the thermocline is a parameter that strongly influences these various processes and hence sea surface temperatures. Valuable information about the nature of this influence should be available from observational and modeling studies of the seasonal cycle during different phases of ENSO, which is associated with large changes in the depth of the thermocline.

Ocean models have been able to simulate some aspects of annual variability in the eastern equatorial Pacific, particularly features with large zonal scale such as the basin-wide pressure gradients and zonal currents, yet they have had trouble simulating the annual cycle of sea surface temperature in the eastern Pacific without resorting to parameterizations that to some extent predetermine the result through either relaxation terms or particular specifications of the heat fluxes. It is unclear to what extent these unsatisfactory results are due to incomplete model physics or insufficiently well-observed surface forcing functions. Efforts to improve these models have often focused on parameterization of mixed-layer physics, upwelling, and entrainment. One of the major motivations for the field studies described in the next section is the need for improved estimates of the surface fluxes for testing the various OGCM parameterizations.

As in the atmosphere, an issue that remains unresolved is the rectification of high-frequency forcing and internal instabilities into the low-frequency variability. Such forcing includes the equatorial intraseasonal waves and instabilities that are prominent particularly north of the equator at periods near 20-30 days; both of these signals are modulated by the annual cycle and by ENSO. Model results suggest that the vertical veloc-

ity field can fluctuate rapidly in connection with these and other phenomena. Since mixing is an irreversible process, the net effect of high-frequency signals on the annual cycle might be quite different than would be deduced from low-frequency averages alone.

Smaller-scale regional variability escapes the resolution of basin-scale OGCMs but may be significant for understanding the heat, mass, and momentum budgets over the eastern tropical Pacific. The region up to a few hundred kilometers off the Central American coast is generally very warm but can cool rapidly in response to winter northerlies blowing through gaps in the American cordillera. South of the equator, the annual coastal upwelling signal has been cited as important for the development of much larger-scale phenomena, but the processes by which the narrow coastal features might influence the larger scale have not yet been clearly elucidated. Present basin-scale OGCMs handle these near-coastal signals poorly.

The question of closure of the equatorial and tropical current systems in the east Pacific remains obscure. The fate of water flowing eastward in the North Equatorial Countercurrent and Equatorial Undercurrent is not known. To date, these current systems have been largely understood as a feature of the dynamics of the broad central Pacific, far from boundaries, where the zonal scales are very long. Similarly, the source of water upwelled in the equatorial cold tongue, the depth from which it originates, and the meridional extent of the upwelling cell have not yet been established, and it is not known whether the upwelling water can be traced back to the surface in extratropical regions, as suggested from theory. These and other questions about the closure of the current systems in the east speak to the most fundamental aspects of the ocean circulation in the Pan American region; they will become tractable as the community develops confidence in the performance of OGCMs in the tropical eastern Pacific.

5.5 Coupled ocean-atmosphere GCMs

Improved prediction of sea surface temperature anomalies and their effects on climate will require the development of coupled GCMs capable of simulating the seasonally varying climate accurately, since it is the mean climate that determines the stability and the dynamical properties of the coupled system. Sea surface temperature anomalies in the tropical Pacific are currently predicted operationally out to several seasons in



advance using simple coupled ocean-atmosphere models, in which the mean state and climatological-mean seasonal cycle are prescribed. The evolution of the complete tropical Pacific system is also predicted operationally using coupled GCMs. Coupled models tend to be more sensitive to small perturbations and to display more complex behavior than their AGCM and OGCM components. The Pan American domain, with its strong ocean-atmosphere-land interactions, provides an attractive test bed for these models. Working correctly, coupled models become the tools needed for predicting seasonal-to-interannual climate variability and for the longer-term response to anthropogenic forcing.

The success of some coupled GCMs in predicting the initiation and termination of the 1997-1998 El Niño indicates that they can potentially predict not only the anomalous sea surface temperature patterns in the tropical Pacific but also their teleconnections to other tropical regions and the extratropics. The El Niño event of 1997-1998 was more intense than other well-documented events of the past. For many months peaking in December 1997, SSTs recorded values that in locations of the tropical Pacific were more than 5°C warmer than average. Coupled models demonstrated skill in predicting the onset of the ENSO event a season to six months in advance, although the amplitude was not well predicted. At longer lead times, neither the onset nor the amplitude of the event was well predicted by most models, and the success in predicting the evolution (growth, decay) of the event once it had begun was mixed. In general, the more comprehensive (primitive equation) coupled models gave better, more skillful results.

Despite the successes of coupled model predictions of ENSO events, coupled models share some troublesome systematic errors. The simulated equatorial Pacific cold tongue generally extends too far west and tends to be too strong and too narrow. The largest biases in sea surface temperature occur along the eastern and western ends of the Pacific basin: simulated sea surface temperature is not cold enough in the east and not warm enough in the west. The models also tend to underestimate the strong equatorial asymmetries in the mean climate of the eastern Pacific: sea surface temperature and rainfall are too high south of the equator. The climatological mean annual march, which strongly influences the characteristics of the ENSO cycle, also tends to be unrealistic: the ITCZ migrates across the equator rather than remaining in the Northern Hemi-

sphere throughout nearly the entire year as observed. A pervasive problem in many of the coupled GCMs is that the western Pacific warm pool extends too far east along 10°S. This feature, combined with the tendency for the cold tongue to extend too far west along the equator, renders simulated meridional gradients too strong and zonal gradients too weak south of the equator. The excessively high sea surface temperatures in the eastern Pacific south of the equator appear to be a consequence of the lack of stratiform cloudiness that allows an excessive amount of insolation to reach the ocean surface. Many of these deficiencies are manifested during the “southerly regime” described in more detail in Sections 4.3.1-4.3.2.

To promote a better understanding and improved simulation of the evolution of the SST anomalies, it will be necessary to consider the coupling between the atmosphere and ocean over a wide spectrum of time scales, ranging from a season to decades. Coupled models will provide the ultimate test of any theory of why the cold tongue/ITCZ complexes exist, why they tend to be asymmetric about the equator, and why they exhibit a strong annual cycle. These models will be the focal point for investigating the stratus decks and their role in global climate. Since they simulate feedbacks not represented in the AGCMs, they provide the most reliable indication of the global response to local boundary forcing. On longer time scales, it will be necessary to understand the mechanisms that give rise to events such as the prolonged warm episode over the tropical Pacific during the early 1990s. At present there is no definitive explanation of this phenomenon. Apparently sea surface temperature in the tropical Pacific varies, not only in response to the ENSO cycle but also in response to processes operating on longer time scales.

Sensitivity studies with coupled GCMs may be used to explore mechanisms determining the seasonal cycle of sea surface temperatures and their controls on precipitation in the Pan American region. For example, the annual cycle of solar heating can be turned off over various regions in the model to modify sea surface temperatures and/or land processes and hence the seasonality of precipitation patterns. Coupled GCMs are the principal tool to be used in support of those studies. The improved understanding of the physical processes responsible for the variability of the tropical oceans and the improved ability to predict them with coupled GCMs will be directly relevant to the methodologies used in operational prediction centers.



A number of important technical issues in the design of coupled models have yet to be resolved. Experiments have been conducted to explore how a change in the resolution of one component of the coupled system affects the results. If the OGCM has high (finer than 1° latitude-longitude) horizontal resolution that can capture the equatorially trapped waves that transmit the signal of the wind forcing across the Pacific basin, then a realistic ENSO cycle can be reproduced in the coupled model. If the resolution of the OGCM is degraded to the point where it fails to capture those modes, other processes dominate the evolution of sea surface temperature in the equatorial waveguide and the simulation of the ENSO cycle is unrealistic. The effect of AGCM resolution on the performance of the coupled system is relatively unexplored. Coupled GCMs in which the AGCM has high horizontal resolution tend to produce a realistic annual cycle in sea surface temperature in the eastern equatorial Pacific but a very weak ENSO cycle. If the AGCM has a substantially coarser horizontal resolution than the OGCM (as is the case for most models), the simulation of the feedbacks between the atmosphere and the ocean is compromised to some extent because the AGCM is incapable of responding to the fine structure in the sea surface temperature field, such as the equatorial cold tongues and narrow coastal upwelling zones. Resolving this problem requires a better understanding of the connection between seasonal and interannual variability.

6. Dataset Development and Management

Pan American investigators have at their disposal a much larger array of observational and model-generated datasets than was available during TOGA. Relevant satellite-based datasets include radiative fluxes, precipitation estimates, cloud parameters, layer-averaged temperature and humidity, wind stress over the oceans, sea level, ocean color, and properties of vegetation. The satellite measurements, in combination with the ongoing components of the in situ global observing system put into place during GARP and TOGA and datasets derived from U.S. CLIVAR and GEWEX field programs, provide unprecedented opportunities for innovative investigations in pursuit of the Pan American scientific objectives. The UCAR Joint Office for Science Support (JOSS) currently provides NOAA's Pan American Climate Studies Program with limited dataset development and management support with online data access for some of the PACS datasets.

U.S. CLIVAR does not fund a major data management activity of its own: it relies heavily on a number of ongoing data management efforts funded by the mission agencies. As a part of their routine operations, weather prediction centers perform the management, quality control, synthesis, and gridding of many of the atmospheric datasets needed by Pan American investigators. Reanalysis projects currently in progress at NCEP and the European Centre for Medium-Range Weather Forecasts (ECMWF) will substantially upgrade historical datasets derived from these analyses, especially for model-generated fields such as precipitation rates. An analogous ocean data assimilation system established at NCEP under the auspices of TOGA produces gridded oceanographic datasets. The Global Precipitation Climatology Project provides precipitation estimates based on infrared and microwave satellite data, rain gauge measurements, and model outputs. Monthly mean precipitation estimates for 1986-2000 are being produced on a 2.5° latitude-longitude resolution grid.

The International Satellite Cloud Climatology Project (ISCCP) provides cloud amount, top temperature and pressure, optical thickness, and water path for cirrus, deep convective, middle, and low clouds on a 30-km grid with 3-hour and monthly time resolution for 1983-1991. A reanalysis of this data with improved cloud detection and an ice-phase microphysical model in the retrieval algorithm was completed in 2000. A limited amount of pixel resolution data is available for COARE, the First ISCCP Regional Experiment (FIRE), and the Atlantic Stratocumulus Transition Experiment (ASTEX) field programs. Radiative flux profiles generated in the retrieval algorithm are being routinely archived. ISCCP continues through the year 2002.

NASA has developed and flown on the Terra satellite a new generation of instruments for getting measurement of land properties. These measurements were made for climate model improvement in 2001. Previous observations have been developed into useful datasets over land by the ISLSCP. Their previously developed data have been widely used in the land surface schemes of operational and research models. Other monitoring products that are satellite based include the NOAA/NESDIS precipitation and precipitable water and soil wetness index products, with high-resolution GOES satellite estimates of rainfall over South America.

The GSWP is producing retrospective multi-model estimates of soil moisture and surface fluxes over the



globe. The NASA Land Data Assimilation System (LDAS) is similar to GSWP but is a higher-resolution operational product, a version of which will eventually be coupled to the NASA DAO atmospheric data assimilation system. LDAS is operational over the United States and is expanding to cover all of North America and eventually the globe.

Many of the datasets needed by Pan American investigators are already available through existing data distribution centers. The NOAA National Climate Data Center offers monthly and seasonal data for precipitation and other variables, from a variety of sources and in a number of different formats. The National Center for Atmospheric Research (NCAR) data library maintains an extensive collection of use to Pan American researchers, including precipitation datasets, gridded atmospheric analyses, selected oceanographic data, and more specialized datasets such as daily global tropical cyclone positions. PMEL offers data from the TAO array, in near real time. The NOAA Atlantic Oceanographic and Meteorological Laboratory (AOML) provides data from the volunteer observing ship/expendable bathythermograph temperature (VOS/XBT) program and temperature and current data from the tropical and global drifting buoy array. It will also provide sea-surface salinity observations and analysis products as they become available.

NOAA's NCEP provides global atmospheric reanalysis data on CD-ROMs and the NOAA Climate Diagnostics Center (CDC) in a self-describing common data format (netCDF). The Climate Diagnostics Center is also archiving monthly mean data from the NCEP ocean model and, more recently, weekly means that include surface fluxes generated by the coupled model. Ocean reanalysis products will be added to this archive as they become available.

U.S. CLIVAR is supporting the assembly of additional daily and monthly precipitation records for Mexican stations, the preparation of 1° latitude-longitude resolution monthly sea surface temperature data for the tropical and extratropical Pacific and Atlantic basins based on the Comprehensive Ocean-Atmosphere Dataset (COADS), and the extension of ISCCP-type convective cloud data back to the early 1970s. Data from U.S. CLIVAR-sponsored field studies described in Section 4 will be available to the scientific community soon after the field observation phase. The data that do not require extensive post-processing should be available

in real or near real time and the more intensively processed datasets should generally be available within a year of the time that the observations are taken.

7. Building the Pan American Climate Observing System

U.S. CLIVAR will promote establishing an integrated network of ocean, atmosphere, and land climate observations in the Pan American region. The network will be built on existing operational networks and the legacy of the TOGA program in the Pacific. Major U.S. CLIVAR enhancements of the global ocean observing system are planned. The Argo system of upper-ocean profiling floats will provide unprecedented coverage of upper-ocean temperature and salinity over large areas of the Pacific and Atlantic oceans during the CLIVAR period. A network of research-quality air-sea interaction buoys will provide information on upper-ocean conditions and air-sea exchanges of heat, water, and momentum in key climatic regimes over the Pan American domain. VAMOS investigators are planning an array of moored upper-ocean buoys extending the full length of the west coast of South America. These profiling and moored systems will provide observations of oceanic and surface conditions over the ocean but vast areas of the tropical and southern Pacific and Atlantic oceans are virtually without routine upper-air soundings (Fig. 43). Upper-air observations are less dense over Latin America than over the U.S., and large areas of South America are without operational upper-air soundings.

- ◆ The U.S. CLIVAR strategy for improving upper-air observations in the Pan American region is to implement all of the Global Climate Observing System (GCOS) priority atmospheric upper-air stations, and then add high-quality stations in key climatic regimes that are inadequately sampled in both time and space.

Highest priority will be to maintain the existing surface and upper-air stations and observation systems with long, uninterrupted records. CLIVAR process studies may contribute to the improvement of existing GCOS stations and will deploy new surface and upper-air stations in data-sparse areas of North and South America in collaboration with CLIVAR VAMOS. An example of U.S. CLIVAR activities that may enhance the upper-air observations system is the NOAA PACSONET (Fig. 42) project that provides seed money for upper-air sounding equipment and training in Latin

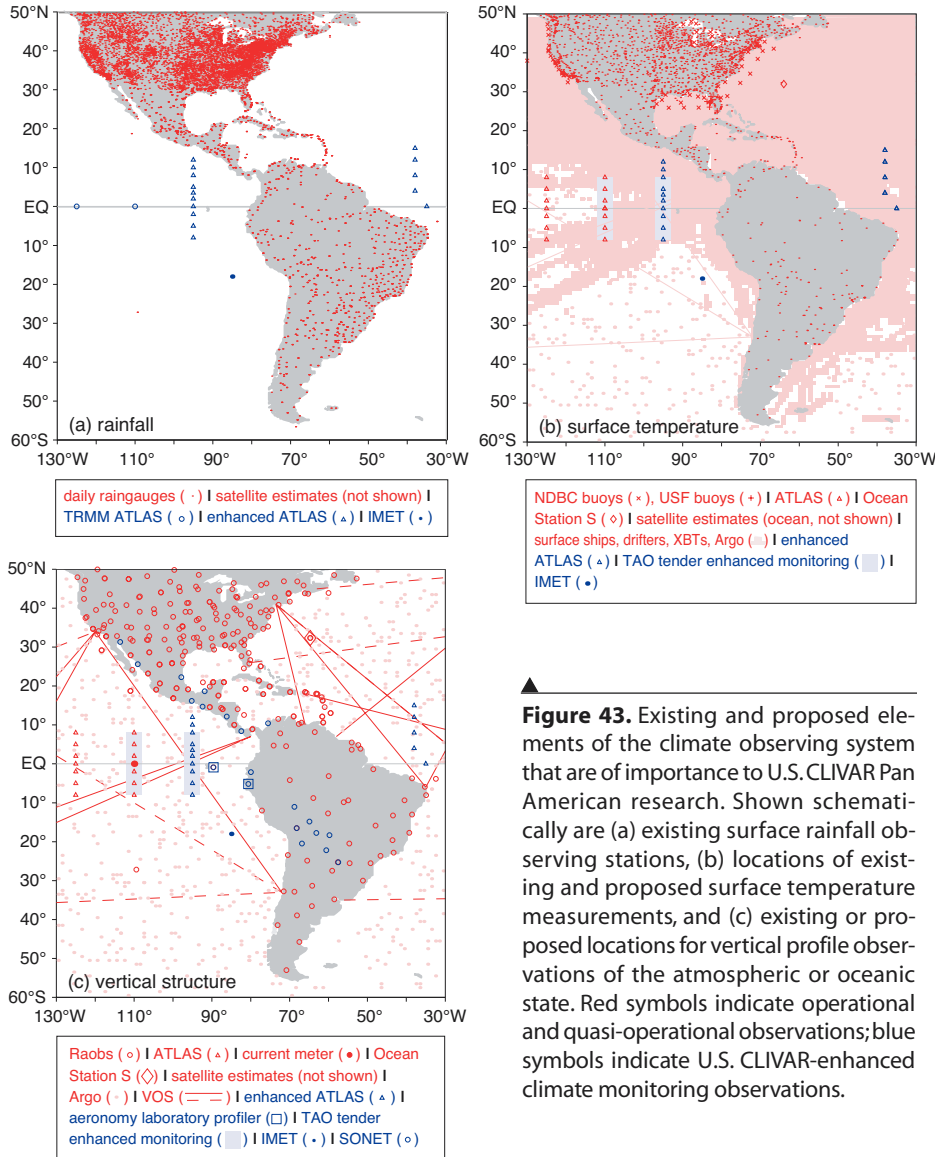


Figure 43. Existing and proposed elements of the climate observing system that are of importance to U.S. CLIVAR Pan American research. Shown schematically are (a) existing surface rainfall observing stations, (b) locations of existing and proposed surface temperature measurements, and (c) existing or proposed locations for vertical profile observations of the atmospheric or oceanic state. Red symbols indicate operational and quasi-operational observations; blue symbols indicate U.S. CLIVAR-enhanced climate monitoring observations.

inclination and altitude maximizes coverage and resolution in the tropics. A 2-cm wavelength radar and passive microwave radiometers with frequencies ranging from 10 to 85 GHz measure the rainfall. These remote measurements must be validated by ground-based rain measurements. The eastern Pacific ITCZ presents a particular problem in this regard because of the sparse island stations in that region. The shipborne radar and other precipitation measurements obtained during U.S. CLIVAR process studies over the tropical eastern Pacific Ocean will provide valuable validation data for TRMM. In addition, wind stress measurements from the NASA QuikSCAT, sea surface temperature from the TRMM microwave instrument, and sea level from TOPEX and its follow-ons are providing data of unprecedented quality for air-sea interaction research.

In the Atlantic, a pilot-scale moored measurement program is being designed as the centerpiece of PIRATA.

America and is involved in enhanced monitoring for the MESA and NAME field studies. Every effort will be made to upgrade or add stations through the World Weather Watch, but failing this, alternative funding will be sought within and outside of CLIVAR.

National and international research satellite missions providing improved global coverage of sea surface temperature, wind stress, sea level, precipitation, and other climatic parameters may become operational during the CLIVAR period. NASA is sponsoring a number of research satellite missions of importance to U.S. CLIVAR. The Tropical Rainfall Measurement Mission (TRMM) launched its first satellite in November 1997 to map tropical precipitation. The satellite orbits between 35°N and 35°S at an altitude of 350 km. The low

The purpose of PIRATA is to provide time series data of surface fluxes, surface temperature and salinity, and upper-ocean heat and salt content to examine processes by which the ocean and atmosphere interact in key regions of the tropical Atlantic. The field phase of PIRATA was 1997-2000. Deployment of up to 14 moorings was part of a multinational effort involving Brazil, France, and the United States. PIRATA will contribute to planning for a CLIVAR Basinwide Extended Climate Studies (BECS) on Atlantic climate variability.

8. U.S. CLIVAR Organization and Links to Other Efforts

U.S. CLIVAR is a national contribution to International CLIVAR that is overseen by the Climate Research



Committee of the National Research Council. Scientific leadership for U.S. CLIVAR is provided by an SSC. The Interagency Group (IAG) is made up of members from the National Science Foundation (NSF), National Oceanic and Atmospheric Administration (NOAA), National Aeronautics and Space Administration (NASA), and the Department of Energy (DOE) who initially appointed the SSC. The SSC has established several standing working groups for specific tasks and three panels with oversight of all U.S. CLIVAR concerns in the three regions of its primary interest. The Atlantic, Pan American, and Pacific Sector Implementation Panels report to the SSC, which appointed the members. The working groups are the Seasonal-to-Interannual Modeling and Prediction (SIMAP) panel, Asian-Australian Monsoon Working Group, a joint Past Global Changes (PAGES) and CLIVAR group, and a joint Study of Environmental Arctic Change (SEARCH) and CLIVAR group. The working groups and sector panels both report to the SSC, which is the main line of communication to International CLIVAR and the Interagency Group. The membership of all U.S. CLIVAR committees, panels, and working groups rotate on a regular schedule to ensure fairness and an infusion of fresh ideas.

The program managers from NASA, NOAA, NSF, and DOE, forming the IAG, promote and coordinate national interests in CLIVAR. They look for and coordinate opportunities within and across federal agencies to secure resources and develop funding mechanisms. They participate in all aspects of the planning process to ensure program viability. Lastly, they approve membership of the SSC and provide support, through the U.S. CLIVAR office, for planning and organizational activities. The SSC provides overall scientific and programmatic guidance to ensure that U.S. CLIVAR progresses toward its scientific objectives, including development and approval of implementation plans. They advise agencies on CLIVAR implementation, promote balance within the various elements (theory, modeling, empirical studies, long-term observations, and field campaigns) of the program, and provide oversight and guidance to advisory groups, particularly on the balance and prioritization of activities.

The Pan American Sector Implementation Panel, in collaboration with the Pacific and Atlantic panels, advises the SSC on needed field, empirical, and model studies in the Pan American region and on appropriate mechanisms (e.g., community meetings, working groups, commissioned studies, etc.) to develop imple-

mentation plans. In developing the regional implementation plans, the Pan American panel organizes open meetings and publicizes planning documents in an effort to develop a comprehensive plan of strongly justified and balanced activities. Together with other national and international groups, the Pan American panel is expected to advise on efficiently coordinating the execution of these plans. The panel calls for workshops and other meetings that will lead to progress in the implementation phase. At the international level, the Pan American panel provides liaison with the CLIVAR VAMOS program. U.S. CLIVAR Pan American research will make a major contribution to VAMOS and will benefit from international coordination and planning of field programs and dataset development and from the development of new empirical and modeling research on the American monsoons by scientists in North, Central, and South America.

U.S. CLIVAR and GEWEX are complementary programs in the Pan American region that emphasize continental precipitation. U.S. CLIVAR emphasizes the planetary-scale context and the variability of the weather systems that produce rain on seasonal and longer time scales while GEWEX emphasizes land-atmosphere interaction on intraseasonal-to-interannual time scales. Mesoscale modeling of continental precipitation in a climate context is a common element of both programs. The GEWEX projects of GCIP focus on North American rainfall and the Brazil/NASA-led LBA hydrometeorology program focuses on rainfall in the Amazon basin. As a contribution to both U.S. CLIVAR and GEWEX, NOAA is currently sponsoring a PACS/GCIP research initiative that focuses on the seasonal-to-interannual variability of warm-season rainfall, surface air temperature, and the hydrologic cycle over North America. U.S. CLIVAR and U.S. GEWEX will bring together the respective strengths and areas of expertise of their participating scientists. There will be cooperation through complimentary projects such as the CLIVAR SIMAP, GLASS, and through the ISLSCP and the GSWP.

The Intergovernmental Panel on Climate Change (IPCC) process marshals scientists to assess the effect of human activity on climate change (see IPCC 2001). There is a U.S. community involved in the IPCC process and a vigorous program of model development and experimentation supporting these activities. U.S. CLIVAR will not, therefore, seek to directly address anthropogenic climate change, but rather facilitate U.S.



activities under the IPCC process by using existing and new knowledge of the record and mechanisms of primarily natural climate variability to improve the models that are the basis for projecting climate change and by assisting the development of ways of separating natural and anthropogenic changes. A high level of cooperation will be required between the academic community and the few national centers capable of supporting the comprehensive climate models needed to study climate change.

The U.S. Carbon Cycle Program is developing plans for atmospheric, land-based, ocean-surface and ocean-interior observations in order to better understand the sources and sinks of carbon (Sarmiento and Wofsy 1999). They are also considering data-assimilative and prognostic models. While the processes involved in the transport and transformation of carbon may be more complex than those affecting heat and water, they are strongly coupled, and there are strong similarities in both the underlying physics and methodologies of climate and carbon research. Consequently, significant synergy between the Carbon Cycle Program and CLIVAR should be anticipated and encouraged. The observing strategies of the two programs, which involve many of the same platforms, their common need to assimilate relatively sparse ocean data, and their desire to better understand ocean transport and mixing, all provide a basis for significant cooperation.

U.S. CLIVAR will be attempting to improve the accuracy and completeness of the instrumental climate record, but this can, at best, add an increment to the length of record available for studying climate variability. Consequently, U.S. CLIVAR will actively support work to understand the implications of the proxy climate record through joint work with the PAGES program. A joint PAGES/CLIVAR working group is being formed to foster this research, but CLIVAR will not directly address efforts to extend the record of proxy data backward in time.

Other activities that are at the scientific heart of CLIVAR research but are organized separately include the significant improvement of the ocean climate observing system through the use of profiling floats by the Argo program and the necessary improvement of the analysis of sustained ocean observations to be carried out in the Global Ocean Data Assimilation Experiment (GODAE). Additionally, coordination with GCOS will help ensure that the components put in place by

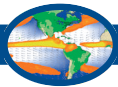
CLIVAR are fully integrated into the global climate observing system. Links to development and application activities within forecast centers (e.g., NCEP, IRI) will be central in establishing developmental pipelines between the research community and the climate forecasters who implement and utilize the climate models that CLIVAR will improve.

U.S. CLIVAR will coordinate its eastern Pacific field studies with the Scripps-Lamont CORC, which has begun enhanced ocean monitoring in the eastern tropical Pacific for 5 years beginning in 1998. It is anticipated that Pan American research activities of U.S. CLIVAR will contribute to the development of a CLIVAR Pacific BECS, focusing on the processes that couple tropical, subtropical, and subarctic wind-driven gyres on seasonal-to-decadal time scales, including the decadal modulation of ENSO.

Selected References

Sections 1.1 and 1.2 Annual mean climate and the seasonal march

- Baden-Dagan, A., C. E. Dorman, M. A. Merrifield, and C. D. Winant, 1991: The lower atmosphere over the Gulf of California. *J. Geophys. Res.*, **96**, 16,877-16,896.
- Barlow, M., S. Nigam, and E. H. Berbery, 1998: Evolution of the North American monsoon system. *J. Climate*, **11**, 2238-2257.
- Berbery, E. H., 2001: Mesoscale moisture analysis of the North American monsoon. *J. Climate*, **14**, 121-137.
- Berbery, E. H., and E. M. Rasmusson, 1999: Mississippi moisture budgets on regional scales. *Mon. Wea. Rev.*, **127**, 2654-2673.
- Berbery, E. H., and E. A. Collini, 2000: Springtime precipitation and water vapor flux over southeastern South America. *Mon. Wea. Rev.*, **128**, 1328-1346.
- Bonner, W. D., 1968: Climatology of the low-level jet. *Mon. Wea. Rev.*, **96**, 833-850.
- Bonner, W. D., and J. Paegle, 1970: Diurnal variations in the boundary-layer winds over the south-central United States in summer. *Mon. Wea. Rev.*, **98**, 735-744.
- Bryson, R. A., and W. P. Lowry, 1955: The synoptic climatology of the Arizona summer precipitation singularity. *Bull. Amer. Meteor. Soc.*, **36**, 329-339.
- Dickinson, R. E., 1987: *The Geophysiology of Amazonia: Vegetation and Climate Interactions*. J. Wiley and Sons, 526 pp.
- DiMego, G. F., L. F. Bosart, and G. W. Enderson, 1976: An examination of the frequency and mean conditions surrounding frontal incursions into the Gulf of Mexico and Caribbean Sea. *Mon. Wea. Rev.*, **104**, 709-718.
- Douglas, M. W., 1995: The summertime low-level jet over the Gulf of California. *Mon. Wea. Rev.*, **123**, 2334-2347.
- Douglas, M. W., R. A. Maddox, K. Howard, and S. Reyes, 1993: The Mexican Monsoon. *J. Climate*, **6**, 1665-1677.
- Douglas, M., M. Nicolini, and C. Saulo, 1998: Observational evidences of a low-level jet east of the Andes during January-March 1998. *Meteorologia*, **23**, 63-72.
- Figuroa, S. N., P. Satyamurty, and P. L. Silva-Dias, 1995: Simulations of the summer circulation over the South American re-



- gion with an eta-coordinate model. *J. Atmos. Sci.*, **52**, 1573-1584.
- Fu, R., B. Zhu, and R. E. Dickinson, 1999: How do the atmosphere and land surface influence seasonal changes of convection in the tropical Amazon? *J. Climate*, **12**, 1306-1321.
- Gandu, A. W., and P. L. Silva-Dias, 1998: Impact of tropical heat sources on the South American tropospheric upper circulation and subsidence. *J. Geophys. Res.*, **103**, 6001-6005.
- Garreaud, R. D., and J. M. Wallace, 1997: The diurnal march of the convective cloudiness over the Americas. *Mon. Wea. Rev.*, **125**, 3157-3171.
- Garreaud, R. D., and J. M. Wallace, 1998: Summertime incursions of midlatitude air into subtropical and tropical South America. *Mon. Wea. Rev.*, **126**, 2713-2733.
- Hales, J. E., Jr., 1974: Southwestern United States summer monsoon source—Gulf of Mexico or Pacific Ocean? *J. Appl. Meteor.*, **13**, 331-342.
- Hastenrath, S. L., 1966: The flux of atmospheric water vapor over the Caribbean Sea and the Gulf of Mexico. *J. Appl. Meteor.*, **5**, 778-788.
- Helfand, H. M., and S. D. Schubert, 1995: Climatology of the Great Plains low-level jet and its contribution to the continental moisture budget of the United States. *J. Climate*, **8**, 784-806.
- Hess, P., D. S. Battisti, and P. Rasch, 1993: The maintenance of the intertropical convergence zones and the large-scale tropical circulation on a water-covered earth. *J. Atmos. Sci.*, **50**, 691-713.
- Holton, J. R., 1967: The diurnal boundary-layer wind oscillation above sloping terrain. *Tellus*, **19**, 199-205.
- Lenters, J. D., and K. H. Cook, 1997: On the origin of the Bolivian high and related circulation features of the South American climate. *J. Atmos. Sci.*, **54**, 656-677.
- Magaña, V., J. A. Amador, and S. Medina, 1999: The midsummer drought over Mexico and Central America. *J. Climate*, **12**, 1577-1588.
- Mitchell, M. J., R. A. Arritt, and K. Labas, 1995: A climatology of the warm season Great Plains low-level jet using wind profiler observations. *Wea. and Forecasting*, **10**, 576-591.
- Mitchell, T. P., and J. M. Wallace, 1992: The annual cycle in equatorial convection and sea surface temperature. *J. Climate*, **5**, 1140-1156.
- Philander, S. G. H., D. Gu, D. Halpern, G. Lambert, N.-C. Lau, T. Li, and R. C. Pacanowski, 1996: Why the ITCZ is mostly north of the equator. *J. Climate*, **9**, 2958-2971.
- Rasmusson, E. M., 1967: Atmospheric water vapor transport and the water balance of North America: Part I. Characteristics of the water vapor flux field. *Mon. Wea. Rev.*, **95**, 403-426.
- Roads, J. O., S.-C. Chen, A. K. Guetter, and K. P. Georgakakos, 1994: Large-scale aspects of the United States hydrological cycle. *Bull. Amer. Meteor. Soc.*, **75**, 1589-1610.
- Rodwell, M. J., and B. J. Hoskins, 1996: Monsoons and the dynamics of deserts. *Mon. Wea. Rev.*, **122**, 1385-1404.
- Satyamurty, P., C. Nobre, and P. L. Silva-Dias, 1999: South America. Chapter 3C, *Meteorology of the Southern Hemisphere*, Meteorological Monographs, AMS, **27**, 119-139.
- Schmitz, J. T., and S. Mullen, 1996: Water vapor transport associated with the summertime North American Monsoon as depicted by ECMWF analyses. *J. Climate*, **9**, 1621-1634.
- Stensrud, D., 1996: Importance of low-level jets to climate: A review. *J. Climate*, **9**, 1698-1711.
- Stensrud, D. J., R. L. Gall, S. L. Mullen, and K. W. Howard, 1995: Model climatology of the Mexican Monsoon. *J. Climate*, **8**, 1775-1794.
- Tang, M., and E. R. Reiter, 1984: Plateau monsoons of the Northern Hemisphere: A comparison between North America and Tibet. *Mon. Wea. Rev.*, **112**, 617-637.
- Velasco, I., and J. Fritsch, 1987: Mesoscale convective complexes in the Americas. *J. Geophys. Res.*, **92**, D8, 9591-9613.
- Whittaker, L. M., and L. H. Horn, 1981: Geographical and seasonal distribution of North American cyclogenesis, 1958-1977. *Mon. Wea. Rev.*, **109**, 2312-2322.

Section 1.3 North American anomalies and climate variability

- Bell, G. D., and J. E. Janowiak, 1995: Atmospheric circulation associated with the Midwest floods of 1993. *Bull. Amer. Meteor. Soc.*, **76**, 681-695.
- Carleton, A. M., D. A. Carpenter, and P. J. Weser, 1990: Mechanisms of interannual variability of the southwest United States summer rainfall maximum. *J. Climate*, **3**, 999-1015.
- Cavazos, T., and S. Hastenrath, 1990: Convection and rainfall over Mexico and their modulation by the Southern Oscillation. *Int. J. Climatology*, **10**, 377-386.
- Enfield, D. B., 1996: Relationships of inter-American rainfall to tropical Atlantic and Pacific SST variability. *Geophys. Res. Lett.*, **23**, 3305-3308.
- Gutzler, D. S., and J. W. Preston, 1997: Evidence for a relationship between spring snow cover in North America and summer rainfall in New Mexico. *Geophys. Res. Lett.*, **24**, 2207-2210.
- Higgins, R. W., and W. Shi, 1999: Dominant factors responsible for interannual variability of the Southwest Monsoon. *J. Climate*, **13**, 759-776.
- Higgins, R. W., Y. Yao, E. S. Yarosh, J. E. Janowiak, and K. C. Mo, 1997: Influence of the Great Plains low-level jet on summertime precipitation and moisture transport over the central United States. *J. Climate*, **10**, 481-507.
- Higgins, R. W., Y. Yao, and X. Wang, 1997: Influence of the North American Monsoon System on the United States summer precipitation regime. *J. Climate*, **10**, 2600-2622.
- Higgins, R. W., K. C. Mo, and Y. Yao, 1998: Interannual variability of the United States summer precipitation regime with emphasis on the southwestern monsoon. *J. Climate*, **11**, 2582-2606.
- Latif, M., and T. P. Barnett, 1994: Causes of decadal climate variability over the North Pacific/North American sector. *Science*, **266**, 634-637.
- Latif, M., and T. P. Barnett, 1996: Decadal climate variability over the North Pacific and North America: Dynamics and predictability. *J. Climate*, **9**, 2407-2423.
- Mo, K. C., J. N. Paegle, and R. W. Higgins, 1997: Atmospheric processes associated with summer floods and droughts in the Central United States. *J. Climate*, **10**, 3028-3046.
- Mock, C. J., 1996: Climatic controls and spatial variations of precipitation in the western United States. *J. Climate*, **9**, 1111-1125.
- Stensrud, D. J., R. L. Gall, and M. K. Nordquist, 1997: Surges over the Gulf of California during the Mexican Monsoon. *Mon. Wea. Rev.*, **125**, 417-437.
- Ting, M., and H. Wang, 1997: Summertime U.S. precipitation variability and its relation to Pacific sea surface temperature. *J. Climate*, **10**, 1853-1873.
- Wang, H., M. Ting, and M. Ji, 1999: Prediction of seasonal mean United States precipitation based on El Niño sea surface temperatures. *Geophys. Res. Lett.*, **26**, 1341-1344.
- Wang, M., J. Paegle, and S. DeSordi, 1999: Global variable resolution simulations of Mississippi basin rains of summer 1993. *J.*



Geophys. Res., **104**, 19,399-19,414.

Yu, B., and J. M. Wallace, 2000: The principal mode of interannual variability of the North American monsoon system. *J. Climate*, **13**, 2794-2800.

Section 1.4 South American anomalies and climate variability

Aceituno, P. F., 1988: On the functioning of the Southern Oscillation in the South America sector. Part I: Surface climate. *Mon. Wea. Rev.*, **116**, 505-524.

Buchmann, J., J. Paegle, L. Buja, and R. E. Dickinson, 1990: The effect of tropical Atlantic heating anomalies upon GCM rain forecasts over the Americas. *J. Climate*, **3**, 189-208.

Buchmann, J., L. E. Buja, J. Paegle, and R. E. Dickinson, 1995: Further experiments on the effect of tropical Atlantic heating anomalies upon GCM rain forecasts over the Americas. *J. Climate*, **8**, 1235-1244.

Diaz, A. F., C. D. Studzinski, and C. R. Mechoso, 1998: Relationships between precipitation anomalies in Uruguay and southern Brazil and sea surface temperature in the Pacific and Atlantic oceans. *J. Climate*, **11**, 251-271.

Garcia, N. O., and W. M. Vargas, 1998: The temporal climatic variability in the Río de la Plata basin displayed by the river discharges. *Climatic Change*, **38**, 359-379.

Grimm, A. M., S. E. T. Ferraz, and J. Gomes, 1998: Precipitation anomalies in Southern Brazil associated with El Niño and La Niña events. *J. Climate*, **11**, 2863-2880.

Karoly, D. J., 1989: Southern Hemisphere circulation features associated with El Niño-Southern Oscillation events. *J. Climate*, **2**, 1239-1251.

Kousky, V. E., 1985: Atmospheric circulation changes associated with rainfall anomalies over tropical Brazil. *Mon. Wea. Rev.*, **113**, 1951-1957.

Kousky, V. E., and M. T. Kayano, 1994: Principal modes of outgoing longwave radiation and 250-mb circulation for the South American sector. *J. Climate*, **7**, 1131-1142.

Lenters, J. D., and K. H. Cook, 1999: Summertime precipitation variability over South America: Role of the large-scale circulation. *Mon. Wea. Rev.*, **127**, 409-431.

Liebmann, B., and J. A. Marengo, 2001: Annual and interannual variability of rainfall in the Brazilian Amazon Basin. *J. Climate*, **14**, 4308-4318.

Liebmann, B., J. A. Marengo, J. D. Glick, V. E. Kousky, I. C. Wainer, and O. Massambani, 1998: A comparison of rainfall, outgoing longwave radiation, and divergence over the Amazon Basin. *J. Climate*, **11**, 2898-2909.

Marengo, J. A., B. Liebmann, V. E. Kousky, N. P. Filizola, and I. C. Wainer, 2000: Onset and end of the rainy season in the Brazilian Amazon Basin. *J. Climate*, **14**, 833-852.

Mechoso, C. R., and S. L. Lyons, 1988: On the atmospheric response to SST anomalies associated with the Atlantic warm event during 1984. *J. Climate*, **1**, 422-428.

Mechoso, C. R., and G. Pérez Iribarren, 1992: Streamflow in southeastern South America and the Southern Oscillation. *J. Climate*, **5**, 1535-1539.

Mo, K. C., 2000: Relationships between low-frequency variability in the Southern Hemisphere and sea surface temperature anomalies. *J. Climate*, **13**, 3599-3610.

Mo, K. C., and R. W. Higgins, 1998: The Pacific South American modes and tropical convection in the Southern Hemisphere winter. *Mon. Wea. Rev.*, **126**, 1581-1596.

Moura, A. D., and J. Shukla, 1981: On the dynamics of droughts in

Northeast Brazil: Observations, theory, and numerical experiments with a general circulation model. *J. Atmos. Sci.*, **38**, 2653-2675.

Namias, J., 1972: Influence of Northern Hemisphere general circulation on drought in northeast Brazil. *Tellus*, **24**, 336-342.

Nogues-Paegle, J., and K. C. Mo, 1997: Alternating wet and dry conditions over South America during summer. *Mon. Wea. Rev.*, **125**, 279-291.

Pezzi, L. P., and I. F. A. Cavalcanti, 2001: The relative importance of ENSO and tropical Atlantic sea surface temperature anomalies for seasonal precipitation over South America: A numerical study. *Climate Dynamics*, **17**, 205-212.

Pisciottano, G., A. Díaz, G. Cazes, and C. R. Mechoso, 1994: El Niño-Southern Oscillation impact on rainfall in Uruguay. *J. Climate*, **7**, 1286-1302.

Robertson, A. W., and C. R. Mechoso, 1998: Interannual and decadal cycles in river flows of southeastern South America. *J. Climate*, **11**, 2570-2581.

Van Loon, H., J. W. Kidson, and A. N. Mullan, 1993: Decadal variation of the annual cycle in the Australian dataset. *J. Climate*, **6**, 1227-1231.

Weiner, I., and J. Soares, 1997: Northeast Brazil rainfall and its decadal-scale relationship to wind stress and sea surface temperature. *Geophys. Res. Lett.*, **24**, 277-280.

Section 1.5 Land surface role and processes

Atlas, R., N. Wolfson, and J. Terry, 1993: The effect of SST and soil moisture anomalies on GLA model simulations of the 1988 summer drought. *J. Climate*, **6**, 2034-2048.

Avisar, R., and R. A. Pielke, 1989: A parameterization of heterogeneous land surface for atmospheric numerical models and its impact on regional meteorology. *Mon. Wea. Rev.*, **117**, 2113-2136.

Betts, A. K., and J. H. Ball, 1998: FIFE surface climate and site-average dataset 1987-1989. *J. Atmos. Sci.*, **55**, 1091-1108.

Betts, A. K., J. H. Ball, A. C. M. Beljaars, M. J. Miller, and P. Viterbo, 1996: The land-surface-atmosphere interaction: A review based on observational and global modeling perspectives. *J. Geophys. Res.*, **101**, 7209-7225.

Chou, C., and J. D. Neelin, 2000: Ocean-atmosphere-land feedbacks in an idealized monsoon. *Quart. J. Roy. Meteor. Soc.*, **126**, 1-29.

Clark, C. A., and R. W. Arritt, 1995: Numerical simulations of the effect of soil moisture and vegetation cover on the development of deep convection. *J. Appl. Meteor.*, **34**, 2029-2045.

Delworth, T. L., and S. Manabe, 1989: The influence of soil wetness on near-surface atmospheric variability. *J. Climate*, **2**, 1447-1462.

Dirmeyer, P. A., and K. L. Brubaker, 1999: Contrasting evaporative moisture sources during the drought of 1988 and the flood of 1993. *J. Geophys. Res.*, **104**, 19,383-19,397.

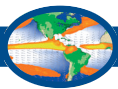
Eltahir, E. A. B., and R. L. Bras, 1994: Precipitation recycling in the Amazon Basin. *Quart. J. Roy. Meteor. Soc.*, **120**, 861-880.

Koster, R. D., and M. J. Suarez, 1995: Relative contributions of land and ocean processes to precipitation variability. *J. Geophys. Res.*, **100**, 13,775-13,790.

Koster, R. D., and M. J. Suarez, 1996: The influence of land surface moisture retention on precipitation statistics. *J. Climate*, **9**, 2551-2567.

Kunkel, K. E., 1989: A surface energy budget view of the 1988 midwestern United States drought. *Bound. Layer Meteor.*, **48**, 217-225.

Mintz, Y., 1984: The sensitivity of numerically simulated climates



- to land-surface boundary conditions. *The Global Climate*, (J. Houghton, Ed.), Cambridge University Press, 79-105.
- Paegle, J., K. C. Mo, and J. Nogués-Paegle, 1996: Dependence of simulated precipitation on surface evaporation during the 1993 U.S. summer floods. *Mon. Wea. Rev.*, **124**, 345-361.
- Rind, D., 1982: The influence of ground moisture conditions in North America on summer climate as modeled in the GISS GCM. *Mon. Wea. Rev.*, **110**, 1487-1494.
- Salati, E., 1987: The forest and the hydrological cycle. *The Geophysiology of Amazonia: Vegetation and Climate Interactions*, J. Wiley and Sons, 273-296.
- Trenberth, K. E., and G. W. Branstator, 1992: Issues in establishing causes of the 1988 drought over North America. *J. Climate*, **5**, 159-172.
- Trenberth, K. E., and C. J. Guillemot, 1996: Physical processes involved in the 1988 drought and 1993 floods in North America. *J. Climate*, **9**, 1288-1298.
- sea surface temperature on surface wind in the eastern equatorial Pacific: Seasonal and interannual variability. *J. Climate*, **2**, 1492-1499.
- Wang, B., and Y. Wang, 1999: Dynamics of the intertropical convergence zone-cold SST tongue complex. *J. Climate*, **12**, 1830-1847.
- Wang, B., and X. Fu, 2001: Physical processes determining the rapid re-establishment of the equatorial cold tongue/ITCZ complex from March to May. *J. Climate*, **14**, 2250-2265.
- Xie, S.-P., M. Ishiwatari, H. Hashizume, and K. Takeuchi, 1998: Coupled ocean-atmospheric waves on the equatorial front. *Geophys. Res. Lett.*, **25**, 3863-3866.
- Yin, B., and B. A. Albrecht, 2000: Spatial variability of atmospheric boundary-layer structure over the eastern equatorial Pacific. *J. Climate*, **13**, 1574-1592.

Section 1.8 Stratus cloud decks

Section 1.6 El Niño/Southern Oscillation

- Halpert, M. S., and C. F. Ropelewski, 1992: Sea surface temperature patterns associated with the Southern Oscillation. *J. Climate*, **5**, 577-593.
- Ropelewski, C. F., and M. S. Halpert, 1986: North American precipitation and temperature patterns associated with El Niño/Southern Oscillation (ENSO). *Mon. Wea. Rev.*, **114**, 2352-2362.
- Ropelewski, C. F., and M. S. Halpert, 1987: Global and regional scale precipitation patterns associated with El Niño/Southern Oscillation. *Mon. Wea. Rev.*, **115**, 1606-1626.
- Ropelewski, C. F., and M. S. Halpert, 1989: Precipitation patterns associated with the high index phase of the Southern Oscillation. *J. Climate*, **2**, 268-284.

Section 1.7 Cold tongue/ITCZ complexes

- Bond, N. A., 1992: Observations of planetary boundary-layer structure in the eastern equatorial Pacific. *J. Climate*, **5**, 699-706.
- Chelton, D. B., F. J. Wentz, C. L. Gentemann, R. A. deSzoeko, and M. G. Schlax, 2000: Satellite microwave SST observations of transequatorial tropical instability waves. *Geophys. Res. Lett.*, **27**, 1239-1242.
- Chelton, D. B., and Coauthors, 2000: Observations of coupling between surface wind stress and sea surface temperature in the eastern tropical Pacific. *J. Climate*, **14**, 1479-1498.
- Deser, C., J. J. Bates, and S. Wahl, 1993: The influence of sea surface temperature gradients on stratiform cloudiness along the equatorial front in the Pacific Ocean. *J. Climate*, **6**, 1172-1180.
- Fu, X., and B. Wang, 2001: Coupled modeling of the Pacific ITCZ/cold tongue complex, Part I: Model performance and sensitivity experiments. *J. Climate*, **14**, 765-779.
- Hayes, S. P., M. J. McPhaden, and J. M. Wallace, 1989: The influence of sea surface temperature on surface wind in the eastern equatorial Pacific: Weekly to monthly variability. *J. Climate*, **2**, 1500-1506.
- Tomas, R. A., J. R. Holton, and P. J. Webster, 1999: The influence of cross-equatorial pressure gradients on the location of near-equatorial convection. *Quart. J. Royal Meteor. Soc.*, **125**, 1107-1127.
- Waliser, D. E., and R. C. J. Somerville, 1994: Preferred latitudes of the Intertropical Convergence Zone. *J. Atmos. Sci.*, **51**, 1619-1639.
- Wallace, J. M., T. P. Mitchell, and C. Deser, 1989: The influence of
- Albrecht, B. A., 1989: Aerosols, cloud microphysics, and fractional cloudiness. *Science*, **245**, 1227-1230.
- Bajuk, L., and C. B. Leovy, 1997: Seasonal and interannual variations in stratiform and convective clouds over the tropical Pacific and Indian oceans from ship observations. *J. Climate*, **11**, 2922-2941.
- Bretherton, C. S., and M. C. Wyant, 1997: Moisture transport, lower-tropospheric stability, and decoupling of cloud-topped boundary layers. *J. Atmos. Sci.*, **54**, 148-167.
- Gordon, C. T., A. Rosati, and R. Gudgel, 2000: Tropical sensitivity of a coupled model to specified ISCCP low clouds. *J. Climate*, **13**, 2239-2260.
- Klein, S. A., and D. L. Hartmann, 1993: The seasonal cycle of low stratiform clouds. *J. Climate*, **6**, 1587-1606.
- Klein, S. A., D. L. Hartmann, and J. R. Norris, 1995: On the relationship among low-cloud structure, sea surface temperature, and atmospheric circulation in the summertime northeast Pacific. *J. Climate*, **8**, 1140-1155.
- Ma, C.-C., C. R. Mechoso, A. W. Robertson, and A. Arakawa, 1996: Peruvian stratus clouds and the tropical Pacific circulation: A coupled ocean-atmosphere GCM study. *J. Climate*, **9**, 1635-1645.
- Nigam, S., 1997: The annual warm-to-cold phase transition in the eastern equatorial Pacific: Diagnosis of the role of stratus cloud top cooling. *J. Climate*, **10**, 2447-2467.
- Norris, J. R., 1998: Low cloud type over the ocean from surface observations. Part I: Relationship to surface meteorology and the vertical distribution of temperature and moisture. *J. Climate*, **11**, 369-382.
- Norris, J. R., 1998: Low cloud type over the ocean from surface observations. Part II: Geographical and seasonal variations. *J. Climate*, **11**, 383-403.
- Norris, J. R., and C. B. Leovy, 1994: Interannual variability in stratiform cloudiness and sea surface temperature. *J. Climate*, **7**, 1915-1925.
- Randall, D. A., B. A. Albrecht, S. Cox, D. Johnson, P. Minnis, W. Rossow, and D. O'C. Starr, 1996: On FIRE at ten. *Adv. Geophys.*, **38**, 37-177.
- Rozendaal, M., C. B. Leovy, and S. A. Klein, 1995: An observational study of diurnal variations of marine stratiform cloud. *J. Climate*, **8**, 1795-1809.
- Short, D. A., and K. Nakamura, 2000: TRMM radar observations of shallow precipitation over the tropical oceans. *J. Climate*, **13**, 4107-4124.



Stevens, B., W. R. Cotton, G. Feingold, and C.-H. Moeng, 1998: Large-eddy simulation of strongly precipitating, shallow, stratocumulus-topped boundary layers. *J. Atmos. Sci.*, **55**, 3616-3638.

Section 1.9 Subseasonal climate variability

Higgins, R. W., and W. Shi, 2001: Intercomparison of the principal modes of interannual and intraseasonal variability of the North American monsoon system. *J. Climate*, **14**, 403-417.

Kayano, M. T., and V. E. Kousky, 1999: Intraseasonal (30-60 day) variability in the global tropics: principal modes and their evolution. *Tellus*, **51A**, 373-386.

Liebmann, B., G. N. Kiladis, J. A. Marengo, and T. Ambrizzi, 1999: Submonthly convective variability over South America and the South Atlantic Convergence Zone. *J. Climate*, **12**, 1877-1891.

Madden, R. A., and P. R. Julian, 1971: Detection of a 40-50 day oscillation in the zonal wind in the tropical Pacific. *J. Atmos. Sci.*, **28**, 702-708.

Madden, R. A., and P. R. Julian, 1994: Observations of the 40-50 day tropical oscillation—A review. *Mon. Wea. Rev.*, **122**, 814-837.

Maloney, E. D., and D. L. Hartmann, 2000: Modulation of eastern north Pacific hurricanes by the Madden-Julian oscillation. *J. Climate*, **13**, 1451-1460.

Nogues-Paegle, J., L. A. Byerle, and K. C. Mo, 2000: Intraseasonal modulation of South American summer precipitation. *Mon. Wea. Rev.*, **128**, 837-850.

Stensrud, D. J., R. L. Gall, and M. K. Nordquist, 1997: Surges over the Gulf of California during the Mexican Monsoon. *Mon. Wea. Rev.*, **125**, 417-437.

Weickmann, K. M., 1983: Intraseasonal circulation and outgoing longwave radiation modes during the Northern Hemisphere winter. *Mon. Wea. Rev.*, **111**, 1838-1858.

Section 2 Motivation

Díaz, H. F., and R. S. Pulwarty, 1997: Decadal climate variability, Atlantic hurricanes, and societal impacts: An overview. *Hurricanes*, (H. F. Díaz and R. S. Pulwarty, Eds.), Springer-Verlag, 292 pp.

Lagos, P., and J. Buizer, 1992: Natural and technological disasters: Causes, effects, and preventative measures. Pennsylvania Academy of Sciences, 16, 223-238. (Available from S. K. Mujumdar, Dept. of Biology, Lafayette College, Easton, PA 18042.)

Neumann, C. J., 1987: *The National Hurricane Center Risk Analysis Program (HURISK)*. NOAA Technical Memorandum NWS NHC 38, 56 pp.

Section 4 Field studies

NAME Project Science Team, 2000: *NAME Science and Implementation Plan*. Available from U.S. CLIVAR Project Office (www.usclivar.org).

Weller, R., B. Albrecht, S. Esbensen, C. Eriksen, A. Kumar, R. Mechoso, D. Raymond, D. Rogers, and D. Rudnick, 1999: *A Science and Implementation Plan for EPIC*. Available from U.S. CLIVAR Project Office (www.usclivar.org).

Section 5 Modeling issues

Boyle, J. S., 1998: Evaluation of the annual cycle of precipitation

over the United States in GCMs: AMIP simulations. *J. Climate*, **11**, 1041-1055.

Davey, M. K., and Coauthors, 2002: STOIC: A study of coupled model climatology and variability in tropical ocean regions. *Climate Dynamics*, **18**, 403-420.

Ghan, S. J., X. Bian, and L. Corsetti, 1996: Simulation of the Great-Plains low-level jet and associated cloud fields by general circulation models. *Mon. Wea. Rev.*, **124**, 1388-1408.

Hahmann, A. N., and R. E. Dickinson, 2001: A fine-mesh land approach for general circulation models and its impact on regional climate. *J. Climate*, **14**, 1634-1646.

Ji, M., A. Leetmaa, and V. E. Kousky, 1996: Coupled model predictions of ENSO during the 1980s and the 1990s at the National Centers for Environmental Prediction. *J. Climate*, **9**, 3105-3120.

Koster, R. D., and M. J. Suarez, 1992: Modeling the land surface boundary in climate models as a composite of independent vegetation stands. *J. Geophys. Res.*, **97**, 2697-2715.

Lu, L., R. A. Pielke, G. E. Liston, W. J. Parton, D. Ojima, and M. Hartman, 2000: Implementation of a two-way interactive atmospheric and ecological model and its application to the central United States. *J. Climate*, **14**, 900-919.

Mechoso, C. R., and Coauthors, 1995: The seasonal cycle over the tropical Pacific in general circulation models. *Mon. Wea. Rev.*, **123**, 2825-2838.

Rasmusson, E. M., and K. C. Mo, 1996: Large-scale atmospheric moisture cycling as evaluated from NMC global analysis and forecast products. *J. Climate*, **9**, 3276-3297.

Section 8 U.S. CLIVAR Organization

IPCC, 2001: *Climate Change 2001: The Scientific Basis Contribution of Working Group I to the Third Assessment Report of the Intergovernmental Panel on Climate Change (IPCC)*. (J. T. Houghton, Y. Ding, D. J. Griggs, M. Noguer, P. J. van der Linden, and D. Xiaosu, Eds.), Cambridge University Press, UK, 944 pp.

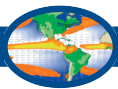
IPCC, 2001: *Climate Change 2001: Adaptation and Vulnerability Contribution of Working Group II to the Third Assessment Report of the Intergovernmental Panel on Climate Change (IPCC)*. (J. J. McCarthy, O. F. Canziani, N. A. Leary, D. J. Dokken, and K. S. White, Eds.), Cambridge University Press, UK, 1000 pp.

IPCC, 2001: *Climate Change 2001: Mitigation Contribution of Working Group III to the Third Assessment Report of the Intergovernmental Panel on Climate Change (IPCC)*. (B. Metz, O. Davidson, R. Swart, and J. Pan, Eds.), Cambridge University Press, UK, 700 pp.

Sarmiento, J. L., and S. C. Wofsy, 1999: *A U. S. Carbon Cycle Science Plan: A Report of the Carbon and Climate Working Group*. U. S. Global Change Research Program, 69 pp. (Copies may be obtained from USGCRP, 400 Virginia Avenue SW, Suite 750, Washington D.C. 20024.)

Notes on Illustrations

Figure 1. The rainfall estimates in the upper panel are a hybrid of two different datasets. Over the oceans they are based on the MSU carried aboard the Television Infrared Operational Satellites (TIROS) for 1979-1991. The method for inferring rainfall from MSU measurements is described in Spencer (1993: *J. Climate*, **6**, 1301-1326). Over land, they are based on a compilation of historical raingauge data by Legates and Willmott (1990: *Int. J. Climatol.*, **10**, 111-127). The GPI is described in Arkin and Meisner (1987: *Mon. Wea. Rev.*, **115**, 51-74), and



based on 1986-1993. MSU data provided by the NASA Marshall Space Flight Center.

Figure 2. Surface winds are based on an analysis of the COADS (Woodruff et al. 1987: *Bull. Amer. Meteor. Soc.*, **68**, 1239-1250; Woodruff et al. 1993: *Earth Syst. Monit.*, **4**, 1-8) performed by Sadler et al. (1987: Tropical Marine Climatic Atlas, Univ. Hawaii, Dep't. of Meteor., Reports 87-01 and 87-02). They represent averages for 1900-1979. Rainfall estimates are as in the upper panel of the previous figure. The outline for the stratus cloud decks corresponds to the 0.3 contour in an albedo map derived from 4 years of visible satellite imagery. Only surface winds in excess of 3 m/s are plotted, and annual precipitation totals in excess of 2 m are shaded.

Figure 3. Surface winds and sea surface temperature climatologies are from Sadler et al. (1987) as in the previous figure. The shading varies from blue to red for cold-to-warm sea surface temperatures, with gray indicating temperatures near 27°C. The wind plotting convention is as in Fig. 2.

Figure 4. As in Fig. 3, but arrows denote surface currents based on the Richardson (1989: *J. Geophys. Res.*, **94**, C5, 6169-6176) climatology of the historical record of ship drift measurements.

Figure 5. Courtesy of G. Feldman, NASA.

Figure 6. Coarse and fine resolution elevation datasets derived from the 5-min latitude-longitude resolution TerrainBase Worldwide Digital Terrain Dataset, which is produced at the National Geophysical Data Center (NGDC) and is available online at both NGDC and NCAR. See Row et al. (1995: *TerrainBase: Worldwide Digital Terrain Data Documentation Manual*, CD-ROM Public Beta Test Release 1.0, NOAA, National Geophysical Data Center, Boulder, CO, KGRD-30, 180 pp).

Figure 7. Snow depth climatology from the U.S. Air Force Environmental Technical Applications Center (Foster and Davy 1988: United States Air Force, Environmental Technical Applications Center, TN-88/006, Scott Air Force Base, Illinois, 48 pp.). Model soil moisture (surface soil wetness) for 1987-88 from the ECMWF (1995) Level III-A global atmospheric data archive. FPAR observations for 1987-88 (Sellers et al. 1994: *Int. J. Remote Sensing*, **15**, 3519-3545; Sellers et al. 1996a: *J. Climate*, **9**, 706-737). All three datasets are taken from the International Satellite Land Surface Climatology Project (ISLSCP) Initiative I CD-ROM (Sellers et al. 1996: *Bull. Amer. Meteor. Soc.*, **77**, 1987-2006). They are also available online through the NASA Goddard Space Flight Center Distributed Active Archive Center.

Figure 8. Circulation data taken from the NCEP/NCAR reanalysis archive. Precipitation estimates are based on merged satellite and station observations. North American panel courtesy of W. Higgins and M. Halpert. South American panel courtesy of V. Kousky and M. Halpert.

Figure 10. Figure provided by W. Higgins of NOAA Climate Prediction Center and A. Douglas of Creighton University.

Figure 12. After Mitchell and Wallace (1992), based on observations from COADS for 1946-1985.

Figure 13. Based on data from the TOGA-TAO array (McPhaden and McCarty, 1992: NOAA Tech. Mem. ERL PMEL-95, U.S. Dept. of Commerce, Washington D.C., 118 pp). The climatology for 140°W is based on observations for July 1983 to December 1991 and for 110°W from March 1980-June 1982 and July 1983-December 1991. The period of large anomalies during the 1982-1983 ENSO event, July 1982-June 1983, were not included in the climatology to prevent large biases due to this single event. Red shading for temperatures greater than 24°C,

with increases in color intensity for each 1°C increase in temperature. Blue contours for temperatures less than and equal to 22°C; contour interval 2°C.

Figure 14. Derived from high-resolution infrared images from geostationary satellites, 8 per day. Courtesy of K. Howard, NOAA NSSL.

Figure 15. Surface wind changes based on the COADS; sea-level pressure based on the ECMWF operational analyses; and rainfall as in the upper panel of Fig. 1. The surface wind and sea-level pressure climatologies are based on data for 1946-1979 and 1980-1989, respectively. Only vector wind changes with magnitudes in excess of 1 m/s are plotted. Pressure changes in increments of 0.6 mb are contoured, and precipitation changes in excess of 5 cm in magnitude are shaded. The sea-level pressure analysis over land is consistent with an analysis of historical airport pressure records (not shown).

Figure 16. Water content and FPAR as in Fig. 7.

Figure 17. Snow data as in Fig. 7.

Figure 18. Rainfall as in upper panel of Fig. 1.

Figure 19. Standard deviation of monthly data for 1982-1990, provided by P. Dirmeyer, University of Maryland. The data is from the ISLSCP Initiative II and is available online from the NASA DAAC. The LAI is discussed in Sellers et al. (1994, 1996: see notes for Fig. 7).

Figure 21. Regression of sea surface temperature and MSU precipitation on an index of eastern equatorial Pacific (6°N-6°S, 180°-80°W) sea surface temperature. The analysis is based on data for 1982-1991 and 1979-1991 for the sea surface temperature and precipitation fields, respectively. The sea surface temperature analyses are from NOAA NCEP. Temperature contour interval 0.2°C per 1 standard deviation of the index, with negative (zero) contours dashed (thickened). Shading for precipitation anomalies greater than 1 cm per 1 standard deviation of the index. Precipitation anomalies range from -4 to +10 cm per 1 standard deviation of the index.

Figure 22. Precipitation estimates from the MSU.

Figure 23. Regression of precipitation over the oceans and mean-tropospheric temperature on an index of eastern equatorial Pacific (6°N-6°S, 180°-80°W) sea surface temperature. The analysis is based on data for 1979-1991. Both the precipitation and the mean tropospheric temperature fields are taken from MSU measurements. The method for inferring precipitation from MSU measurements is described in Spencer (1993: *J. Climate*, **6**, 1301-1326) and the mean-tropospheric temperature estimates are described by Spencer and Christy (1990: *Science*, **247**, 1558-1562). Temperature contour interval of 0.1°C per 1 standard deviation of the index, with the positive and zero (negative) isotherms are drawn in gold (green). Precipitation plotting convention as in Fig. 21.

Figure 25. After Thompson et al. (1979: *J. Atmos. Sci.*, **32**, 53-72).

Figure 26. The QuikSCAT wind vectors are the simple average over one degree bins and one month. The divergence is calculated from the averaged wind vectors and then zonally smoothed along each latitude with a Loess smoother having a half span of 10°. Courtesy of D. Chelton, Oregon State University.

Figure 27. Figure provided by D. Chelton, Oregon State University.

Figure 28. Analysis provided by W. Higgins, NOAA Climate Prediction Center.

Figure 29. Analysis provided by W. Higgins, NOAA Climate Prediction Center.

Figure 30. Map of QuikSCAT 10-m vector wind overlaid on sea surface temperature measurements from a satellite microwave



radiometer (TMI). Courtesy of D. Chelton, Oregon State University.

Figure 31. As in Fig. 14.

Figure 32. U.S. series obtained from the National Climate Data Center Climate Division dataset; Brazil from the NCAR World Monthly Surface Station Climatology; and Ecuador from the Instituto Nacional de Meteorología e Hidrología (Ecuador) as provided to the Trade Convergence Climate Complex program (courtesy of D. Enfield and P. Cornejo).

Figure 33. Analysis provided by W. Higgins, NOAA Climate Prediction Center.

Figure 34. Precipitation time series as in Fig. 32. Sea surface temperature for 1950-1991 from Smith et al. (1996: *J. Climate*, **9**, 1403-1420) and for 1992 from Reynolds and Smith (1994: *J. Climate*, **7**, 929-948). As in Fig. 24.

Figure 35. Global tropical cyclone data produced by the National Climatic Data Center, and available online at the NOAA National Hurricane Center and at NCAR.

Figure 36. As in Fig. 35.

Acronym Glossary

ABL: Atmospheric Boundary Layer
 ADCP: Acoustic Doppler Current Profiler
 AGCM: Atmospheric General Circulation Model
 ALLS: American Low-Level Jets
 AOML: Atlantic Oceanographic and Meteorological Laboratory
 ASTEX: Atlantic Stratocumulus Transition Experiment
 ATLAS: Automated Temperature Line Acquisition System
 AVHRR: Advanced Very High Resolution Radiometer
 BECS: Basinwide Extended Climate Studies
 CCN: Cloud Condensation Nuclei
 CDC: Climate Diagnostics Center
 CDF: Common Data Format
 CEOP: GEWEX Coordinated Enhanced Observing Period
 CIRES: Cooperative Institute for Research in Environmental Sciences
 CLIVAR: Climate Variability and Predictability
 COADS: Comprehensive Ocean-Atmosphere Dataset
 COARE: Coupled Ocean-Atmosphere Response Experiment
 CORC: Consortium for the Ocean's Role in Climate
 CTD: Conductivity Temperature Depth
 CTIC: Cold Tongue/ITCZ Complex
 DAO: Data Assimilation Office
 DOE: Department of Energy
 ECMWF: European Centre for Medium-Range Weather Forecasts
 ENSO: El Niño/Southern Oscillation
 EPIC: Eastern Pacific Investigation of Climate Processes in the Coupled Ocean-Atmosphere System
 EPOCS: Equatorial Pacific Ocean Climate Studies
 EUC: Equatorial UnderCurrent
 FIRE: First ISCCP Regional Experiment
 FPAR: Fraction of Photosynthetically Active Radiation
 GAPP: GEWEX Americas Prediction Project
 GARP: Global Atmospheric Research Program
 GATE: Global Atlantic Tropical Experiment
 GCIP: GEWEX Continental-scale International Project
 GCM: General Circulation Model
 GCOS: Global Climate Observing System
 GEWEX: Global Energy and Water Experiment
 GLASS: Global Land Atmosphere System Study
 GOALS: Global Ocean-Atmosphere-Land System
 GODAE: Global Ocean Data Assimilation Experiment

GOES: Geostationary Operational Environmental Satellite
 GPCP: Global Precipitation Climatology Project
 GPI: GOES Precipitation Index
 GSWP: Global Soil Wetness Project
 IAG: U.S. CLIVAR Interagency Group
 IMET: Improved Meteorological Instrument
 IOP: Intensive Observing Period
 IPCC: Intergovernmental Panel on Climate Change
 IRI: International Research Institute for Climate Prediction
 ISCCP: International Satellite Cloud Climatology Project
 ISLSCP: International Satellite Land Surface Climatology Project
 ITCZ: InterTropical Convergence Zone
 JOSS: UCAR Joint Office for Science Support
 LAI: Leaf Area Index
 LBA: Large-Scale Biosphere-Atmosphere Experiment in Amazonia
 LDAS: Land Data Assimilation System
 LLJ: Low-Level Jet
 MESA: Monsoon Experiment South America
 MJO: Madden-Julian Oscillation
 MSU: Microwave Sounding Unit
 NAME: North American Monsoon Experiment
 NASA: National Aeronautics and Space Administration
 NCAR: National Center for Atmospheric Research
 NCEP: National Centers for Environmental Prediction
 NDBC: National Data Buoy Center
 NECC: North Equatorial CounterCurrent
 NESDIS: National Environmental Satellite Data and Information Center
 NetCDF: Network Common Data Format
 NGDC: National Geophysical Data Center
 NOAA: National Oceanic and Atmospheric Administration
 NSF: National Science Foundation
 NSSL: NOAA National Severe Storms Laboratory
 OAR: NOAA Office of Oceanic and Atmospheric Research
 OGCM: Ocean General Circulation Model
 OGP: Office of Global Programs
 OSEPA: Ocean Southeast Pacific Array
 PACS: Pan American Climate Studies
 PAGES: Past Global Changes
 PBL: Planetary Boundary Layer
 PIRATA: Pilot Research Moored Array in the Tropical Atlantic
 PLATIN: VAMOS La Plata River Basin hydroclimatology field program
 PMEL: Pacific Marine Environmental Laboratory
 PNA: Pacific North American
 PSA: Pacific South American
 PSU: Practical Salinity Unit
 QuikSCAT: NASA "quick" scatterometer mission
 SACZ: South Atlantic Convergence Zone
 SALLJ: South American Low-Level Jet
 SEARCH: Study of Environmental Arctic Change
 SEC: South Equatorial Current
 SIMAP: U.S. CLIVAR Seasonal-to-Interannual Modeling and Prediction
 SNET: PACS pilot upper-air sounding network
 SSC: U.S. CLIVAR Scientific Steering Committee
 SST: Sea Surface Temperature
 SWG: Science Working Group
 TAO: Tropical Atmosphere-Ocean
 TEW: Tropical Easterly Wave
 TIROS: Television Infrared Operational Satellite
 TMI: TRMM Microwave Imager



TOGA: Tropical Ocean-Global Atmosphere
 TOPEX: Ocean Topography Experiment
 TRMM: Tropical Rainfall Measurement Mission
 UCAR: University Corporation for Atmospheric Research
 USF/ADCP: University of South Florida Acoustic Doppler
 Current Profiler
 USGCRP: U.S. Global Change Research Program
 VAMOS: Variability of the American Monsoon Systems
 VEPIC: VAMOS EPIC field study
 VOS: Volunteer Observing Ship
 WCRP: World Climate Research Programme
 WWW: World Weather Watch
 XBT: eXpendable BathyThermograph

Color Maps for Selected Figures

Figure 16











	RGB	CYMK	Web
	R=176, G=196, B=216	C=30.59, Y=12.94, M=2.75, K=0.39	AFC8E1
	R=26, G=70, B=157	C=94.9, Y=57.65, M=0, K=11.37	1A469D
	R=213, G=236, B=30	C=16.47, Y=0, M=91.76, K=0	D5EC1E
	R=114, G=164, B=29	C=45.1, Y=0, M=94.9, K=19	72A41D
	R=37, G=122, B=76	C=83.92, Y=11.76, M=69.41, K=14	257A4C

Figure 19

	RGB	CYMK	Web
	Pantone DS277-4U R=217, G=239, B=127	C=15, Y=3, M=50, K=0	D9EF7F
	Pantone DS278-1U R=140, G=207, B=127	C=45, Y=1, M=50, K=0	8CCF7F
	Pantone DS278-3U R=89, G=182, B=91	C=65, Y=2, M=70, K=0	59B65B
	Pantone DS278-5U R=26, G=148, B=49	C=91, Y=4, M=96, K=0	1A9431
	Pantone DS302-6U R=63, G=128, B=70	C=75, Y=20, M=75, K=6	3F8046



Notes

U.S. CLIVAR is a major contributor to the international CLIVAR program,
an element of the World Climate Research Programme (WCRP).

For additional information on the U.S. CLIVAR program,
see our web page: www.usclivar.org

